Alma Mater Studiorum - Università di Bologna

Dottorato di Ricerca in: MECCANICA E SCIENZE AVANZATE DELL'INGEGNERIA
Ciclo: XXXIII
Settore concorsuale di afferenza: 09/A3
Settore scientifico disciplinare: ING/IND 14

Novel advance for smart batteries testing and monitoring

Presentata da:
JURI BELCARI

Supervisore:
Andrea Zucchelli, PhD

Coordinatore Dottorato:
Marco Carricato, PhD

co-Supervisore:
Catia Arbizzani, PhD

Esame finale Anno 2021

ad Elias.

Abstract

The aim of this thesis work is to contribute to the technological advancement of energy storage systems, especially batteries, in terms of efficiency and safety. The thesis to be demonstrated argues that on the one hand, the possibility of testing electrode materials with a more performing and versatile system than those present in the state of the art allows to reach a level of characterization and understanding of the working behaviour of these materials higher than the current state. On the other hand, the use of economic and at the same time effective sensors makes it possible to improve the production process of electrochemical cells and to monitor their state of health during their useful life, ultimately achieving the desired high level of reliability.
The main activity of this work consists of three different experimental phases aimed at improving the performance of an instrument for testing the electrodes in rechargeable batteries, as well as the search for an economic and high-performance sensor to detect electrolyte losses in the production process of lithium-ion batteries and the study of an innovative sensor that can be integrated into the electrochemical cell that can closely monitor its stability by intercepting any malfunctions.
The first phase of the work involved the study of a system for measuring the volumetric expansion of the electrodes during the charge/discharge cycles: the accurate choice of materials, careful design and the use of two temperature sensors combined with the choice of a contact-less gauge for transduction of the volume variation made it possible to obtain a compact system able to measure the cell assembly expansion under different conditions of applied compression force. The tests have been carried out at room temperature. However, subsequent characterization in the thermal chamber made it possible to validate the measurement provided by the instrument in a temperature range from 10 to 60°C, finding the calibration characteristic that allows the instrument to work correctly at different temperatures. This offers the opportunity to perform tests on electronic materials in conditions closer to those of real applications on electric vehicles, in all portable applications or in stationary storage systems. Electrochemical tests have validated the correctness of the measurements made with the designed instrument. They have also highlighted the possibility of evince phenomena that occur in the cell under test other than that of electrode expansion/contraction due to the insertion/deinsertion of the lithium ion in the electrode structure. Finally, it was necessary to provide the instrument with a sample holder for the "half-cell" test, so as to be able to appreciate the contribution to the dilation of only one electrode at a time. A second sample holder has therefore been designed for this purpose.

In the second phase a technology was identified that allows to detect the possible presence of dimethyl carbonate, the main component of the electrolyte in lithium-ion batteries currently on the market. After the analysis of the state of the art on sensors for the detection of gas, in particular VOC (Volatile Organic Compounds), we selected the photoionization as detection technique. Laboratory tests were carried out using a commercial sensor based on the technology identified and a machine layout was proposed to detect the possible presence of coarse electrolyte losses.
In the third phase, a new approach was proposed for monitoring the state of health of lithium-ion batteries: a new smart-sensor concept that can be integrated into the electrochemical cell, based on the colorimetric measurement of a chemical species at precise points in the cell. After the realisation of the first prototype, the first laboratory tests were carried out using water-based coloured solutions simulating the presence of transition metal ion salts. The electrochemical test cells show how there is a correlation between colour variation and the triggering of undesirable phenomena that degrade battery performance. The encouraging results obtained leave plenty room for improvement both from the point of view of the sensor principle and the miniaturisation of the prototype device and the interface system between the sensor and the world outside the battery, making it possible to integrate it into future batteries.

Sommario

Scopo del presente lavoro di tesi è quello di contribuire all'avanzamento tecnologico dei sistemi di accumulo dell'energia, in particolare delle batterie, in termini di efficienza e sicurezza. La tesi che si intende dimostrare sostiene che da un lato, la possibilità di testare i materiali elettrodici con un sistema più performante e versatile rispetto a quelli presenti nello stato dell'arte consente di raggiungere un livello di caratterizzazione e comprensione del comportamento in opera di questi materiali superiore allo stato attuale. Dall'altro l'utilizzo di sensori economici ed allo stesso tempo efficaci consente di migliorare il processo produttivo delle celle elettrochimiche e di monitorare il loro stato di salute durante la loro vita utile, ottenendo in ultimo l'elevato livello di affidabilità auspicato.
L'attività principale di questo lavoro consiste in tre differenti fasi sperimentali rivolte al miglioramento della performance di uno strumento per il test degli elettrodi nelle batterie ricaricabili, oltre alla ricerca di un sensore economico e performante per rilevare le perdite di elettrolita nel processo di produzione delle batterie litio-ione ed allo studio di un sensore innovativo integrabile nella cella elettrochimica che possa monitorarne da vicino la stabilità intercettando eventuali malfunzionamenti.
La prima fase del lavoro ha riguardato lo studio di un sistema per la misura dell'espansione volumetrica degli elettrodi durante i cicli di carica/scarica: la scelta accurata dei materiali, un'attenta progettazione e l'utilizzo di due sensori di temperatura unito alla scelta di un misuratore contact-less per la trasduzione della variazione di volume ha permesso di ottenere un sistema compatto in grado di misurare l'espansione della cella completa in condizioni di differente forza di compressione applicata. I test sono stati condotti a temperatura ambiente. Tuttavia, la successiva caratterizzazione in camera termica ha permesso di validare la misura fornita dallo strumento in un range di temperatura da 10 a 60 $°C$, trovando la caratteristica di calibrazione che permette allo strumento di poter lavorare correttamente a temperature diverse. Questo ha dato l'opportunità di effettuare i test sui materiali elettronici in condizioni più vicine a quelle delle applicazioni reali sui veicoli elettrici, in tutte le applicazioni *portable* o negli impianti di accumulo stazionari.I test elettrochimici hanno validato la correttezza delle misure fatte con lo strumento progettato. Hanno evidenziato inoltre la possibilità di apprezzare ulteriori fenomeni che avvengono nella cella sotto test altra a quello dell'espansione/contrazione elettrodica dovuta all'inserzione/deinserzione dello ione litio nella struttura degli elettrodi. Infine si è manifestata la necessità di predisporre a corredo dello strumento anche un porta campione per il test a "mezza cella", in modo da poter apprezzare il contributo

alla dilatazione di un solo elettrodo per volta.
Quindi è stato progettato un secondo porta campione a tal proposito. Nella seconda fase è stata individuata una tecnologia che permette di rilevare l'eventuale presenza di dimetilcarbonato, il principale componente dell'elettrolita nelle batterie agli ioni di litio attualmente in commercio. Dopo l'analisi dello stato dell'arte dei sensori per la rilevazione dei gas, in particolare dei VOCs (Volatile Organic Compounds), abbiamo selezionato la fotoionizzazione come tecnica di rilevazione. Sono state condotte prove di laboratorio utilizzando un sensore commerciale basato sulla tecnologia individuata ed è stato proposto un layout di macchina in grado di rilevare l'eventuale presenza di perdite grossolane di elettrolita.
Nella terza fase, è stato proposto un nuovo approccio per il monitoraggio dello stato di salute delle batterie litio-ione: è stato quindi pensato un nuovo concetto di *smart-sensor* integrabile nella cella elettrochimica che si basa sulla misura colorimetrica di una specie chimica in punti precisi della cella. Dopo la realizzazione del primo prototipo i primi test di laboratorio sono stati condotti utilizzando soluzioni colorate a base acquosa simulando la presenza di sali di ioni metallici di transizione. Quindi le celle elettrochimiche di test hanno mostrato come ci sia correlazione tra variazione di colore ed innesco di fenomeni indesiderati che degradano la prestazione della batteria. Gli incoraggianti risultati ottenuti lasciano ampi margini di miglioramento sia dal punto di vista del principio del sensore sia per quanto riguarda la miniaturizzazione del dispositivo prototipato e del sistema di interfaccia tra il sensore ed il mondo esterno alla batteria, favorendone la possibilità di integrazione nelle batterie future.

Contents

List of Figures

List of Tables

Introduction

Electromobility is undoubtedly the background to this thesis work. Electric mobility is one of the phenomena that is redesigning the economic and social order in recent decades and of one thing we can be sure: the evolution towards electric mobility will be a revolution. Imagining the mobility needs of tomorrow means taking into account multiple factors concerning energy, environment, socio-economic, political and technological aspects, in a context of social transformation that goes far beyond the automotive industry. We are facing with a "new industrial revolution" on a global level that poses new challenges very quickly. In an articulated context like the one we are going through, technological change is a key-feature, but other factors are also playing an important role. The aim of this thesis work is precisely to contribute to the technological advancement of some technical aspects of e-mobility.

E-Mobility

Before tackling the technological aspect, it is useful to make an overview of the context in which we will move. It is now common opinion that the desired goal of this transition is a sustainable and ecological society and for this reason there are three flywheels that are moving: the ecological, economic and political ones. From an ecological point of view, there are numerous studies that highlight the environmental impact of fuel transportation. The transport sector accounts for approximately a quarter of global greenhouse gas (GHG) emissions and is one of the major sectors where emissions are still rising[35]. Within the transport sector, road transport is by far the biggest emitter, accounting for more than half of all transport-related GHG emissions. At the local scale, transport activities cause urban air pollution, noise, congestion, water and soil degradation, asthma, obesity, road deaths and social and urban fragmentation [36]. At the international/national scale, mobility contributes to greenhouse gas emissions, trans-boundary air pollution, and the depletion of oil resources. Global greenhouse gas emissions from transport doubled over the 1970-2010 period to 7.0 $GtCO_2$-eq, increasing at a faster rate than any other end-use sector [37].
Unfortunately, the concentration of CO_2 and gases in the atmosphere in the modern era is constantly growing: the continuous fluctuations of the last 800,000 years (Figure 1), coinciding with the onset of ice ages (low CO_2) and interglacials (high CO_2) [1] and due to changes in the orbit of the earth around the sun (Milankovitch cycles), are turning into a growing trend in recent centuries and in particular in recent decades.

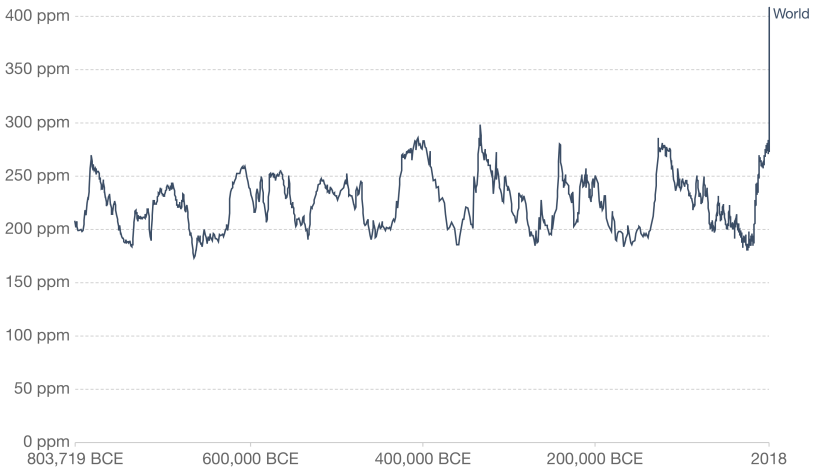

Figure 1: Atmospheric CO_2 concentration: global average long-term atmospheric concentration of carbon dioxide (CO_2), measured in parts per million (ppm). Long-term trends in CO_2 concentrations can be measured at high-resolution using preserved air samples from ice cores. Reprinted with permission from [1]. Available online at https://www.esrl.noaa.gov/gmd/ccgg/trends/data.html.

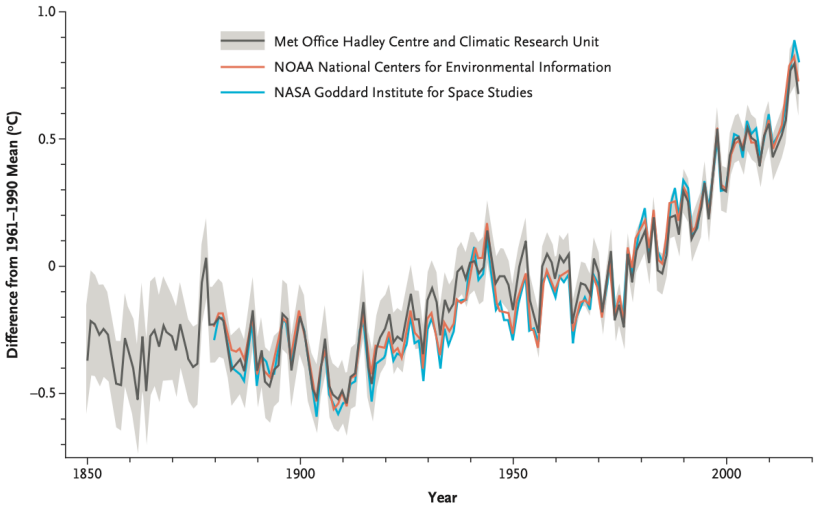

Figure 2: Annual global mean temperature anomalies relative to the means during 1961-1990 from the HadCRUT4 data set (produced by the Met Office Hadley Centre and University of East Anglia Climatic Research Unit, in gray shaded, the confidence intervals). Plots of the mean anomalies from two order data sets (from NASA and NOAA) show similar patterns. Adapted from the Met Office Hadley Centre (www.metoffice.gov.uk/research/monitoring/climate/surface-temperature). Reprinted with permission from [2].

What is frightening is not so much the fact that for the first time we go beyond the average of the last 800,000 years (300 ppm), up to 400 ppm in recent decades, but the speed of this increase: we have gone from thousands of years to a few decades to assess the fluctuations in CO_2 concentration. Moreover, the link between CO_2 concentration and the increase of the Earth's temperature [38] is not "in phase": given the delay between the increase of concentration in the atmosphere and the increase of the Earth's temperature (Figure 2), it is expected that even if the CO_2 concentration will stabilize now, the temperature increase will continue for the next decades [39]. In this context, ecosystems and species have no more or no time to adapt.

The effects of climate change on health (Figures 3) are very important, including: direct effects such as prolonged exposure to high environmental temperatures[40]; effects mediated by natural systems (the transmission of diseases by vectors or the influence of the concentration of carbon dioxide on cereal crops) or by social systems such as increased poverty [2]. Between 2030 and 2050 the WHO (World Health Organization) estimated 250.000 deaths in the elderly due to temperature rise, increased disease and disastrous climatic events [41].

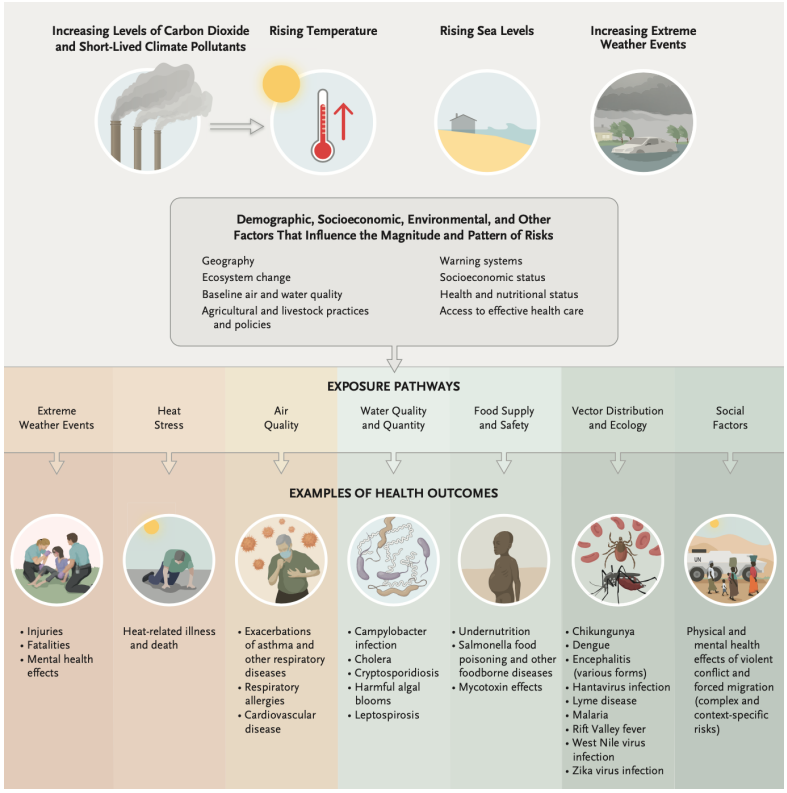

Figure 3: Major Health Risks Associated with Climate Change: examples of potential health outcomes and exposure pathways linking climate change with human health are shown, together with factors that can influence the magnitude and pattern of risks. Reprinted with permission from [2].

In order to slow down climate change, it is now clear that in the short term it

is necessary to strongly reduce greenhouse gas emissions and zero them in the long term: it would be necessary to limit global warming to less than $2°C$ above pre-industrial values [42], trying to avoid the unfavorable projections associated with temperature extremes and occupational heat stress, air quality, undernutrition, and vector-borne diseases.The e-mobility represents one of the answers to the above cited needs: but, as mentioned, the scenario is not yet complete. It is therefore necessary to take into consideration another fundamental aspect related to the climate issue, namely the political one.

From the political point of view there are two interesting aspects to consider: what has been done by states to face climate change; moreover, what other reasons can lead countries to favour development policies based on electric mobility. An historical excursus of the main stages that have led to the political evolution of the states towards an environmental regulation in automotive industry is shown in Figure 4: a

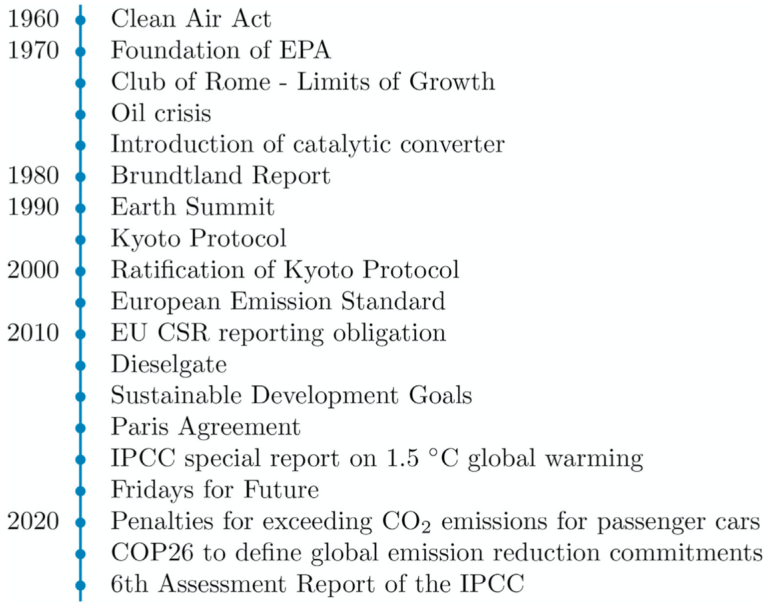

Figure 4: Important events that have been (or are expected to be) drivers for the development of sustainability.EPA=Environmental Protection Agency; CSR=Corporate Social Responsibility; IPCC=Intergovernmental Panel on Climate Change; COP26=26th United Nations Climate Change Conference. Reprinted with permission from [3].

Beginning with the Clean Air Act, introduced in the United States by the Environmental Protection Agency (EPA) in 1963 and amended several times, which is the basic regulation of air quality [43], deforestation in Europe and the appearance of smog in large cities in the United States of America due to high NO_X concentrations led the European Union (EU) and the United States Environmental Protection Agency (EPA) to ban leaded fuels and forced OEMs (Original Equipment Manufacturers) to use catalysts [44]. Subsequently the United Nations Framework Convention on Climate Change of 1992 [45] and the Kyoto Protocol [46], pushed the European Union (EU) to the introduction

of CO_2 for passenger cars [47]. In addition the European Measures of 2014 [48], the adoption of Paris Agreement [49] and the IPCC Special Report on 1.5°C Global Warming [50] led to thinking on the one hand about a long-term strategy[51] and to increase the legal emission limits for passenger cars [52]. The "Dieselgate" scandal of 2015-2016 that revealed the real non-compliance of vehicles that were on the market has undoubtedly accelerated the change of test procedure for emission measurements: we have moved from the NEDC protocol (New European Driving Cycle) to the WLTP protocol (Worldwide Harmonized Light Vehicle Test Procedure [53] to have a measured data closer to real data of the vehicle on the road [54]. The need to adopt policies that lead towards eco-sustainability and the protection of the environment and climate is evident. It is even more evident if you look at the Figure 5 in which the Climate Action Tracker, an independent scientific analysis that tracks and measure government climate action, correlates CO_2 emissions with the policies adopted by world governments.

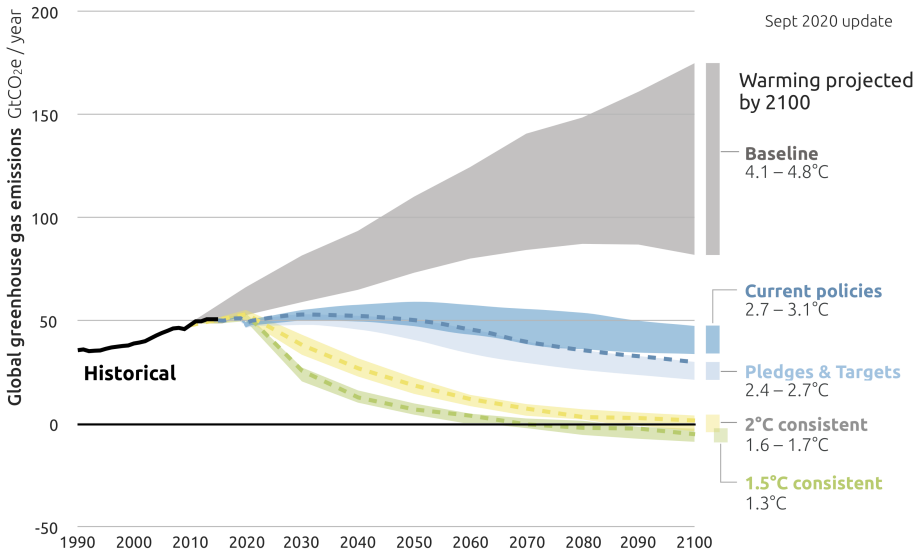

Figure 5: 2100 Warming Projection: emission and expected warming based on pledges and current policies (data source from Climate Action Tracker). Reprinted with permission from [4]. Available at https://climateactiontracker.org/global/temperatures/

.

In the absence of policies, global warming is expected to reach 4.1°C- 4.8°C above pre-industrial levels by the end of the century. The emissions that determine this warming are often called "Baseline" scenarios and are taken from IPCC AR5 Working Group III [55]. Current policies around the world are expected to reduce base emissions and lead to a warming of about 2.9°C above pre-industrial levels. However, from these data it is clear that in order to reach the ambitious target set by the Paris Accord, to limit the heating below 1.5°C-2°C compared to the baseline, urgent and rapid reductions would be necessary to return the estimated curve in the right direction [56].
At present, the trajectories of the policies and efforts made are well above the

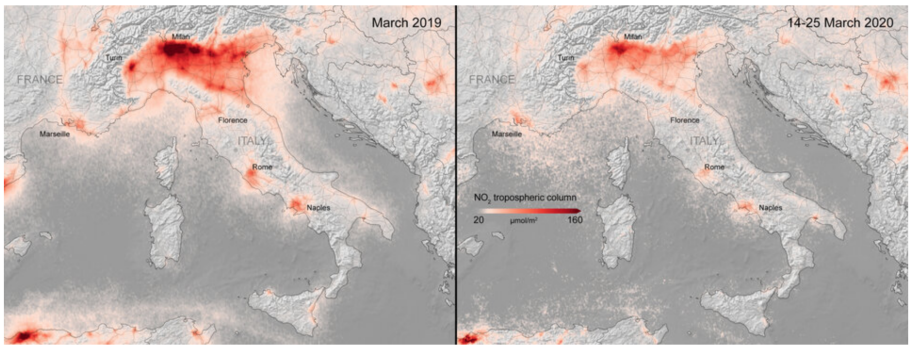

Figure 6: Nitrogen Dioxide concentration over Italy: comparison between 2019 March and the same period in 2020. Reprinted with permission from [5].

emission paths consistent with long-term international targets [4]. In 2020, the pandemic situation that involved the entire planet and the consequent blockage of economic activities also had a partially positive impact on the climate. The images of Italy provided by the satellite Copernicus Sentinel 5P speak for themselves (Figure 6). Despite the sharp decrease in climate-altering emissions, there was no immediate effect on global warming: the time period affected by the drop in emissions was too short to have an effect on the long-term trend[57]. However, we will have gained real experience that the adoption and implementation of climate policies can have tangible effects on air quality, health and global warming.

The political choices are fundamental in outlining the scenario of electromobility and in this the differences between geographical areas are already evident: if in Europe there is a strong push to consolidate and establish the EV (electric vehicle) market by taking advantage of this push to raise a market in crisis, the European automotive market, in the U.S. there is no strong national policy that "sponsors" the use of EVs; on the other hand, many are the American states that have independently set themselves targets to reduce emissions by pushing economically on EV. In Asia, there are countries like India with a concrete strategy for the transition to electric mobility, promising to stop selling fossil fuel vehicles by 2030. Japan has set 2050 as the year by which the domestic car market will be fully electric [58]. And case in point it is China, an economy in strong ascent to the global level that sees this transition as a huge opportunity. On the one hand it aims to solve its ecological problems, due to the enormous urbanization of industrialized areas, by launching a plan that prohibits the production and sale of fossil fuel only cars and a fleet of fully electric vehicles by 2050; on the other hand it has the opportunity to consolidate the automotive sector, accelerating with the production capacity of batteries and laying the foundations for a global expansion of Chinese car manufacturers [59]. Leading countries are therefore looking for a new structure and new opportunities from this transition; it is of interest that while historically the main driver for more sustainable technological solutions has been politics, recent developments in many areas show that we may have overtaken this policy-pull regime in favour of a business-push system, where companies reveal their intrinsic motivation to act to seize new opportunities from an economic point of view. In this context,

even in a more sustainable way: in fact, the current "electric car race" has already led to unprecedented investments in the automotive industry. [60]. The economic aspect therefore plays a fundamental role and will redesign the global car market structure in the decades to come.

Electric-driven Vehicle

Speaking of e-mobility, the electric vehicle must clearly be introduced. As a low-polluting, oil-independent transport solution, the electric vehicle has an extremely simple operating principle: an electric motor (instead of the internal combustion engine) powered by batteries (instead of the fuel tank) provides propulsion to the vehicle, with greater overall efficiency and excellent acceleration; when not in use, the vehicle can be "recharged" by attaching the batteries to a current source, possibly produced by renewable energy. Guaranteeing the autonomy of the vehicle, the batteries (Â§1.1) are managed by an auxiliary system, the Battery Management System (BMS), which monitors the battery pack of the vehicle during the charging and discharging phases. The parameters that are monitored are the single cell and the pack voltages, the pack incoming and outgoing current, the temperature of the pack. In addition to these parameters the BMS provides the State of Charge, SoC (or DoD, Depth of Discharge, the inverse concept of SoC) which in percentage provides the battery charge level (*SoC%=100-DoD%*). Finally, the SoH (State of Health), another parameter monitored by the BMS with various possible evaluation strategies evaluated by the designer of the BMS [61]. As mentioned, one of the strengths of the EV is undoubtedly the efficiency: the electric motor, generally mounted in direct drive, has an internal efficiency of around 90%; after all, the best internal combustion engine working with Diesel Cycle reaches 45% and no more. Considering that in the electric vehicle there is no need for clutch and gearbox, it is clear that the variable that determines the choice between EV and ICE is the capacity of the battery pack or the autonomy of the vehicle [62].
Historically, contrary to what one might think, the electric motor was the first solution adopted for the automotive industry and retracing the fundamental stages of technological development, it can be seen that at a certain point, the decision not to pursue its development was dictated by economic-political interests related to the promotion of oil development, neglecting the environmental effects in the long term. In an excerpt taken from "The history of the electric vehicle", the starting point of this technology is summarized [63]. *"Ferdinand Porsche, founder of the sports car company by the same name, developed an electric car called the P1 in 1898. Around the same time, he created the world's first hybrid electric car, a vehicle that is powered by electricity and a gas engine. Thomas Edison, one of the world's most prolific inventors, thought EVs were the superior technology and worked to build a better EV battery. Even Henry Ford, who was friends with Edison, partnered with Edison to explore options for a low cost electric car in 1914. Yet, it was Henry Ford's mass-produced Model T that dealt a blow to the electric car. Introduced in 1908, the Model T made gasoline-powered cars widely available and affordable. By 1912, the gasoline car cost only $650, while an electric roadster sold for $1,750. That same year, Charles Kettering introduced the electric starter, eliminating the need for the hand crank and giving rise to more gasoline-powered vehicle sales."*

Here are some fundamental dates of the beginnings of the electric vehicle:

- 1836: Birth of the electric motor car
- 1853: Invention of the internal combustion engine
- 1881: Electric car diffusion in France and Germany
- 1897: Whole fleet of cabs in New York electric cab fleet
- 1898-1909: Invention of Porsche car manufacturer and patent of hybrid-parallel propulsion and later hybrid-series propulsion

Therefore, at the end of 1800 the circulating car fleet consisted of steam, electric and gasoline cars. Subsequently:

- 1912: Electric car boom in USA
- 1920: Decline of the electric traction due on the one hand to the reduction of the price of the gasoline and the discovery of new oil fields in Texas; on the other hand, to the strong reduction of the cost of the gasoline engine due to the introduction of the assembly lines designed by Ford and the invention of the electric starter [64].

In the last 20 years it is observed that in advance of emissions policies, some car manufacturers have started to introduce some electrically driven models on the market. It should be emphasized that the first models with electric traction were immediately derived from homologous models with thermal engine: they were therefore technologically deficient projects, because the derivation from models born with different design philosophies, necessarily implied technical compromises, which reduced efficiency. [65]. Since 2015, automotive manufacturers have been showing an impetus to offer various models of electric vehicles. Recent studies show a growing market potential for EV vehicles, not only passenger cars but also buses and other passenger transport vehicles, light commercial vehicles (LCVs) for goods transport, and heavy vehicles for construction and construction sites. In addition, electrification will also invest in air transport (electric aircraft) and maritime transport (electric vessels) [66]. Vehicle cost, way of using the vehicle, battery weight and autonomy, type of battery pack charging and related infrastructure are some of the main factors that will influence the growth and diffusion of electric vehicles.

Before taking a look at the EV market it is necessary to briefly list the main types of electric vehicles available (Figure 7).

There are 3 main categories of electric vehicles, classified according to how much electricity is used as primary energy for propulsion:

- All-electric vehicles (AEV): a vehicle using electric power as only sources to move the vehicle. Currently, AEV have six types of power transfer configurations, but only three types are famous for use by an auto-maker. The vehicle configuration for BEV or FCEV is similar [6]. Battery Elelctric Vehicles (BEV): more frequently called EVs, they are vehicles without petrol engine, fully electric and with winged rechargeable batteries: these power the vehicle's electric motor and all the auxiliary electronics on

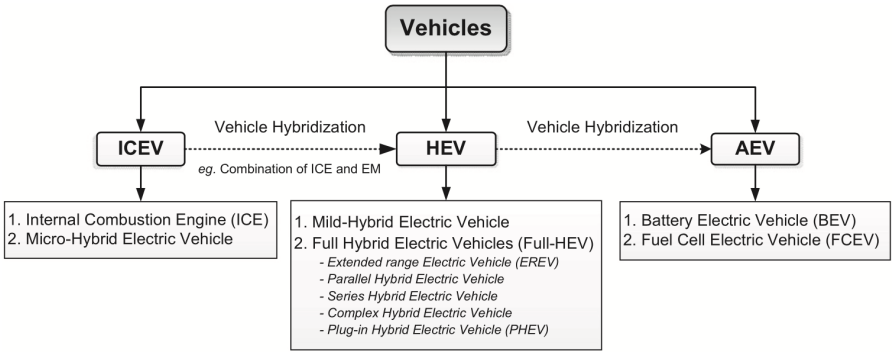

Figure 7: Classification of the vehicle. Reprinted with permission from [6].

board. BEVs are recharged with electricity from an external source. There are 3 types of recharging, based on the speed at which the batteries are recharged: level 1, the most common one currently uses a standard domestic socket (120 V) to connect to the electric vehicle and requires more than 8 hours to recharge the average battery pack of an EV. Level 2 recharging requires a specialized station that provides 240 V power with half the charging time compared to Level 1. Finally, level 3 recharging, or fast DC recharging, can be done in dedicated EV charging stations with extremely short times. Fuel Cell Electric Vehicle (FCEV): the fuel cell (it is not a rechargeable battery) in the vehicle is fed by hydrogen stored in a special tank. The advantage of this system is that it has zero emissions, since the only waste product is water vapor. However, pollution is not completely eliminated because of the way the hydrogen is produced [67].

- Hybrid Electric Vehicle (HEV): these are vehicles in which the energy for propulsion comes from two sources, one of which is abattery. Unlike a pure electric vehicle, a hybrid electric vehicle does not require an external battery charging system, so it can be independent of the charging infrastructure: in fact, the electric energy that recharges the battery comes from "regenerative braking", i.e. in which the electric motor contributes to the braking of the vehicle by recovering that part of the energy that is normally dissipated in brake heat or by the ICE like the recharge of SLI lead acid batteries occurs. Depending on the levels of "hybridization" (power of the electric engine compared to the total installed power), can be distinguished: Micro-hybrid, i.e. with start/stop system and regenerative braking, power supply at 12-48 V and the power of the electric motors installed on board the vehicle, which generally does not exceed 10 kW; Mild-Hybrid, can also operate with electric power supply during the start and departure of the vehicle and accommodate batteries with a higher voltage from 100-200 V and a power of the electric motors of about 20 kW; finally, Full-Hybrid, in which the vehicle is driven by the electric motor, the thermal motor or both depending on the driving speed. Usually batteries are used with a voltage between 200-300 V and an electric motor power of over 50 kW. [68]. Speech apart it could be done for Plug-in Hybrid electric Vehicle (PHEV): vehicles in which the traction

is entrusted to the electric motor until the energy of the battery pack is exhausted, or to the internal combustion engine. The batteries can be recharged by connecting to an external source, as well as recovering energy from the vehicle's braking. The battery pack installed is larger than HEV vehicles. The three PHEV configurations, PHEV series, PHEV parallel, PHEV series/ parallel are shown in Figure 8.

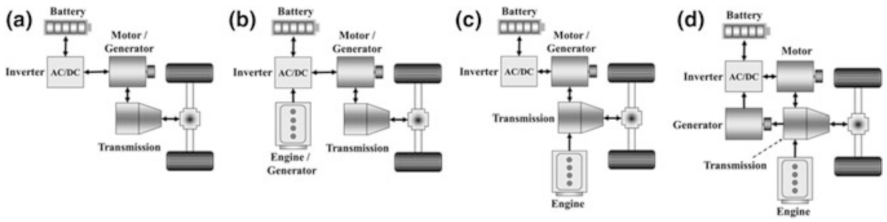

Figure 8: Electrified vehicle type powertrain (a) EV, (b) *Series* PHEV, (c) *Parallel* PHEV, (d) *Series/ Parallel* PHEV. Reprinted with permission from [7].

Therefore, new technologies available and new challenges to the design of structures with new requirements; above all, new opportunities for creativity: a new vehicle concept (Figure 9) [8].

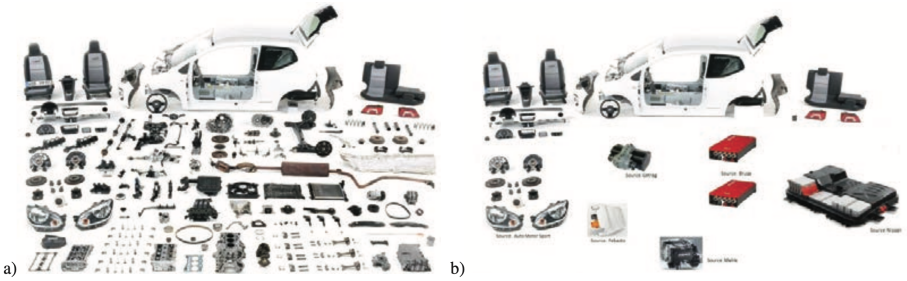

Figure 9: Example of a) dismantled conventional vehicle compared to the b) analogous electric one. Reprinted with permission from [8].

From numerous studies it is clear that in addition to technological changes other factors will shape the growth of the EV market, such as: economic reasons (countries are competing to build the next high value-added industry clusters; car manufacturers and large fleet operators are increasingly taking GHG emission reduction targets seriously), ecological reasons (urbanization continues its steady march around the world, leading to growing concerns about congestion and urban air quality, and changing consumer preferences) and policies (policy makers are pushing the automotive market towards low-carbon options and greater fuel efficiency) will drive its growth. According to Bloomberg, in its annual report EVO2020 (Electric Vehicle Outlook 2020) [10], which photographs the current state of the EV market and provides a forecast of how the EV market will evolve, more than 7 million road passenger vehicles are electric so far and electrification is spreading to other road transport segments. (Figure 10): over

500,000 electric buses, nearly 400,000 electric vans and trucks and 184 million electric mopeds, scooters and motorcycles on the road globally (Figure 11).

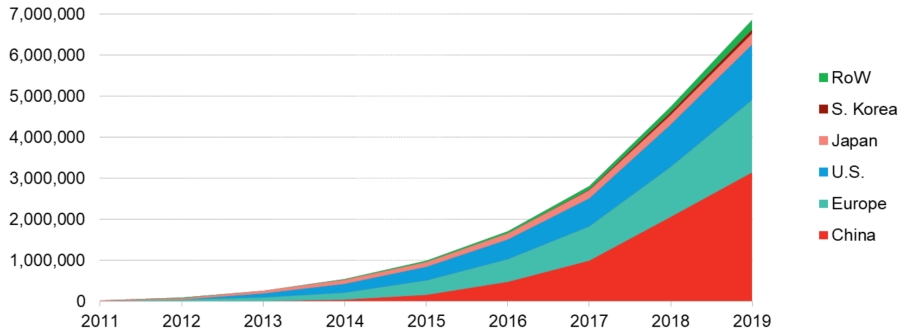

Figure 10: Cumulative BEV and PHEV sales by market. Reprinted with permission from [9].

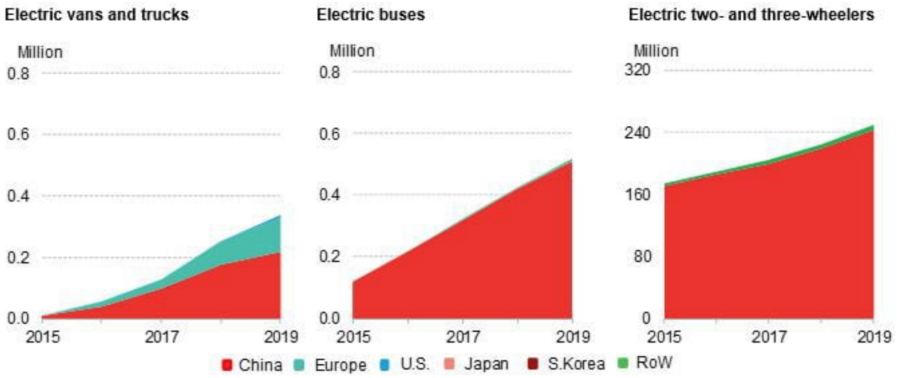

Figure 11: Current fleet of electric buses, vans, trucks and electric two-and three weelers. Reprinted with permission from [10].

Compared to the 2019 sales forecast [11] (Figure 12), the current global pandemic is bound to leave its mark (Figure 13): global sales are expected to fall by 23%, an event recorded for the first time in the modern era.
The market recovery estimated for 2021 is not expected until 2025 at the earliest. Commercial vehicle sales will also decline, but will recover by 2022 due to increased e-commerce and growing demand for freight in China and emerging economies. The growth of the PHEV market is confirmed and a market share related to fuell cells (FCEV) will appear.
In the long term, the EV market will remain good (Figure 14): in 2025 electric vehicles will reach 10% of global passenger vehicle sales, growing to 28% in 2030 and 58% in 2040.
It is expected the price parity between EVs and ICEs around 2025, with significant variations dependent on vehicle type and geographical area. In addition by 2035 (Figure 15) the global share of EV vehicles is expected to be equal to the global share of ICE vehicles sold.
It is appropriate to mention the study of Deloitte Insight [12] which, in addition

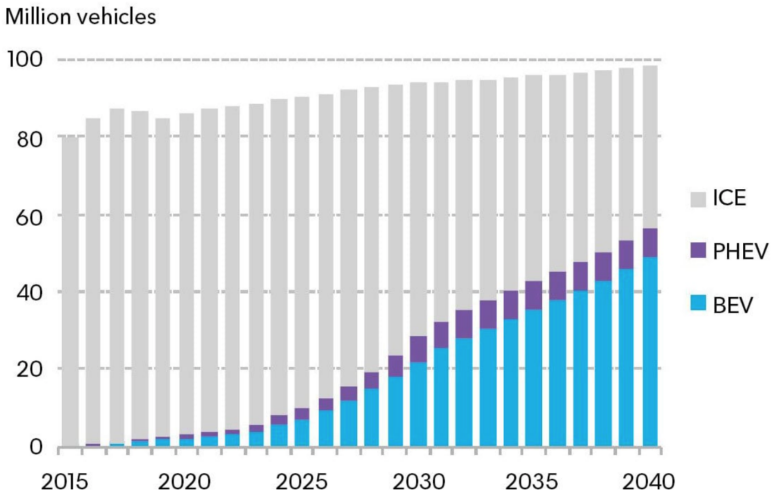

Figure 12: Global long-term passenger vehicle sales by drivetrain. Reprinted with permission from [11].

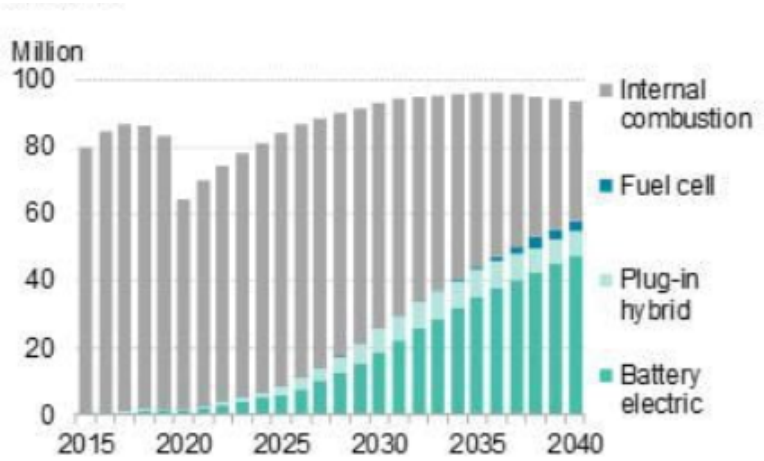

Figure 13: Global annual passenger vehicle sales by drivetrain. Reprinted with permission from [10].

to confirming Bloomberg's forecasts, specifies that the growth of the EV market in the coming years will be dictated by the corporate strategies of car manufacturers that promise to increase the supply of car models; no less, it will depend on "consumer sentiment" (Figure 16) i.e. how they welcome the adoption of an electric vehicle.

As it is easy to think among the key factors for the growth and affirmation of the EV market, in addition to policies (e.g. government incentives for the purchase of electric vehicles) adopted and public investment (e.g. the construction of charging infrastructure (Figures 17) and private (economic efforts by car manufacturers to expand the offer of EV models (Figures 18) there is battery technology.

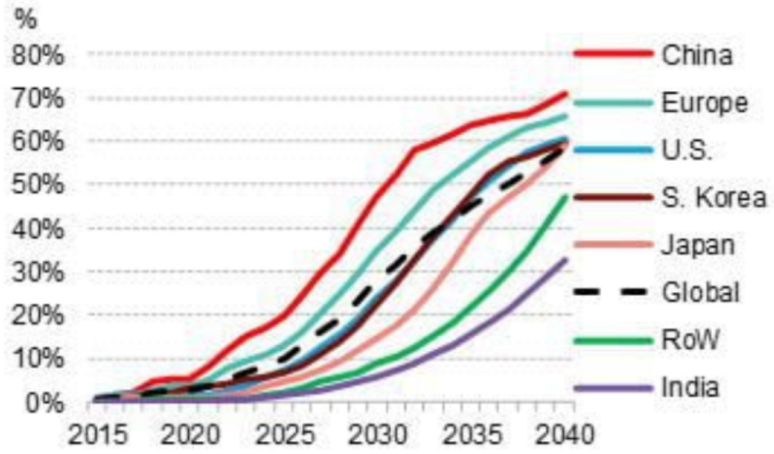

Figure 14: Global long-term EV share of new passenger vehicle sales by region. Reprinted with permission from [10].

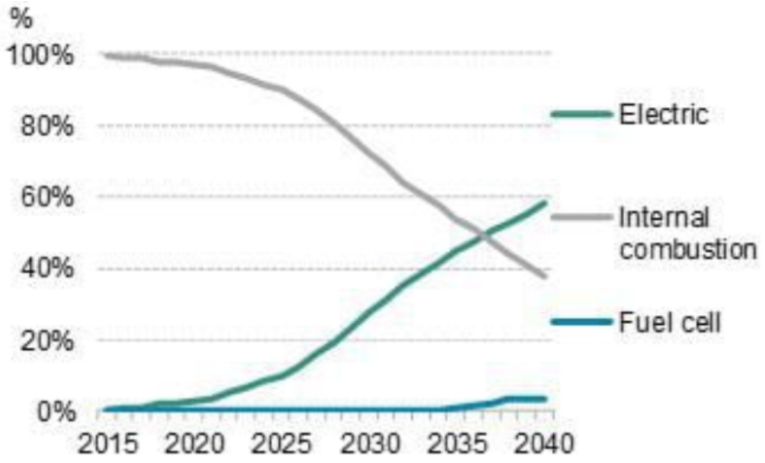

Figure 15: Global share of total annual passenger vehicle sales by region. Reprinted with permission from [10].

The importance of batteries in the growth of the electric vehicle market is linked to their ability to store energy and make it available during vehicle use. The commitment of the global scientific community to the improvement and evolution of this technology is tangible: in Europe in particular (§1.4) there are several medium to long term initiatives aimed at consolidating know-how and production lines in the old continent. The technological evolution of energy storage systems (§1.1) and the different battery configurations available (§1.2.1) show that especially in the last decades enormous steps have been taken with regard to performance, reliability and safety of these systems. Thanks to their technological maturity, lithium-ion batteries (§1.2.3) play a central role in electric vehicles: the core of this work is to enhance the study and monitoring

2020 Global Auto Consumer Study	FRANCE		GERMANY		ITALY		UK		CHINA		US	
In your opinion, what is the greatest concern regarding all battery-powered electric vehicles?	2018	2020	2018	2020	2018	2020	2018	2020	2018	2020	2018	2020
Driving range	31%	28%	35%	33%	4%	27%	26%	22%	25%	22%	24%	25%
Cost/price premium	32%	22%	22%	15%	19%	13%	24%	16%	9%	12%	26%	18%
Time required to charge	11%	15%	11%	14%	18%	16%	13%	16%	12%	15%	10%	14%
Lack of electric vehicle charging infrastructure	16%	22%	20%	25%	44%	32%	22%	33%	18%	20%	22%	29%
Safety concerns with battery technology	4%	11%	5%	10%	7%	10%	6%	12%	22%	31%	8%	13%
Others	6%	2%	7%	3%	8%	2%	9%	1%	14%	0%	10%	1%
Total	100%	100%	100%	100%	100%	100%	100%	100%	100%	100%	100%	100%
Sample size	1,083	1,266	1,287	3,002	1,048	1,274	965	1,264	1,606	3,019	1,513	3,006

Figure 16: Deloitte global auto consumer study. Reprinted with permission from [12].

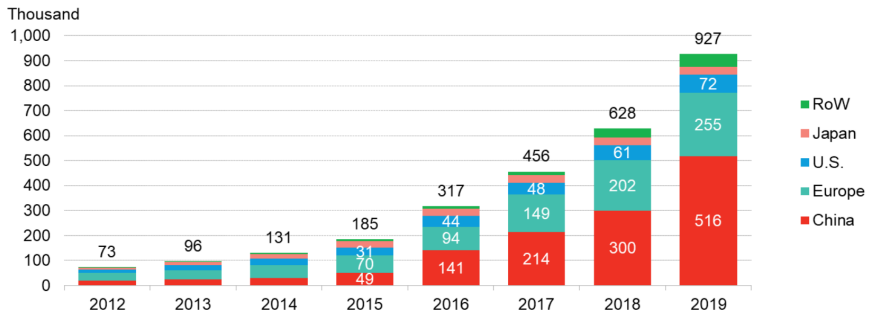

Figure 17: Cumulative public charging connectors: the public charging infrastructure stock rose by 47% in 2019. Reprinted with permission from [9].

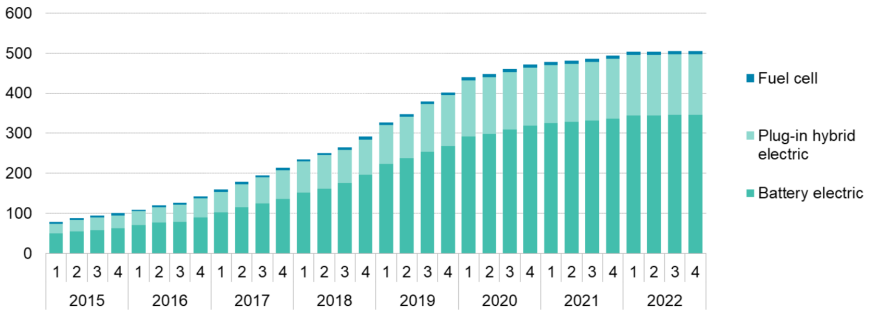

Figure 18: Current and upcoming passenger EV/FCV models. Reprinted with permission from [9].

reliability of these energy storage systems. Therefore, there are two paths that simultaneously pursue the goal, on the one hand by improving the performance of laboratory systems that measure the expansion of electrode materials during the charge and discharge cycles of the electrochemical cell; on the other hand, by first proposing a system for the industrial monitoring of leaks on the battery packs of the vehicle and then, a sensor that goes to monitor the health of the electrochemical cell closely. From the point of view of materials testing then, after a brief analysis of the state of the art (§2.3.1), a new test bench has been proposed to measure the expansion of electrochemical materials during the electrochemical cell cycling, with features that improve its reliability and give the experimenter the opportunity to test the materials in conditions closer to real conditions (§4.1). The single battery, Lithium ion for example, is the basic element of an articulated system that stores energy and provides a certain autonomy to the electric vehicle, the battery pack. In the automotive industry, during the various assembly operations of the battery pack, i.e. from the closing of the single cell to the closing of the complete pack, it is crucial to verify the tightness (§2.3.2) of all the cells that compose it and of the whole assembled pack. This verification must be done in a time consistent with the cycle times of the automotive production lines, so often it is necessary to give up the classic laboratory systems to detect gas leaks, also depending on the typologists of the leak test you need to find the right sensor to apply. After an overview of the types of industrial sensors (§2.3.3) and the techniques for monitoring the health of batteries (§2.1.1) the two contributions of this work are presented. First, we describe the application of a PID sensor for the detection of leaks in batteries and battery pack. Then, we present a new idea of a sensor for monitoring each individual cell that makes up the battery pack of an electric vehicle (§4.2). For all the proposed contributions, the results of laboratory tests are also presented, offering ideas for future developments: laboratory tests on electrochemical dilatometer show not only that the proposed instrument is able to measure the expansion and contraction of electrode materials in charge and discharge cycles, but also show how the presence of the proposed new features such as the regulation of the force acting on the sample under test are actually of interest to collect useful information to predict the real behavior in the electrochemical cell. The tests with the PID sensor, show how it is able to detect the presence of dimethyl carbonate leaks and then highlight how with a proper design of the test system, you can conduct leak tests in line at a lower cost, compared to the costs to be incurred for the purchase of a mass spectrometer, for example. The results of the preliminary tests on the new sensor for the monitoring of the single electrochemical cell during its entire life cycle, validate the new proposed idea of using color as a significant signal of a possible internal cell malfunction and leave open new development scenarios for this sensor.

1. Batteries

Non mi preoccupo mai del futuro,
arriva sempre abbastanza presto.
Albert Einstein

1.1. Overview

The adoption of the electric vehicle intended as a vehicle for passenger transport inevitably passes from the capacity of the battery pack to accumulate enough energy to be able to give a certain autonomy to the vehicle, comparable or even greater than that of the vehicle with internal combustion engine. Batteries are therefore a key element to exploit this type of mobility and in the panorama described in the introduction chapter considerable efforts are made to increase the technological knowledge and quantity/quality of these devices. In order to analyze battery technology it is necessary to briefly introduce the most generic energy storage systems. An energy storage system consists of a set of devices and equipment that, coordinated according to a management-control logic, absorbs and releases electrical energy. Electrical Energy Storage (EES) refers then to a process of converting electrical energy from a power network into a form that can be stored for converting back to electrical energy when needed [69]. Storage technologies for electricity then be classified by the form of storage [70]:

- Electrical energy storage: (i) Electrostatic energy storage including capacitors and supercapacitors; (ii) Magnetic/current energy storage including SMES.
- Mechanical energy storage: (i) Kinetic energy storage (flywheels); (ii) Potential energy storage (PHS and CAES).
- Chemical energy storage: (i) Electrochemical energy storage (conventional batteries such as lead-acid, nickel metal hydride, lithium ion and flow-cell batteries such as zinc bromine and vanadium redox and unconventional one such as metal-air betteries); (ii) thermochemical energy storage (solar hydrogen, solar metal, solar ammonia and solar methane dissociation-recombination).
- Thermal energy storage: (i) Low temperature energy storage (Aquiferous cold energy storage, cryogenic energy storage); (ii) High temperature

energy storage (sensible heat systems such as steam or hot water accumulators, graphite, hot rocks and concrete, latent heat systems such as phase change materials).

EES is characterized by energy and power density, energy efficiency in charge and discharge, self-discharge, charging and discharging times, behavior in different conditions of state of charge, life time (Table 1.1). In addition, depending on the application, the type and consequently the materials used, the costs to be incurred, the time of realization and eventual disposal / recycling is chosen appropriately .

Storage System	**Power** (MW)	**Efficiency** (%)	**Life Time Time** (y)	**Total Capital Cost** (USD/kW)
CAES	15-400	54/76/88	35	600-750
PHS	250-1k	87	30	2700-3300
Li-ion	5	90 (CC)	15	4000-5000
Lead Acid	3-20	75-80(CC) 70-75(CA)	4-8	1700-2500
NaS	35	80-85(CC)	15	1850-2150
VRB Flow Cell	4	75-80(CC) 63-68(CA)	10	7000-8200
ZnBr Flow Cell	0.04/0.1-2	75-80(CC) 60-70(CA)	20	5100-5600
High Power Flywheels	0,75-1,6	93	20	3700-4300
ZEBRA	< 10	80-85(CC)	1500 (cyc.)	1500-2000
Fe/Cr flow Battery	< 10	50-65	20	200-2500
Zn/Air	0.02-10	40-60	hundreds cyc.	3000-5000
SMES	1-3	90	$> 30{,}000$	380-490
Supercapacitors	10	90	500K cyc.	1500-2500

Table 1.1: Different storage systems for power grid applications comparison (Source: IEA, International Energy Agency).

Below, a brief description of the mentioned energy storage technologies [71].

Pumping Hydroelectric plant (PHS): technology suitable for daily, seasonal and grid support storage, in each plant there are two basins located at different altitudes: the water transferred from one basin to another allows the storage or release of energy. In the discharge mode, the water is conveyed from the upper basin to the turbines, generating electricity. In charging mode, the same turbines pump water upwards. For the application of this technology, morphologically suitable locations are required; moreover, the energy storage capacity of these plants can vary from 100 MW (small-scale plants) to 3,000 MW.

FlyWeels: suitable for short-term storage of a high amount of energy and are ideal for network services that require very fast response times, the flywheels have an electric motor that turns a rotor up to 100000 rpm. This technology is not suitable for medium-long term storage due to the rapid performance degradation (-15% of the stored energy after about 1 hour).

Compressed-air energy storage (CAES): used sometimes open seasonal storage both as a support to the electricity grid, these plants use underground caves

for the storage of compressed air. In charging mode, the air is compressed and can be stored underground at high pressure for several months. Once released, the air expands into a turbine to regenerate electricity.

Liquid Air (LAES): liquid air energy storage is an economical form of storage, as plants are built using standard industrial components. There are only a few plants on a normal scale. Air is cooled until it liquefies, after which it is stored in an insulated tank. To reverse the process and generate electricity, the air is expanded so that it drives a turbine. Its low efficiency, less than 50 %, compared to 75 / 90 % of batteries, limits its use.

Thermal Storage: electric water heaters for domestic use can be used as a storage device: the heat can be stored in an insulated water tank, offering homes the possibility to store energy for a few hours. Cold storage is also possible, through the use of chilled water or ice. Alternatively, for solid-state heat storage, radiators filled with bricks heated with cheap electricity are used. The heat is then released as required. Storage in wells uses heat pumps connected to a borehole for underground heat storage for a seasonal or large scale duration.

Molten Salt Storage: In this form of thermal storage, electricity or solar energy is used to heat a container filled with molten salt. This storage medium reaches a temperature hot enough to generate steam; at this point, steam turbines can be used to generate electricity from the stored heat. Combined with concentrated solar energy, this system allows daily storage of electricity from photovoltaic solar energy. The molten salt storage currently accounts for 75 % of the world's thermal storage capacity.

The electricity storage systems until used in a vehicle are briefly described below.

Supercapacitors: a form of short-term energy storage that absorbs and releases large amounts of electricity very quickly. A supercapacitor consists of two layers of conductive material separated by an insulating layer. The electricity is accumulated by generating an electrical charge between the two conductive layers.They require minimal maintenance and are installed to provide network services as well as components of braking and acceleration devices. They are characterized by extremely long cycle-life; on the other hand, this technology shows much lower energy density than batteries.

Superconducting magnetic energy storage (SMES) is a technology through which it is possible to store energy in the magnetic field created by a direct current flowing in a superconducting coil when cryogenically cooled. Power can be available immediately and a high power output can be provided for a short period of time. Their high cost strongly limits any commercial application.

Batteries can store energy through electrochemical reactions. When the battery is charged, electrical energy is converted in chemical energy and when is discharged, the chemical energy is converted back into electrical energy. There is a wide range of technologies used in the fabrication of electrochemical accumulators and their main assets are their energy and power densities and technological maturity. Used both for portable devices and stationary use batteries have as a sore point their duration, i.e. the number of charge-discharge cycles they can withstand.

From an economic point of view the storage systems can allow to store energy produced at low cost (or purchased at low price) at the time not needed, and then deliver it to the need, avoiding to pay more at a later time for the purchase

or production. Moreover they are expressly designed to cope with the "intermittent" nature of many renewable energies (solar, wind, marine, etc..)..Peak load problems could be reduced, electrical stability could be improved, and power quality disturbances could be eliminated. Indeed, the energy storage plays a flexible and multifunctional role in the grid of electric power supply, by assuring more efficient management of available power [69].

It is important to note that the charge/ discharge time (Figures 1.1) is particularly significant because it determines the applicability of an energy source and a specific storage system.

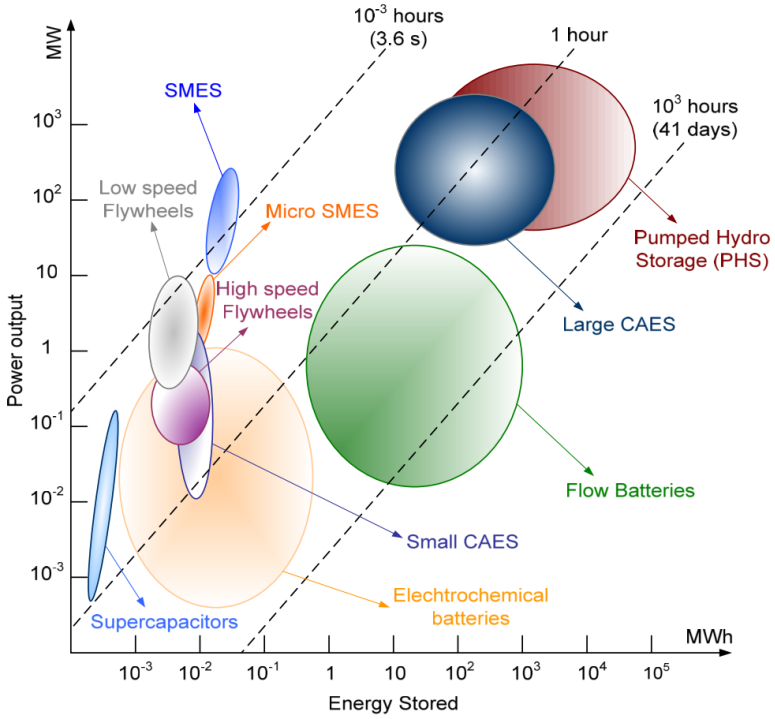

Figure 1.1: Discharge time vs. energy stored for various energy storage technologies. Reprinted with permission from [13].

1.2. Batteries

A battery, or electrochemical cell, is a device able to directly converting chemical energy into electrical energy. Together with super (or ultra) capacitors, they are considered the most suitable systems for storing electricity and powering modern systems. In fact from this point of view the technological advancement (Figure 1.2) is oriented towards obtaining small and equally light devices able to power everything that is "portable" and "transportable" [13].
It is possible to compare battery systems from the state of the three main components (Figure 1.3): the electrode A and the electrode B, i.e. the "chemistry", and the electrolite. The electrodes usually are solid phases, but they also can be liquid (catholyte and anolyte), as well as the electrolyte can be liquid, plastic,

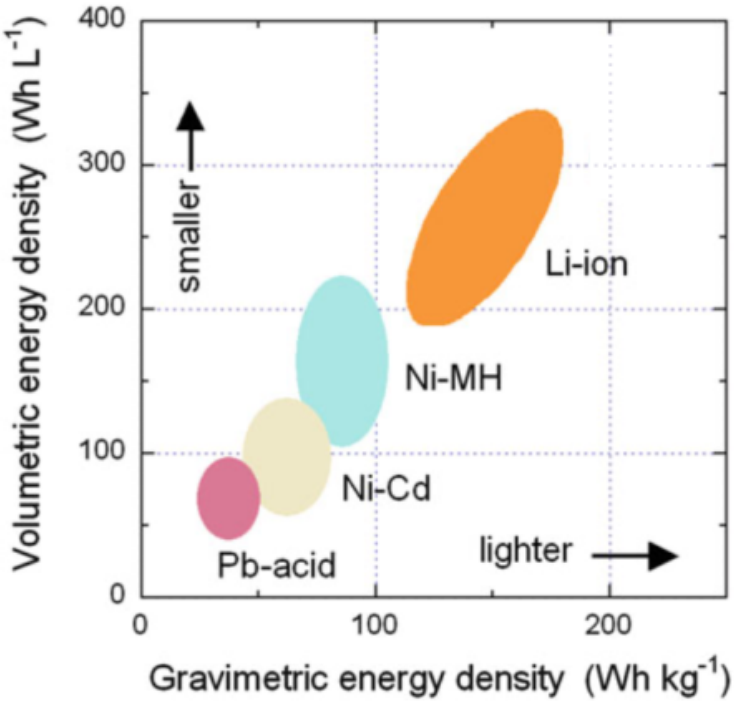

Figure 1.2: Various electrochemical systems in a plot of specific volumetric energy against gravimetric volumetric. Reprinted and modified with permission from [13].

or solid phase. This is crucial because certain interfaces are difficult to handle [14]. Not all possible combinations are realized, because although they may be interesting from the point of view of energy density, they may present difficulties with respect to their realization, cost or ease of application. Electrochemical cells are generally identified as "primary", i.e. not rechargeable, or "secondary", i.e. rechargeable. The most common ones are reported in Table 1.2.

	Aqueous Cell	**Nonaqueous Cell**
Primary Battery	Manganese Dry cell Alkaline Dry cell Magnesium cell	Metallic Lithium battery
Secondary Battery	Lead-acid battery Ni-Cd battery Ni-MH battery	Li-ion battery

Table 1.2: Classification of Batteries [13]

Through particular architectures inside the battery, the flow of electrons produced by the internal oxidation-reduction reactions (redox) from one material to another through an electric circuit, is conveyed and used to power electrical loads. In the case of a rechargeable system, the battery is recharged by a rever-

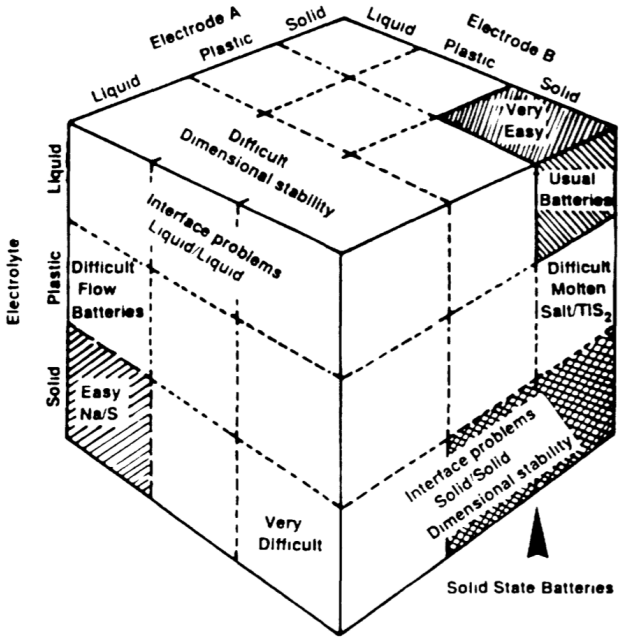

Figure 1.3: The three main components of electrochemical cells. Reprinted with permission from [14].

sal of the process [72]. In this conversion the efficiency is high and far superior to machines that convert thermal energy into mechanical energy through the Carnot cycle: ICE vehicles lose their energy through friction on a moving part and heat loss from total energy in fuel (Figure1.4).

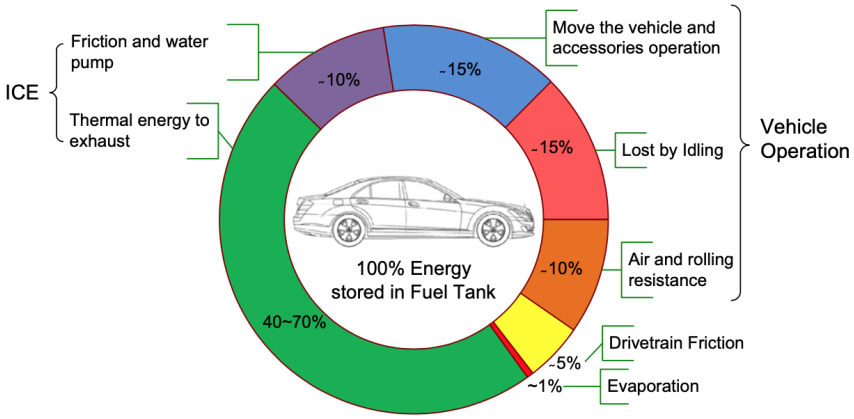

Figure 1.4: Typical energy flow of conventional internal combustion engine vehicle. Reprinted with permission from [6].

While the term "battery" is often used, the basic electrochemical unit being referred to is the "cell". A battery, consists of one or more of these cells,

connected in series or parallel, or both, depending on the desired output voltage and capacity.
The cell consists of three major components:

1. The anode (the reducing electrode) which gives up electrons to the external circuit and is oxidized during the spontaneous electrochemical reaction. It is selected with the following properties in mind: efficiency as a reducing agent, high coulombic output (Ah/ g), good conductivity, stability, ease of fabrication, and low cost. Practically, metals are mainly used as the anode material.

2. The cathode or positive electrode (the oxidizing electrode) which accepts electrons from the external circuit and is reduced during the spontaneous electrochemical reaction. It must have efficiency as oxidizing agent, be stable when in contact with the electrolyte, and have a useful working voltage. Most of the common cathode materials are transition metal oxides.

3. The electrolyte (the ionic conductor) which provides the medium for transfer of charge, as ions, inside the cell between the anode and cathode. The electrolyte is typically a liquid, such as water or other solvents, with dissolved salts, acids, or alkalis to impart ionic conductivity. Some batteries use solid electrolytes, which are ionic conductors at the operating temperature of the cell.

The two solid electrodes could be completely immersed in the electrolyte or, more often, are separated by a layer of electrically insulator material called separator so as to avoid internal short circuits. The separator is soaked with the electrolyte and in addition, to physically separating the electrode materials, is permeable to the ions so as to maintain ion conductivity and good ion balancing. The cell architecture can take different configurations and shapes: prismatic, cylindrical, button-shaped, flat among the most common. Once assembled the cell is sealed to prevent leakage and dryness. The type of active materials used and their quantity, determines the maximum theoretical energy that can be supplied by an electrochemical system: while the cell voltage is given by the nature of the active electronic materials; their amount determines the cell capacity (Ah). The presence of the electrolyte and other non-active but necessary materials, which increase the weight and volume of the cell, decreases the theoretical energy performance of the cell: in practice, the actual available energy of a real cell is 25-35% of the theoretical one [72].

1.2.1. Main battery technologies

In recent years, various electrochemical storage systems have been developed and applied for applications both in electric vehicles and for stationary systems in electrical networks. Below, a brief description and the range of specific power and specific energy for different battery technologies in Figure 1.5.

Lead acid battery: it is the most common and cheapest battery used by a conventional ICE vehicle; with a low specific energy, typically between 20 and 40 Wh/kg [73]. The application of this battery is more preferable when weight is least concern (a range of 200 km would necessitate about 150 kg of lithium-ion batteries but more than 500 kg of lead acid cells [74]).Moreover,it is not an

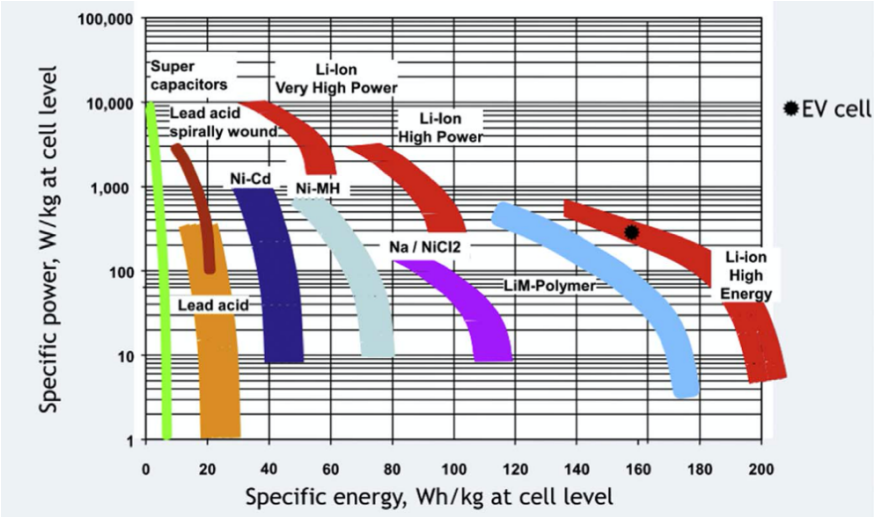

Figure 1.5: Specific energy and power of the main battery technologies. Reprinted with permission from [6].

environment-friendly battery and being a mature and well known technology, the feasibility for its improvement is low.

Nickel Metal Hydride battery (Ni-MH): recently used in hybrid vehicles and, it is considered a mature technology, that has reached its best potential, both in cost reduction and characteristics. Its energy density is between 60 and 80 Wh/kg [75] and it is considered as insufficient for the needs of BEVs. It is not suitable to use in high charge/discharge rate like automobile application but it performs well under rigorous working conditions.

Lithium batteries: there are different types of lithium batteries, which differ from each other due to the different electronic and electrolytic materials used. The common element is the charge carrier, i.e. the lithium ion, Li^+. They are generally divided into two main types:

- lithium metal batteries: having lithium metal to the anode, they can have solid or liquid electrolyte; they have advantages from the point of view of the high specific energy because lithium possesses both the highest electrochemical potential and a low equivalent mass but, being the lithium metal very reactive, they have had a difficult commercial diffusion related to safety aspects. The problem that is mostly found in this type of accumulators is the formation of dendrites, or protuberances, due to the inhomogeneity of the Li plating at the interphase lithium/electrolyte (SEI), which can cause an internal short circuit [76]. This family includes lithium metal polymer batteries: at present the only strategy pursued to avoid dendrite problems. However, the volume variation of all solid components of the cell would lead to the loss of contact at the interphase and its deactivation.

- lithium ion batteries (Li-ion): this is one of the promising energy storage devices due to its light weight, high specific energy, high specific power and high energy density [77]. It has high efficiency and a long lifespan

and its potential to improve is considered as very high [78]. In addition, lithium batteries have no memory effect and do not have poisonous metals, such as lead, mercury or cadmium [6]. The main disadvantage is that lithium ion batteries require high production cost. But as already highlighted, the trend towards decarbonisation and related policies have also had an impact on the battery market: in fact, as we see in Figure 1.6, volume-weighted lithium-ion battery pack prices have fallen 87% in the last ten years and forecasts give a price around 60 dollars around 2030, manufacturing capacity set to quadruple by 2025 (Figure1.7). This family includes lithium ion-polymer batteries [76]: they can have the electrolyte gelled in a polymeric matrix (for example PVDF) or consisting of a polymeric matrix, laminated in thicknesses of 30-50μm, and assembled at the same time as the electrodes or before cell forming.

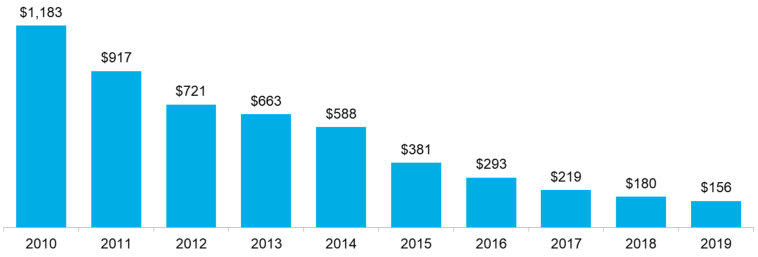

Figure 1.6: Lithium-ion battery pack price (real 2019 % (USD/kWh)). Reprinted with permission from [9].

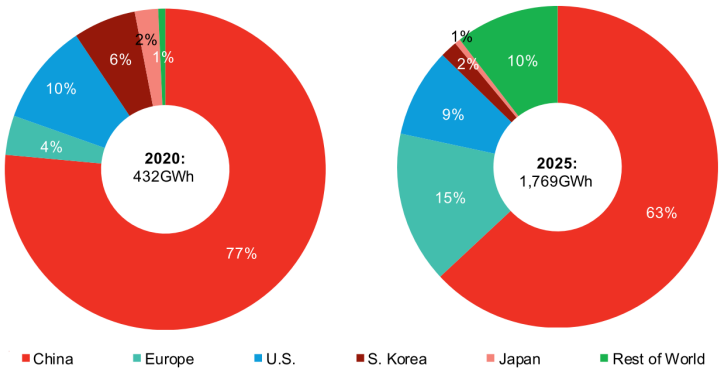

Figure 1.7: Lithium-cell manufacturing capacity forecast. Reprinted with permission from [9].

Currently on the market there are three different cell structures: cylindrical, prismatic and pouch (Figure 1.8)cells. The cylindrical cell remains one of the most widely used packaging architectures for primary and secondary batteries, given their ease of fabrication and good mechanical stability characterised by the fact that their tubular body can withstand high internal pressures without

deforming. Cylindrical cells, whose dimensions generally follow the commercial standard *18650*, have a volumetric energy density about 20% higher than their prismatic and pouch counterparts: this is because are wound with a higher tension. Introduced in the early 1990s, the prismatic cell satisfies the demand for thinner sizes. Prismatic cells make optimal use of space by using the layered approach. These cells are predominantly found in mobile phones, tablets and low-profile laptops ranging from 800mAh to 4,000mAh. No universal format exists and each manufacturer designs its own. The pouch cell makes more efficient use of space and achieves 90-95% packing efficiency, the highest among battery packs. Since its introduction in 1995, the pouch has improved several aspects and offered new opportunities in the battery world: the elimination of the metal casing reduces weight, but the cell needs support and space to expand into the battery compartment. Pouch packs are used in consumer, military and automotive applications. There are no standardised pouch cells; each manufacturer designs its own. Where the application has high requirements in terms of the volume occupied by the batteries, prismatic and pouch cells can be preferred in favor of cylindrical cells [15], although this is not always the case: *Tesla Motors*© is emblematic in this respect, having chosen cylindrical cells over pouch cells or prismatic cells (*BMW*©*i3*) from the outset, focusing on greater energy density and retaining the advantage of being able to support a greater number of recharges, thus extending their life.

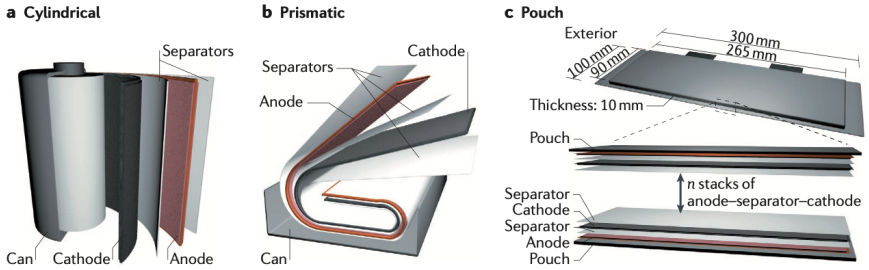

Figure 1.8: Three representative commercial cell structures: (a) Cylindrical-type cell. (b) Prismatic-type cell. (c) Pouch-type cell. Reprinted with permission from [15].

1.2.2. Battery Packs

Based on the requirements of cost, energy, power, weight and volume of the vehicles, the most suitable chemistry can be chosen for the cells that will power it. Lithium-ion technology is well suited to meet these requirements compared to older lead and nickel-metal hydride chemistry due to its higher specific energy. It is worthwhile to briefly well on the assembly of the cells in the battery pack, describing its main features.
The assembly of the cells forms the module; the assembly of the modules forms the battery pack (Figure 1.9). This seemingly simple sequence actually requires a good engineering, as several mechanical, electrical and thermal requirements must be met.

From the mechanical point of view, the battery packs, which are the result of module assembly and often contain electrical and thermal control hardware

Figure 1.9: Rechargeable lithium ion battery cell, cell frame, module and larger system. Reprinted with permission from [16].

and software, must be integrated into the existing structure of the vehicle, so as to be safe in normal use of the vehicle, i.e. with respect to vibrations and in the case of random accidents such as road accidents. Depending on the model of the vehicle there are different strategies for the positioning of the battery pack (Figure 1.10) [17] : typically a favorable area in this regard, taking advantage of the structural parts already present in the chassis, is between the semi-axles of the vehicle and inside the part of the chassis called "rocker panels"; after all, it is possible to choose other areas, but considering the need for structural reinforcements that add weight, volume and costs. The battery pack container is one of the most critical components in the design of electric propulsion: in fact, it must meet many requirements including being water and dust tight. In addition, depending on the chemistry of the batteries it contains must provide a safety valve that intervenes in case of strong overpressure inside the battery pack due to malfunctioning.
The sealing issue will be discussed in more detail in paragraph .

Equally precise are the electrical requirements, which allow the battery pack, through appropriate control electronics, to remain in normal operating conditions when it delivers the power needed to propel the vehicle. Through a series of contactors, the battery pack is self-connected to the vehicle as soon as it changes from off to running condition. In addition, the battery pack is equipped with manual service switches to exclude, for example, a module for any maintenance operations (Manual Service Manual Disconnections, DMSs). For added safety, battery packs often contain high-voltage interlock circuits (HVIL) which, in the event of a breakage, signal to the vehicle a possible loss of insulation. The voltages and currents of the pack/module/cell are measured and controlled by the battery pack management system (BMS): according to the strategies and algorithms implemented within it, which we will talk more specifically in the specific paragraph , the BMS imposes the limits of voltage/current and energy/power on the battery pack. It also communicates with other vehicle control systems the status of the battery pack contactors, HVIL, MSD, and provides temperature information. It also manages the charging interface and the internal charger in

OEM Model	BMW i3	VW E-Up	Nissan Leaf	Mitsubishi i-MiEV	Tesla Model S	Opel Ampera	Ford Mondeo
Position of battery in the car							
Type of drive	EV	EV	EV	EV	EV	EREV	HEV
Manufacturer	Samsung SDI	Samsung SDI	AESC	GS Yuasa	Panasonic/ Sanyo	LG Chem	Panasonic/ Sanyo
Cell shape	prismatic	prismatic	pouch	prismatic	cylindrical	pouch	prismatic
Capacity [kWh]	18,8	18,7	24	16	16,2- 17,7	16	7,6
Nominal voltage [V]	360	374	360	330	402	360	
Number of cells	96	204	192	88	7104	288	76
Number of modules x Cells	8 x 12	17 x 12	48 x 4	10 x 8 2 x 4	16 x 444	7 x 36 2 x 18	2 x 38
Module dimensions (l x w x h in [mm])	-	1726 x 1132 x 303	303 x 223 x 35	1. 350 x 194 x 116 2. 175 x 194 x 116	178 x 102 x 152	1. 230 x 220 x 25 2. 140 x 220 x 25	-
Module weigth [kg]	-	10,5	3,8	1. 15 2. 7,5	-	1. 19 2. 9	-
Arrangement of modules (top view)		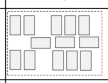				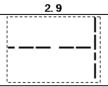	
Arrangement of modules (side view)			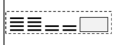				
Electric range [km]	190	160	175	160	400	40 - 80	34
Pack weigth [kg]	230	230	300	200	600	198	240

Figure 1.10: Examples of current (H)EVs and their batteries. (OEM: original equipment manufacturer, EREV: extended-range electric vehicle). Reprinted with permission from [17].

those vehicles where it is possible to charge the pack from outside. As far as the thermal requirements are concerned, each battery pack must have a thermal management system designed to keep the temperatures of the cells within a normal operating range and provide for uniform temperatures across the entire battery pack. Having a uniform temperature of all cells in the pack minimizes the risk of cell voltage variation due to internal resistance variation. Moreover, since self-discharge is highly temperature-dependent, it allows to have a uniform charge level on all cells. The ideal temperature range is generally determined according to the type of cells that make up the pack; in practice, the battery pack tends to work in a range between 10 $°C$ and 40 $°C$, in which the best compromise between available energy and delivered power is obtained. Regardless of the various levels of complexity, the cooling systems that serve the battery packs fall into three categories: passive air, active air or liquid cooling [79]. Passive air cooling, i.e. natural convection cooling, involves the entry of air from outside or from the passenger compartment to the battery pack. The simplicity and low cost, makes this system suitable to be used in the most common electric commercial vehicles. This system has the advantage that it does not need any openings or channels in the battery pack, so it does not affect the level of sealing of the pack itself. Sometimes, however, it is not able to dissipate all the heat necessary to bring the pack back into the desired temperature range: therefore, forced air cooling systems are adopted. Depending on the vehicle model, you can find systems that use the car's air conditioning system,or , systems that have an air conditioning system dedicated to the battery pack. Due to the additional weight, volume and cost of a dedicated air conditioning system and air ducts, the active air approach is much less common than the passive approach. Liquid cooling is undoubtedly the most effective from the point of view of heat dissipation from the battery pack: it uses a heat exchanger that through a cooling circuit in which a mixture of water and ethylene glycol flows (50 / 50 %), removes excess heat from the cells. Unfortunately, although it is advantageous also from the point of view of the occupied volume, it is more expensive, heavier and more complex than the air one; consequently it is used where there is the

actual need for a higher degree of thermal control. [7].

1.2.3. Li-ion batteries: the rocking-chair battery

Li-ion batteries, as one of the most advanced rechargeable batteries, have been attracting much attention in the past few decades. They are currently the dominant mobile power sources for portable electronic devices, exclusively used in cell phones and laptop computers. Li-ion batteries are considered the powerhouse for the personal digital electronic revolution starting from about two decades ago, roughly at the same time when Li-ion batteries were commercialized [19].

The history of lithium-based chemistry starts far back: after lithium discovery by Berzelius and Arfwedson in 1817 and its isolation by Brande and Davy in 1821, research on lithium-based batteries materialized in 1912 when G.N. Lewis began to explore its electrochemical properties: it soon emerged that, given its excellent physical properties such as its low density (0.534 gcm^{-3}), high specific capacity (3860 $mAhg^{-1}$), and low redox potential (-3.04 $Vvs.SHE$), lithium could be an excellent candidate for the electrochemical cell anode [80]. Since the late 1960s nonaqueous lithium cells, especially the 3-V primary systems, have been developed. In early 1958, Harris examined the solubility of lithium in various non-aqueous (aprotic) electrolytes, molten salts, and inorganic lithium salt. He observed the formation of a passivation layer that was capable of preventing a direct chemical reaction between lithium and the electrolyte while still allowing for ionic transport across it, which led to studies on the stability of lithium-ion batteries. These studies also increased interest in the commercialization of primary lithium-ion batteries [80], such as lithium-manganese oxide (Li//MnO_2) cells commercialized by Sanyo in 1975 and lithium-iodine (Li//(P2VP)I_n) cells that has been used to power more than four million cardiac pacemakers since its introduction in 1972. During this time the lithium-iodine system has established a record of reliability and performance unsurpassed by any other electrochemical power source [13]. However, an aqueous electrolyte limits the voltage of the cell and, therefore, the density of electric power a battery can deliver [81]. Simultaneously, advances in the understanding of the intercalation of lithium in different materials gave birth to rechargeable (secondary) lithium-ion batteries. Indeed in the early 1970s, research was rekindled in the area of the intercalation reactions of an ion, atom, or molecule into a crystal lattice of a host material without destroying the crystal structure: Armand suggested to use two different intercalation compounds as a positive and negative electrode, the lithium ions being transferred from one side to the other during the charge / discharge process in the so called rocking-chair battery [13, 82]. The first rechargeable Li-ion batteries with cathode of layered TiS_2 and anode of metallic Li was reported by Whittingham while working at Exxon in 1976. Exxon subsequently tried to commercialize the Li-ion batteries, but was not successful due to the problems of Li dendrite formation and short circuit upon extensive cycling. Dendritic growth brught to short circuits with the related safety concerns [83, 84]. To overcome these safety problems two solutions were proposed: on the one hand a solid electrolyte was proposed, instead of the liquid one, less reactive with lithium and more resistant to dendritic growth; this solution brought rechargeable lithium metal batteries in solid state [85]. On the other hand, an attempt

was made to replace the lithium anode with another material capable of receiving lithium ions reversibly, thus paving the way for batteries called lithium-ion batteries. In 1976, Besenhard proposed to reversibly intercalate Li^+ ions into graphite and oxides as anodes and cathodes, respectively [19]. The year of the turning point was 1980, when Scrosati and Lazzari demonstrated the concept of lithium ions rocking between the two electrodes [86]. In the same year for the first time is demonstrated the possibility to design Li-ion batteries with specific energy even four times higher than lead batteries, which at that time were the most common ones: a cobalt oxide is able to accumulate charge in a reversible way and exchange lithium ions at the same time; so it is possible to think about the two electrodes of the battery that accumulate energy by exchanging lithium ions in one direction and then release energy by exchanging lithium ions in the opposite direction. Hence the concept of "rocking-chair battery", i.e. with lithium ions passing from one electrode to the other [87] has consolidated. This type of battery can also have the electrode materials close to each other and separated by a thin polymer membrane. This arrangement makes it possible to bend and overlap many layers of these materials in order to confine a large amount of energy in a small space. Interestingly, layered $LiCoO_2$ did not attract much attention initially. However, this concept has gained renewed attention following the success of Japanese industries that with Sony (1985) and Sanyo (1988) started to apply new electrodes materials following the fundamental researches of Goodenough in Oxford and of Armand and Touzain in Grenoble, who evidenced the fast motion of lithium ions in layered host structures (named as lithium intercalation compounds). This battery design enabled the large-scale manufacturing of Li-ion batteries in the early 1990s [13]. Thanks to the discovery of carbonaceous intercalation materials for negative electrodes, in 1991 Sony put on the market the first "modern" lithium ion batteries: these materials solved the problems of low rechargeability of lithium metals due to the formation of dendrites and mossy lithium metal deposits [88]. It also greatly increased the safety aspects of the high-energy battery system [89].

Reversibly intercalating ions into host materials for electrochemical energy storage is the essence of the working principle of rocking-chair type batteries. The most relevant example is the graphite anode for rechargeable Li-ion batteries which has been commercialized in 1991 and still represents the benchmark anode in Li-ion batteries 30 years later [90]. The typical lithium-ion battery (LIB) configuration is as shown in Figure 1.11:

- a graphite anode with a stratified structure in which Lithium ions can intercalate, thus preventing dendritic growth.
- a lithium metal oxide cathode, in the typical $LiMO_2$ form with M a generic metal, e.g. $LiCoO_2$.
- a polymeric separator
- a liquid electrolyte composed of a lithium salt typically dissolved in a mixture of organic solvents

The negative electrode is a graphitic carbon that holds Li in its layers, whereas the positive electrode is a Li-intercalation compound (usually an oxide

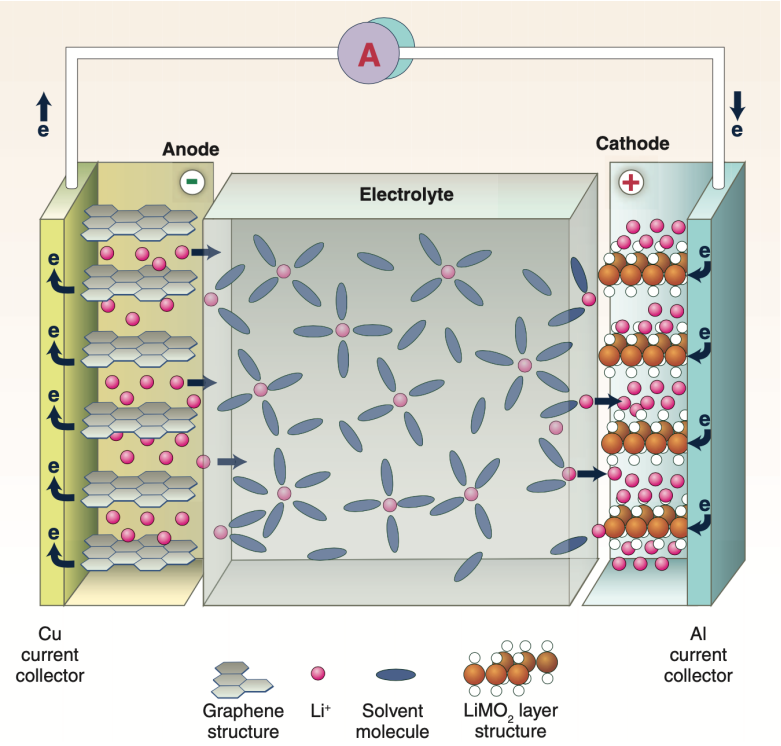

Figure 1.11: Schematic of a LIB. Reprinted with permission from [18].

because of its higher potential) that often is characterized by a layered structure. Both electrodes are able to reversibly insert and remove Li ions from their respective structures. In the first state, i.e. when the cell is completely discharged [note: the commercial cells are typically assembled in discharged state. The discharged cathode materials (e.g., $LiCoO_2$, $LiFePO_4$) and anode materials (e.g., carbon) are stable in atmosphere and can be easily handled in industrial practices], the lithium ions are found in the positive electrode material (cathode,layered oxide compound in Figure 1.11). In addition, lithium ions are present in the electrolyte. In the first moments of the charging phase, electrons present in the cathode migrate to the anode (negative electrode) through an external conductor; the cathode oxidizes and the anode reduces. To ensure charge balance, lithium ions leave the cathode, migrate through the electrolyte and intercalate in the anode (graphite layers in Figure 1.11). In this first cycle,part of the charge is consumed and the following deintercalation of Li^+ does not recover the full charge, but only about 80-95%.The charge consumed in the first cycle is due to solid electrolyte interphase (SEI) formation at the electrolyte/cathode and anode/electrolyte interfaces, and to reactions like Li_xC_6 [91]. This thin layer, insulating for electrons but very conductive for lithium ions, stops further decomposition of the electrolyte allowing lithium ions to intercalate. It is generally made up of a mixture of compounds (mainly lithium compounds) which clearly depend on the components used in the electrolyte, temperature and voltage [92]. That interface is very complex with a structure generally in layers parallel to the electrodes, not homogeneous, which can lead

to an uneven distribution of the lithium ion flow and therefore to the formation of a gradient of current density. For this reason,electrolyte additives have been studied, which form a homogeneous solid interphase, with optimal ionic conductivity and flexible to absorb volume variations of the intercalation electrodes [93]. After the formation of the SEI, the de-intercalation of lithium ions to the cathode and the intercalation of lithium ions to the anode continues. The described process is reversed during cell discharge, i.e. the lithium ions leave the anode and return to the cathode through the electrolyte. The intercalation compounds are often thermodynamically unstable in organic electrolytes. Therefore, passivation films like SEI protect their surfaces, which exposed to the electrolyte, and guarantees the reversibility of the cell cycles. This charge loss is irreversible and leads to a cell capacity reduction. The cycleability of lithium-ion systems mainly depends on the dimensional stability of the intercalation materials during insertion/de-insertion of Li^+ ion. Indeed, mechanical stress occurring during charge/discharge cycles can crack the electrodes, leading to contact losses between active material and possible oxidation/reduction phenomena on current collectors [91]. We report as an example the complete reaction that takes place in a cell, considering the graphite anode and the cathode of $LiCoO_2$:

$$6C + LiCoO_2 \rightleftharpoons Li_xC_6 + Li_1 - xCoO_2$$

As these equations show, during the charge process, lithium is inserted into the graphite. Using $LiCoO_2$, reaction reversibility is obtained only with a value of x lower than 0.5, thus keeping the degree of lithium insertion no lower than 0.5 because the stability domain of lithiated cobalt oxide $Li_(1-x)CoO_2$ lies between x = 0 and 0.5. If more than half of the Li ions is extracted from the cathode, a permanent structural modification occurs, blocking ion intercalation in the material and following oxygen release. Oxygen can react with the electrolytic organic solvents with important risks of fire and explosion. Thus, the charge voltage in a $Li_(1-x)CoO_2$ cell has to be limited to 4.2V in order to keep the threshold value of 0.5 [94].
As already mentioned, the components of the electrochemical cell are the electrodes (anode and cathode), the separator and the electrolyte: the latter is usually in the liquid state and impregnates the separator. Electrodes are "composite" materials. Graphite anodes are composed of the active material (about 90%) and a polymeric binder such as polyvinylidene fluoride (PVdF) (less than 10%) and carbon black. The cathodes are composed of the active material (about 85%), a polymeric binder (less than 10%) and a small quantity of carbon black as conductive carbonaceous additive [25]. The main features of the individual Li-ion cell components are briefly listed below.
Electrolyte: usually is composed of one or more polar organic solvents in which one or more lithium salts such as $LiPF_6$, $LiAlCl_4$, $LiAsF_6$, etc. are dissolved. It has been noted that the conductivity of lithium ions, under the same conditions, cell configuration, salt used, is always considerably higher using pairs of solvents (usually one with high dielectric constant and the other with low viscosity) compared to the use of single solvents. The solvent must be polar to dissolve lithium salt and must be stable (not decompose) over the entire range of voltage and current used: it generally belongs to one of three families of organic products, such as alkyl carbonates, esters and ethers [25]. Commonly used

solvents are Ethylene Carbonate (EC), Propylene Carbonate (PC), DiMethyl Carbonate (DMC). Several lithium salts can be used in the lithium-ion cell: Lithium hexafluoro phosphate, ($LiPF_6$), it is the most used salt because of its high ionic conductivity and electrochemical stability with EC. But it must be treated in an extremely controlled environment because it could easily decompose, reacting with water, forming hydrofluoric acid,extremely corrosive. It is also very sensitive to temperature. The choice of solvent and salt should be weighted according to the type of electrode, temperature and stability of the two electrodes in the voltage range in which the cell should work. In the electrolyte there are various types of additives, each having a specific function: from those that promote the formation of SEI, to those that stabilize the salt avoiding its decomposition; others that in case of excessive temperature increase polymerize blocking the ionic conductivity and acting as intrinsic safety. There are also additives that prevent the corrosion of the carriers and the precipitation of the lithium ion [13].

Anode: is generally composed of graphite or carbon or, more rarely, another insertion material or lithium metal alloys. These compounds all have the characteristic of being able to accept (insert) lithium ions within their structure. Usually graphite is used because of its low cost, high capacity to intercalate lithium ions up to a maximum ratio of 1 Li^+ per 6 carbon atoms and potential close to those of lithium metal. Its theoretical specific capacity is 372 mAh/g, much lower than Lithium metal, but graphite is much more stable for safety issue and its potential is higher than that of Lithium only of about 100 mV. Li^+ ions intercalate between graphene plates, slightly deforming the layer structure. Volume changes during cycles are about 10-15 %. For Li-alloy anodes, the volume variation between the lithium alloy and the corresponding lithium-free matrix metal could reach 300% as in the case of Sn or Si. After few cycles, the alloy becomes fragile, strongly limiting cycle life. A "*zero strain*" material is $Li_4Ti_5O_12$ (LTO), which displays very small volume changes during cycles. Moreover, lithium insertion potential is about 1.55 V (vs.Li/Li^+) and this feature prevents Li plating on the anode surface leading to dendritic growth, even at high currents. Finally, LTO displays very fast charge acceptance and excellent cycle performances. However, it displays low voltage when coupled with cathodes such as $LiMO_2$, i.e. 2.5 V, strongly limiting the energy density of the cell [33].

Cathode: generally as cathodic materials transition metal oxides and sulfides suitably lithified, having a lamellar structure, are used, as for example $Li_(1-x)MO_2$ (where M is one or more metals such as Co, Ni, etc.) or $Li_(1-x)Mn_2O_4$ or lithiated iron phosphates $Li_(1-x)FePO_4$[95]. Lithium ions can be inserted/de-inserted in the host structure over a wide range of potentials (3-5 V) [76]. Many cathodic lithium-ion materials have been synthesized (Table 1.3).
Among the best known:

- $LiCoO_2$: is the most used cathodic material so far for its stability and high capacity. It has not a very high thermal stability and besides being a toxic and expensive material, geographic and ethic concerns about mining are the driving force to limit its use in the next generation of batteries.

- $LiFePO_4$:with three-dimensional structure, has a potential lower than the

Material	Theoretical Gravimetric Capacity ($mAh/\ g$)	Theoretical Gravimetric Capacity based on degree of insertion ($mAh/\ g$)	Average Practical Gravimetric Capacity ($mAh/\ g$)	Cost
$LiCoO_2$	274	137	120	high
$LiNiO_2$	275	275	220	medium
$LiMn_2O_4$	148	148	120	low
$LiCo_{0.2}Ni_{0.8}O_2$	274	247	180	medium
$LiFePO_4$	170	170	150	low

Table 1.3: Cathodic materials for lithium-ion batteries. [33]

above mentioned materials but it is interesting because of the low cost, non-toxicity, long cyclic life and good resistance to high temperatures.

Separator: he has two essential functions, i.e. prevention of short-circuit between electrodes and ionic conduction throughout its porous structure. The choice of the separator is generally made according to the composition of the materials used, the solvents present in the cell, the estimated operating temperature and its mechanical characteristics. Among the characteristics of this membrane, the porosity has a primary role, for the passage of lithium ions. Usually, these membranes are constituted microporous films of polyethylene (PE) or polypropylene (PP) or a combination of these.

Current collectors: the role of current collectors (usually about 10 ?m thick) is to conduct electrons from the active materials to the electrode terminals and then to the external circuit. Aluminum foil is typically used for the cathode, while copper foil for the anode .

1.3. Future scenarios for batteries

To meet the future needs of our society, a huge improvement in the performance of batteries is a key factor. In many cases, and certainly for e-mobility batteries, this means simultaneously fulfilling a number of criteria, such as high power and high-energy density, long autonomy, long life, low cost and excellent safety, while also minimising their negative environmental impact, for example, by ensuring that they are easy to re-use and recycle and based upon abundant and sustainable resources. At present, no battery ticks all these boxes [96]. Therefore, active research is continuing in all aspects of batteries, from anode, cathode, separator, electrolyte, safety, thermal control, packaging, to cell construction and battery management. The electrode materials selected are critical to the performances of Li-ion batteries, as they generally determine cell voltage, capacity, and cyclability [19]. There are a number of potential alternative electrode materials (Figure 1.12): a large number of anode candidates that could dramatically increase the specific capacities, in particularly, with highly attractive $Si-$ and $Sn-$ based anodes; also, since the capacity of the cell is mainly influenced by the capacity of cathode, development efforts have long focused on these materials.

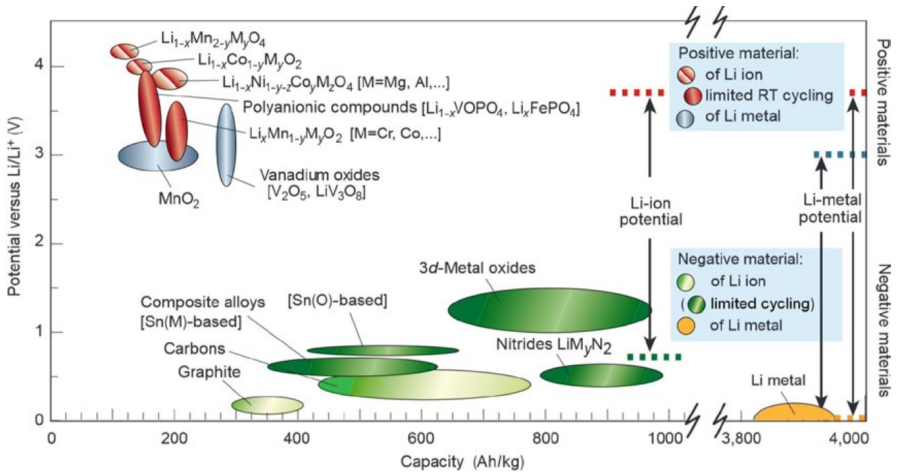

Figure 1.12: Voltage versus capacity for positive and negative electrode materials presently used or under considerations for the next generation of Li-ion batteries. Reprinted with permission from [19].

This issue should be creatively addressed, most likely by nanotechnology and nanocomposites. The future low-cost cathode materials could be $Mn-$ and / or $Fe-$based: in addition $Ni-Co-Mn-$based cathodes are highly attractive, especially from industrial prospective but in the next future cathode materials should try to avoid the use of either Co or Ni, or other toxic elements, from environmental perspectives [19]. The safety concern,which will be briefly described in the following paragraph, is another challenge that needs to be properly addressed. Additionally, future batteries research start with life cycle assessment (LCA) to evaluate whether the batteries are truly green or not: in this regard, the issue of lithium supply and recycling (less than 1% of lithium is currently recycled [77]) for mass production of Li-ion cells is undoubtedly of primary interest. [17]. There are still several types of new generation lithium-ion cells whose environmental impact is unknown (impact in terms of production that could lead to large volumes of waste and contaminated places where agricultural production will not be possible and where air quality is poor, to use and to disposal) [97].Then, it is still challenging to develop electrode materials with low carbon footprint, or the so-called "green batteries" [98]. The trend (Figure 1.13) is to arrive at new generation batteries that are smaller and smaller but perform better than the state of the art.

Among the most promising reliables technologies of the future are $Li-S$ cells (Figure 1.15) and $Li-O_2$ cells (Figure 1.14).

With a theoretical energy density even five times higher than that of Li-ion cells, close to that of fossil fuels [99], the Li-air cell uses Li as the anode and a cathode consisting of a porous conductive composite, usually carbon and a catalyst, that is flooded with electrolyte. Oxygen from the atmosphere dissolves in the electrolyte and is reduced. On discharge, Li ions pass through the electrolyte and react with the reduced oxygen. The process is reversed on charging. Either aqueous or nonaqueous electrolytes could be used. For the former, a Li-ion conducting solid electrolyte separates the metallic Li from the aqueous

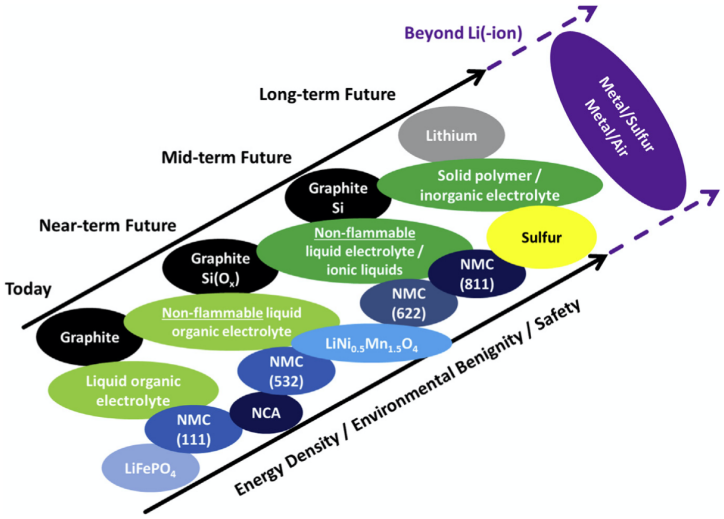

Figure 1.13: General trend for the present automobile battery R & D objectives with respect to the employed anode, electrolyte, and cathode materials. Reprinted with permission from [20].

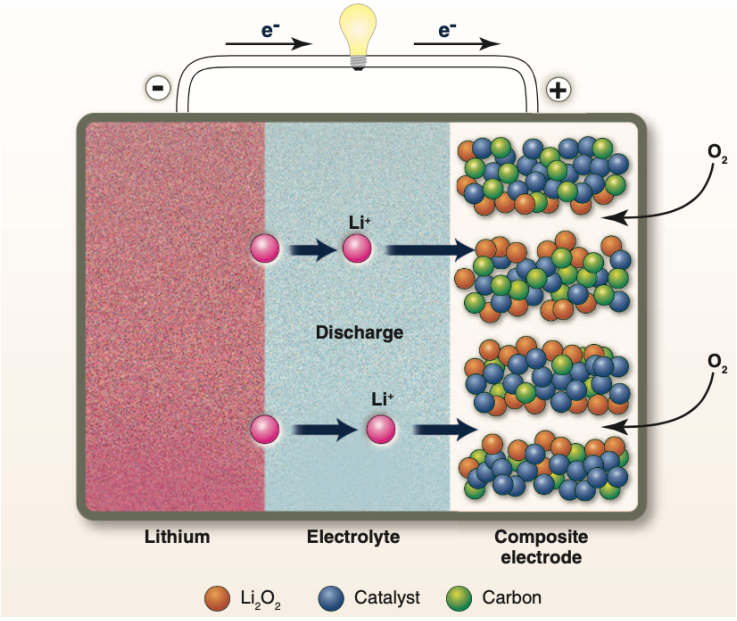

Figure 1.14: Schematic diagram of a $Li - O_2$ cell. Reprinted with permission from [21].

electrolyte [21].

The rechargeable $Li-S$ cell operates by reduction of S at the cathode on discharge: during the reaction, lithium metal is oxidized at the negative electrode to produce lithium ions and electrons. The lithium ions produced move to the

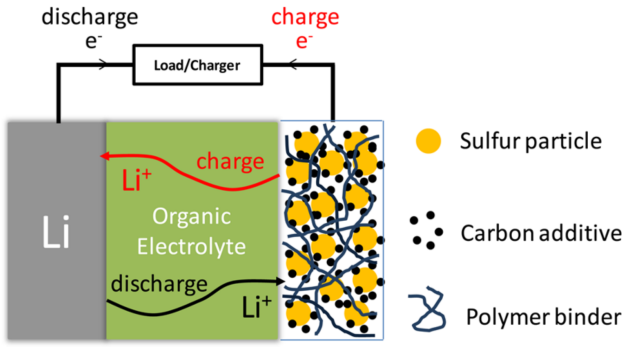

Figure 1.15: Schematic diagram of a $Li - S$ cell. Reprinted with permission from [22].

positive electrode where sulfur is reduced to produce lithium polysulfides and finally lithium sulfide by accepting the lithium ions and electrons. The backward reactions will occur during charge. Such cells have many attractive features, including: the natural abundance and low cost of S; and high theoretical energy storage [100].

However, despite recent scientific progress, the promise of a device with greater energy storage and a longer life cycle than lithium-ion cells has not yet materialised. And it may not materialise for the next ten years.

1.4. European context for batteries

Driven by the current transition to clean energy, demand for batteries will increase rapidly in the coming years, making this market increasingly strategic worldwide. As can be seen in the Figure 1.16, the gravity centre of cell production capacity is in Asia, particularly in China.
In this context, the European Union has strategically proposed a plan of actions with the aim of becoming a world leader in the production of eco-sustainable batteries: the consequences of these actions affect politics, the economy and the environment. Mainly, the EU aims at energy independence and to become a major player in the EV automotive sector [101]. In support of this ambitious goal, the European Commission launched the European Battery Alliance (EBA) cooperation platform [102] in October 2017 and endorsed a Strategic Action Plan on Batteries in May 2018 as part of sustainable mobility initiatives. The Action Plan [103] aims to put Europe on a firm path towards leadership in this key industry, supporting jobs and growth in a circular economy, whilst ensuring clean mobility and an improved environment and quality of life for EU citizens. As part of a "circular economy", sustainability is promoted along the entire battery value chain, from materials, design, use and recycling and disposal. The clear negative impact on the environment of incorrect disposal of batteries, whether in landfills or even worse in incinerators, leads the EU to address this problem by issuing a Battery Directive [104]:

- encourages the study and adoption of new chemistry for the composition of batteries, so as to minimise the use of hazardous or poisonous substances.

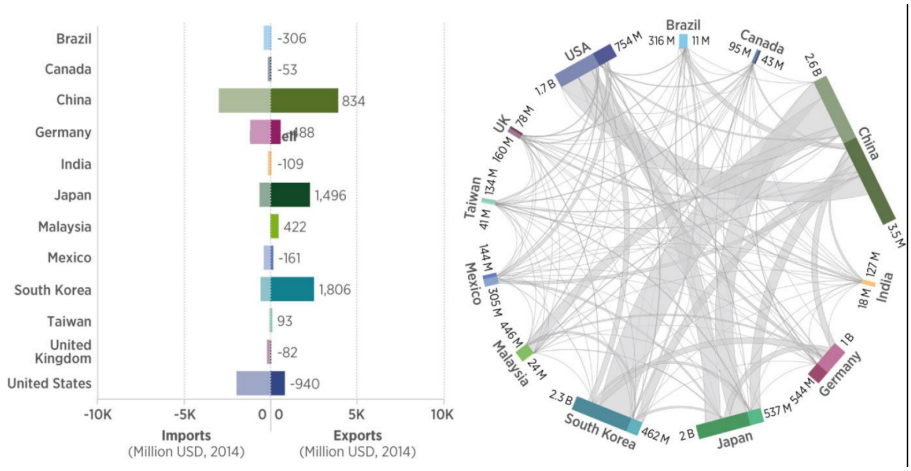

Figure 1.16: Flow of LIB cells between major trading partners (dark shades represent exports, lighter shades represent imports). Reprinted with permission from [23].

- establishes a regulatory framework with which it guarantees the correct management of batteries at the end of their life, encouraging their recycling

In the more general context of the European Strategic Energy Technology Plan [105], the EU has included a specific action on batteries, underlining the key role it intends to give to this technology. This plan is dedicated to promoting the competitiveness of EU industry in the global battery sector as a contribution to the development and deployment of low carbon technologies. This is achieved by coordinating national research efforts and contributing to project funding. Considered as fundamental, in electric mobility and in energy transition in general, batteries play a key role in global and particularly European investment initiatives. From a practical point of view, the European Union, in response to the Asian overwhelming power over electromobility and batteries, has established a well-structured and organised network with very specific objectives (Figure 1.17).
To address the issue synergistically, the network created embraces all levels of technology (TRL, *Technology Readiness Level*): therefore starting from the highest, European Battery Alliance (EBA) launched in October 2017, gathers the European Commission, interested EU countries, the European Investment Bank, key industrial stakeholders and innovation actors with the objective to create a competitive manufacturing value chain in Europe, promoting industrial projects with sustainable battery cells at its core [106]. Therefore, for lower level TRL, we find Batteries Europe the European technology and innovation platform of the European Battery Alliance (EBA), lauched in 2019: this platform, jointly managed the European Commission and stakeholders in the battery industry, has the operational aim of accelerating and organising the creation of a globally competitive European battery industry, guiding the implementation of the battery related research and innovation actions of the Strategic Energy Technology (SET) Plan and the Strategic Transport Research and Innovation

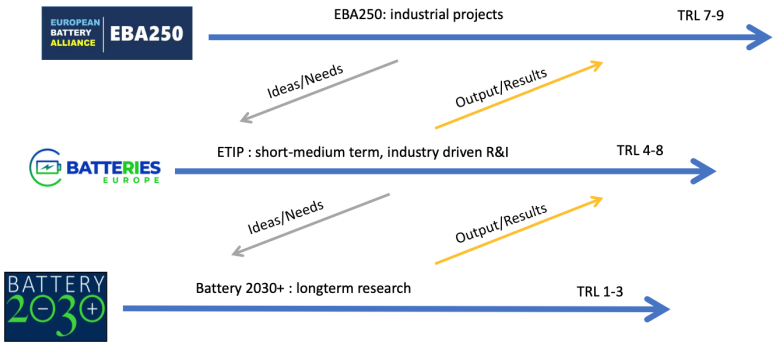

Figure 1.17: European Battery Networks. Reprinted with permission from [24].

Agenda [107]. The Strategic Energy Technology Plan (SET-Plan) is a central pillar of EU energy and climate policy. With its ten key actions, one of which is dedicated to batteries, it sets out the strategy for pursuing the objectives outlined by the European Community. As far as batteries are concerned, several research and innovation activities have been planned with the aim of making the battery value chain in Europe more competitive. At the same time, some Member States are collaborating on important projects of common European interest (IPCEI) on battery research and innovation [108].

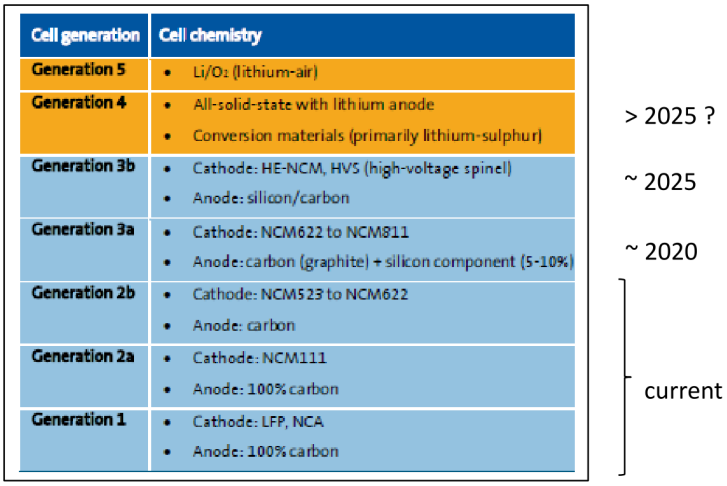

Figure 1.18: LIB cell chemistries generations. Reprinted with permission from [23].

In terms of basic research, Battery 2030 is the long-term programme (10 years) by which the European Union aims to close the technology gap with Asian manufacturers on the batteries of the future (Figure 1.18) by developing new battery that can store more energy, have a longer life and are safer and more environmentally friendly than today's batteries. The programme, coordinated by the Swedish University of Uppsala, is divided into three macro areas: the first, aimed at developing a platform that uses algorithms and AI to help

model the complex reactions present in a battery; the second concerns sensors that, integrated in the cell, examine the state of health of the battery and saw malfunctions in real time; the third, finally, focuses on the search for self-healing materials able of extending the life and reliability of batteries [109]. *Recyclability*, *Producibility*, *Sustainability*: these are the key words to build the future vanguard of energy storage systems in Europe.

2. Sensing, Health and Monitoring in EV

Una tecnologia abbastanza evoluta nei suoi effetti
non è dissimile da una magia.
A.C. Clarke - scrittore di fantascienza ed inventore

2.1. Li-ion Batteries Safety Issues

Lithium ion batteries have a high energy density: this feature, which leads to weight and volume savings (approx. 70%) in transport vehicle applications compared to lead-acid or Ni-MH batteries, makes lithium-ion cells very attractive [13]. Secondary elctrochemical cell are rarely used individually (Figure 2.1): in fact, with the exception of mobile phones and small consumer electronics devices powered at 3.7 V they are usually connected (in series and\or parallel) to obtain the supply voltages requested by the application in which they are used i.e. electric vehicle or stationary system. An assembly of individual cells in the same container is called *module*. Usually for each module there are some sensors, for example temperature, voltage and current sensors, a load/discharge balancing system of the cells and a thermal management system of the module itself that through a cooling system keeps the set of cells within ideal temperature limits. A set of modules, connected to each other in series and/or in parallel, makes up the battery pack: inside it there is a management system called Battery Management System (BMS) which electronically monitors, through different management strategies, the correct functioning of the battery pack and intervenes in case of malfunction. Moreover, the BMS interfaces the battery pack with the external apparatus in which it is mounted, for example the electric vehicle [25]. To summarize, a *cell (C)* is an energy storage device composed of at least one cathode and one anode, and other necessary electrochemical and structural components; a *module (M)* is the grouping of interconnected cells in series and/or parallel into a single unit; a *pack (P)*: is made of interconnected modules including all auxiliary subsystems for mechanical support, thermal management and electronic control [27].

The high energy density and high power achieved in industrial applications has therefore brought the issue of battery safety to the forefront, sometimes limiting its use on a large scale. There are in fact well-known episodes in which

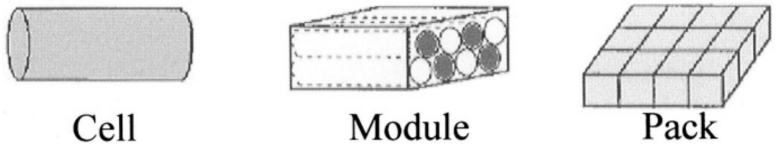

Figure 2.1: Progression from cell to module to pack. Reprinted with permission from [25].

batteries, both large and small, have caused dangerous or even disastrous situations [110]. Therefore, safety is a fundamental aspect, which must be addressed from the cell level to battery pack level. From a certain point of view, it is important to understand that batteries contain both oxidant agents (cathode), a reducing agent (anode) and a fuel (solvent) in a sealed container. Under normal operating conditions, the reductant and oxidant agents convert chemical energy into electrical energy with minimal heat and negligible gas. In the event of a malfunction or accident or short circuit they can react chemically generating heat and gas. Unfortunately, once started, the chemical reaction will probably proceed to completion due to the intimate contact of electrodes and the presence of flammable solvent. Failures at cell level can quickly degenerate into much more serious failures at a module or pack level [111]. Since it cannot be evaluated with a single parameter, safety must be a priority in every phase: from the selection of electrode materials, to the design of cells/modules/packs, to the design of electronic controls monitoring the operating parameters.

2.1.1. Key Facts of Safety

The safety issues associated with LIBs may arise underl abuse conditions. Abuse operating conditions may have different causes. Some environmental factors, for example, present in the application of the battery or battery pack, including ambient temperature, (external) pressure or vibration conditions, can lead to abuse conditions: in this regard it has been suggested that the temperature of the battery should be kept below 50 °C for safe operation [112]. When designing the battery packs, the natural vibration frequencies close to those of the vehicle suspension system, the sprung mass, the powertrain (driveline and gearbox) and the chassis must also be cut to avoid resonance phenomena potentially harmful to the life cycle of the battery pack (i.e. all frequencies from 0 to 40 Hz) [113]. Moreover, situations involving the vehicle in an accident with consequent deformation of the battery pack can produce risks in terms of safety and reliability: episodes are known, especially in the initial phase of diffusion of electric vehicles for passenger transport, in which manufacturers (Tesla, GM, Boeing i.e) were forced to withdraw their products from the market [114]. It is also reported that the causes of malfunctions can also arise in the production process of cell, module and battery pack. The most important are chemical factors, such as impurities, and assembly procedures, i.e. material processing and cell closures, either hermetic or crimp [115]. In addition to these, electrochemical factors can be considered, which in the same way can trigger inefficient, or even worse, dangerous situations: they range from a possible "failure" of an electrochemical cell component (electrodes, separator, current collector or elec-

trolyte) to a higher level of malfunction involving the entire storage system, for example in conditions of overload/discharge, dendritic growth, short circuits. Schematically, therefore, the conditions of abuse can be summarized [116]:

- *mechanical abuse* (crush, nail penetration, drop, vibration etc.)
- *electrochemical abuse* (overcharge, overdischarge, short circuits of full or half charged batteries, gas generation etc.)
- *thermal abuse* (external heating, flame attack, hot combustion gases from a fire etc.)

Regardless of the starting abuse condition, this could lead to the *thermal runaway* (Figure 2.2). The thermal runaway (TR) at single cell level, both in EV and stationary systems, would cause reactions to chains propagate to the entire battery pack, resulting in a catastrophic effect. Therefore, it is vital to understand the factors that can potentially lead to TR in the individual cells and avoid that this phenomenum occurs [26].

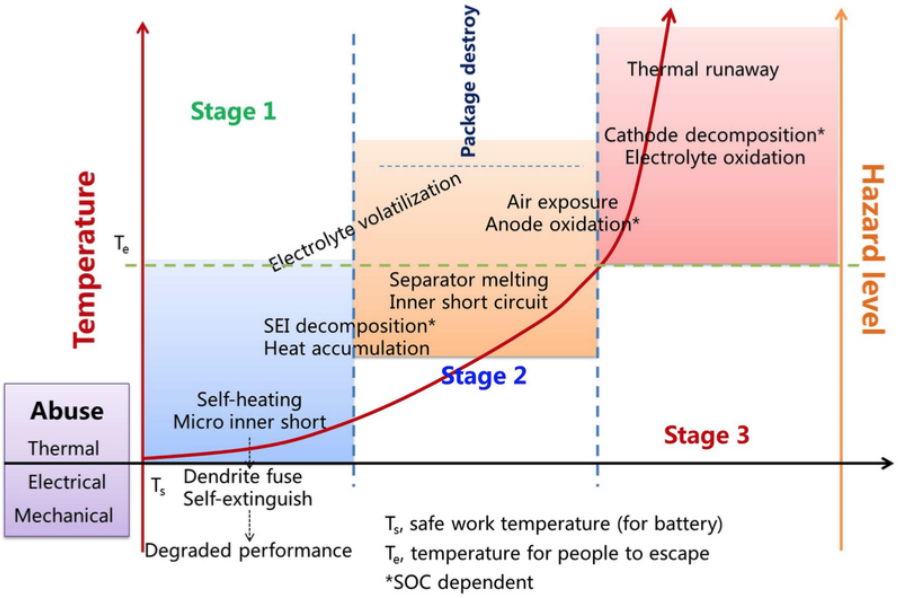

Figure 2.2: Three stages in battery thermal runaway. T_S=safe work temperature (for battery); T_e= temperature for people to escape. Reprinted with permission from [26].

There are three phases in which the TR can be divided, depending on the degree of internal short circuit or the speed of heat generation: in the first stage overheating starts due to small short-circuits caused, as an example, by dendritic processes. If the heat generated melts the dendrites, the process self extinguishes. If the heat generation process continues (Stage 2) the anode/electrolyte interphase could break contributing to unwanted exothermic reactions between electrode and electrolyte and also to the melting of the separator. In the stage 3 an uncontrollable overheating is reached, with an average heat increase rate of $10°C/min$ and the formation and leakage of flammable gas.

Beyond the combination of factors leading to TR, it is commonly believed that improving or solving the safety aspects of Li-ion batteries is necessary:

- developing materials that make the cell safer (electronic materials, electrolytes i.e.)
- increasing the safety requirements in the design of the casing and battery packs.
- developing systems for the thermal management of cells, modules and battery packs

Since the risks associated with a given battery technology are highly dependent on the materials that make up the cells, it is important to consider all these components relevant from the safety point of view: for electrode materials, the cathode LFP (*lithium iron phosphate*) has proved to be thermally stable and non-toxic; the anode LTO (*lithium titanate*) has attracted a lot of attention thanks to its long cycle life without producing significant structural changes and its thermal stability and high potential that prevents the formation of dendrites. The electrolyte has a great weight in the safety evaluation: in fact generally the most used ones are mainly based on highly flammable organic solvents. In case of uncontrolled temperature increase the electrolyte decomposes leading to the formation of gas with consequent internal overpressure and probability of breakage. The presence of fluorinated compounds in the electrolyte represents an additional risk because in case of thermal runaway toxic and corrosive hydrogen fluoride (HF) is released. The addition of "flame retardant" additives has produced the so called *"non-flammable electrolytes"*; moreover the use of high flammability point electrolytes or ionic liquids at room temperature is considered, which have a high electrochemical and thermal stability and low volatility. In addition, the use of solid polymer electrolytes is considered to be intrinsically safer because their state of the matter hinders leakages. Of fundamental importance is the choice of the separator, which physically avoids the short circuit between the electrodes. Among the solutions proposed, we cite an exotics solution proposed by Liu's group, which develops a separator from the regenerated egg membrane, with excellent mechanical properties, thermal and ability to avoid the formation of dendrites. [117]. A compromise is necessary in the choice of the components of a cell according to the application and must be found among the issues of safety, performance and cost [27].

As far as design aspects are concerned, optimization at all levels has the best impact in terms of improving safety. Thus, it ranges from a smarter vehicle design considering the positioning of the battery pack away from the most dangerous areas in case of an accident [114], to considerations related to the choice of cell casings. In fact, cylindrical cells have high energy density, good mechanical stability and cheaper in terms of production costs compared to prismatic cells. However they have a low packaging efficiency and in case of overpressure they could have damaged the roll of internal components before the opening of the vent valve. From this point of view prismatic cells are more advantageous because they are more efficient in packaging and have a safety vent in their casing in case of overpressure (in case of blocked vent valve the risk of explosion increases). A different point is that of the pouch cells, which have a higher energy density than the other two versions, their manufacturing

cost is not very high and they are much lighter. However they tend to swell during abnormal operation and in their classical configuration they do not have an output mechanism in case of internal overpressure. Moreover, due to their "soft" construction, they need a more robust case when assembled to form the battery pack [118].

As regards the management systems, the safety of the batteries goes from designing systems that can control the stored energy and can monitor the entire battery pack. These systems can be internal systems within the cell, module or pack, or external systems. Internally, voltage, temperature, current and pressure are usually controlled. Then, through electronic architectures, these internal parameters are detected, which, suitably processed, allow the Battery Management System (BMS)(§2.2.1) to monitor and manage the entire battery pack. Given the high importance of the thermal aspect on the safety of Li-ion batteries, it is necessary to give a brief description of the systems that allow to keep the cells in an adequate temperature range during their operation (§2.2.2).

In order to facilitate the use of lithium ion batteries in efficient and safe conditions, a multitude of regulations and standards have been drawn up at the international, national and regional level, from the experiences of industry, academia and regulatory bodies. These regulations and tests, summarily summarized in Figures 2.3, are performed to identify the battery's weaknesses and vulnerabilities under real-life and abusive conditions (e.g., a car accident or thermal shock). Many of the tests presented in this review are dedicated to the evaluation of the consequences of a short circuit, which could be followed by a thermal runaway, as this is one of the scenarios that can create a great risk, both for the occupants of the vehicle and for first aiders. [27]. The final aim of the tests is to evaluate the safety level and the field of application of the different types of batteries: following the SAE J2464:2009 standard, the tests are carried out both at cell, module and package level [27].

2.1.2. Safety at cell level

Generally in the rechargeable batteries commonly used for mobile devices there are mechanical or electronic safety devices that intervene before the cell reaches critical and unstable conditions, "disabling" the battery. Safeguards must be included to control charging to prevent damage to the battery due to abusive charging. Proper control of the charge process is critical to the ultimate life and safety of the battery. The two major considerations to be addressed include:

- Voltage and current control to prevent overcharge
- Temperature sensing and response to maintain the battery temperature within the range specified by the battery manufacturers

The controls for voltage and current during charge for most batteries are contained in the charger. Protective devices are installed within the battery to stop the charge in the event of an unacceptable temperature rise. Below is a list of the main protection devices on the cell [72]:

- *Thermal fuse*: Most of the circuits for battery charging incorporate a thermal fuse, wired in series with the cell stack. It opens the circuit when a

		Region of applicability	International				EU and further countries[a]	USA			Korea	India	China
	Test	Section	SAE J2464 (2009) [61]	SAE J2929 (2013) [66]	ISO 12405-1 (2) (2012) [67,68][f]	ISO 12405-3 (2014) [69][f]	IEC 62660-2 (3) (2011 (2016)) [70,71]	UN/ECE-R100.02 (2013) [62]	UL 2580 (2013) [63]	US ABC (1999) [72]	FreedomCAR (2005) [65]	KMVSS 18-3 (2009) [73]	AIS-048 (2009) [74]	QC/T 743 (2006) [75][g]
Mechanical	**Mechanical shock**	**3.1.a**	C M P	C M P V	P	P	C	C M P V	C M[e] P	M P	M P		M	
	Drop	**3.1.b**	P	P					C P	P		P		C
	Penetration	**3.1.c**	C M P							C M P	C M P		C M	C P
	Immersion	**3.1.d**	M P	P		P			M P	M P	M P	P		
	Crush/crash	**3.1.e**	C M P	P V		P V	C	C M P V	C M P	C M P	C M P			C P
	Rollover	**3.1.f**	M P	P					P	M P	M P		M	
	Vibration	**3.1.g**		C M P	P	P	C	C M P	C M P	C M[e] P	C M P		M	P
Electrical	**External short circuit**	**3.2.a**	C M P	P	P	P	C	C M P	C M P	C M P	C M P	P	C M P	C P
	Internal short circuit	**3.2.b**					C							
	Overcharge/ overdischarge	**3.2.c**	C M P[d]	P	P	P	C	C M P V	C M P	C M P	M P	P	C M P[c]	C P
Environmental	**Thermal stability**	**3.3.a**	C				C		C	C M P	C M P	P		C P
	Thermal shock and cycling	**3.3.b**	C M P	C M P	P	P	C	C M P	C M P	C M P	C M P			
	Overheat	**3.3.c**	M P	P				C M P V		M P				
	Extreme cold temperature	**3.3.d**								C M P				
	Fire	**3.3.e**	M P	P		P V[b]		C M P V	C M P	C M P	C M P	P		
Chemical	**Emissions**	**3.4.a**	C M P	P					C M P	C M P	C M P			
	Flammability	**3.4.b**	C M P	P					C M P	C M P	C M P			

[a] Norway, Russia, Ukraine, Croatia, Serbia, Belarus, Kazakhstan, Turkey, Azerbaijan, Tunisia, South Africa, Australia, New Zealand, Japan, South Korea, Thailand and Malaysia.
[b] Vehicle body may be included.
[c] Also possible at battery pack subsystem: representative portion of the battery pack (energy storage device that includes cells or cell assemblies normally connected with cell electronics, voltage class B circuit, and overcurrent shut-off device, including electrical interconnections and interfaces for external systems.
[d] Applicable to the LIB cell and pack whose rated voltage is 3.6 V and nx3.6 V (n: quantity of batteries), respectively.
[e] At the module level for those electric energy storage assemblies intended for use in applications larger than passenger vehicles. The module level testing shall be representative of the electric energy storage assembly.
[f] Overdischarge not at pack level.
[g] Overdischarge not performed.

Figure 2.3: Overview of tests in standards and regulations applicable to lithium ion batteries in automotive applications. Test level is indicated as C: Cell, M: Module, P: Pack and V: Vehicle. Reprinted with permission from [27].

predetermined temperature is reached. Thermal fuses are included as a protection against thermal runaway and are normally set to open at approximately 30-50°C above the maximum battery operating temperature.

- *Thermistor*: intervenes by switching off loads to lower the battery temperature, in the event that excessively high temperatures are reached during the discharge.
- *Temperature Cutoff, TCO*: this device operates at a fixed temperature and is used to cut off the charge (or discharge) when a preestablished internal temperature is reached inside the battery. TCOs are usually resettable. They are connected in series within the cell stack.
- *Positive Temperature Coefficient (PTC)*: This is a resettable device, connected in series with the cells, whose resistance increases rapidly when a preestablished temperature is reached, thereby reducing the current in the battery to a low and acceptable current level.

2.2. BMS AND BTMS

For the safe use of devices powered by one or more energy storage elements, cell phone batteries, battery packs in an electric vehicle or stationary energy storage systems from alternative intermittent sources, the safety aspect is equally important as the energy efficiency aspect in order to avoid the abuse situations previously described and summarized in Figure 2.4. In the case of Li-ion batteries, safety is generally declined in, monitoring and management of electrical parameters and monitoring and management of thermal parameters. The Battery Management System performs the first task. The Battery Termal Management System is used for thermal management. In the next two paragraphs we will briefly describe the two systems according to the state of the art. After all, the systems for monitoring and control evolve at the same speed as electrochemical systems. This implies a strong push of innovation in this field. And it is precisely here that the research contribution of this work is inserted.

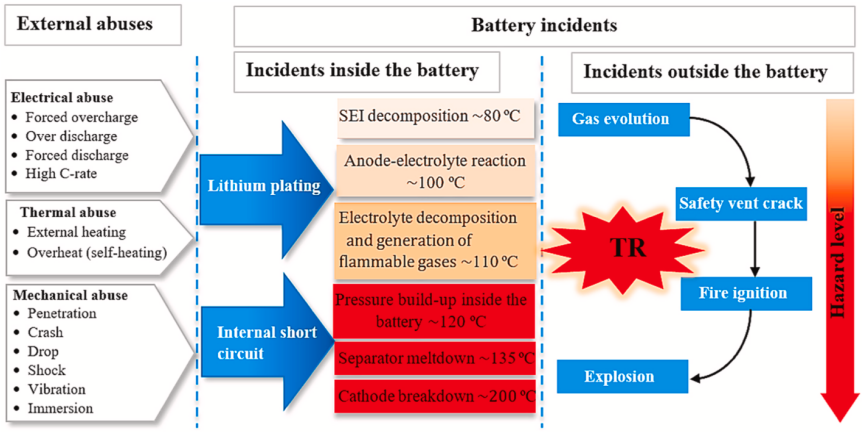

Figure 2.4: A chain of reactions after abusing a Lithium-ion battery. Reprinted with permission from [28].

2.2.1. Battery Management System (BMS)

To ensure the wide acceptance of electric vehicles and expanded the market of Li-ion battery powered vehicles, automakers should invest significantly on the battery management systems to enhance safety of the huge battery packs in vehicles. According to ref.[119] , *the basic task of a Battery Management System (BMS) is to ensure that optimum use is made of the energy inside the battery powering the portable product and that the risk of damage inflicted upon the battery is minimized. This is achieved by monitoring and controlling the battery's charging and discharging process.* Beyond the architecture and strategies that it implements internally to pursue the desired requirements of the application for which it is built, BMS generally serves the ultimate purpose of protecting cells, modules and packages from all forms of abuse and damage, maximizing battery life and ensuring that it is always ready for use in optimal conditions. An overview of the BMS controls can be seen in Figure 2.5.

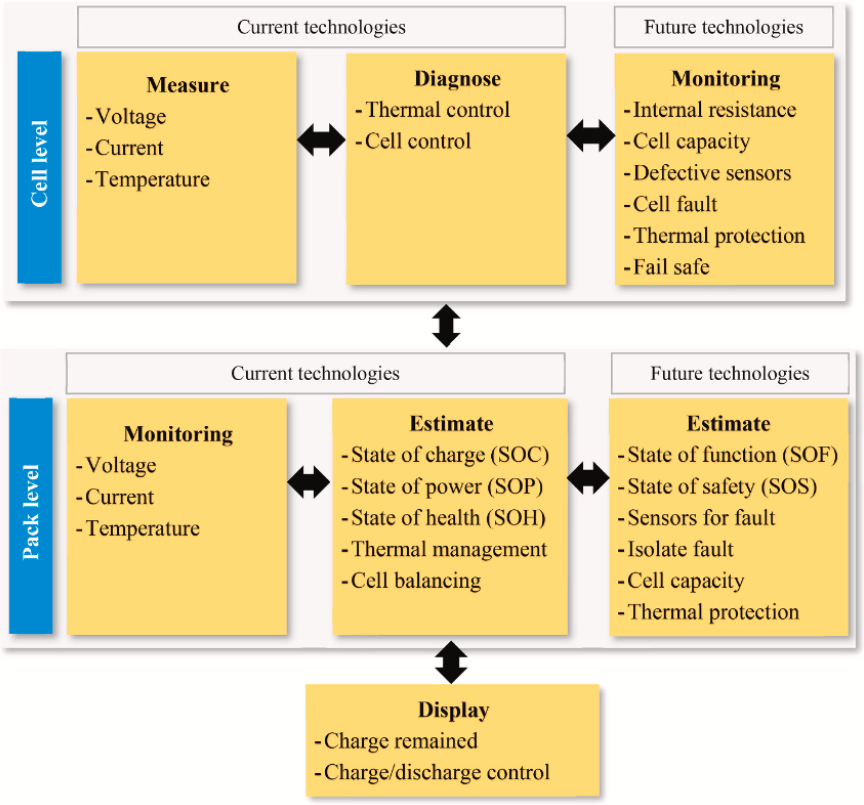

Figure 2.5: Functions of the BMS in cell and pack level for the current and future technologies. Reprinted with permission from [28].

The BMS equipped inside the battery pack is mainly used to protect the battery from overloads and excessive discharges in order to extend its life cycle: in case of overload in charge or over-discharge it could generate heat that if accumulated or uncontrolled would probably lead to thermal runaway and the consequent unstable and sometimes disastrous phenomena. Anomalous charges

and discharges can induce imbalances in some cells, and consequently limiting the usable capacity of the battery pack and reducing its energy. In this situation the BMS acts by re-balancing the energy in the battery pack through passive techniques (dissipation of energy in access through a resistor) or more effectively through more sophisticated techniques that actively redistribute the charge over all the cells in the pack by increasing operating time and reducing the heat generated. The BMS integrated at the level of the single cell, on the other hand, balances its energy and monitors its temperature and communicates with external devices such as displays, battery chargers and data logger [28]. Along with controlling the charge and discharge of the cells and balancing them and intervening in case of malfunctions on the battery pack, the BMS, in order to avoid potentially dangerous situations, determines certain parameters, including:

- Depth of Discharge
- State of Charge
- State of Health
- State of Power
- State of Function

Below is a brief description of the listed variables. For further information please refer to the specific literature starting from [120–122].

Depth of Discharge (DOD: is an indication of the amount of charge (also indicated as capacity) already extracted from a battery in relation to its initial (nominal) capacity. It's given by:

$$DOD = \frac{\int_0^t i_{Dchg}(t)dt}{Q_{nom}} \tag{2.1}$$

[94]

The depth of discharge is the complement of state of charge: as one increases, the other decreases.The DOD is usually expressed as a percentage.

State of Charge (SOC): is an indication of the amount of charge still available in a battery in relation to its capacity in given conditions of discharge past and future. It's given by:

$$SOC = \frac{Q_{av}}{Q_{nom}} = 1 - DOD \tag{2.2}$$

The SOC is associated with a chemical energy. Therefore, it can be used to evaluate the remaining available energy [94].

State of Health (SOH): is an indication of the state of aging or failure of a battery. It can be evaluated as the amount of charge measured during a complete discharge in relation to the nominal capacity. It's given by:

$$SOH = \frac{Q_{Dchg}}{Q_{nom}} \tag{2.3}$$

Thus, this parameter characterizes its degradation over the course of its use. The SOH is usually expressed as a percentage [94].

State of Power (SOP): is defined as the ratio of peak power to nominal power. According to literature, under the designed voltage, current, SOC, and power constraints, the maximum power that a battery can persistently provide for t seconds is defined as the peak power [123]. SOP is used to evaluate whether the battery pack has sufficient power to meet the starting, acceleration or climbing demand of EVs. In the braking state, SOP can help to determine the maximum power recovered by the battery and thus avoid overcharging. On the other hand SOP contribute to optimization of power distribution between the engine and the electric motor in PHEVs and HEVs [124].

State of Function (SOF): recently introduced, gives an account of the ability to render the service for which the secondary battery was intended. This state needs to be defined on the basis of the application. Depending on the application, the definition may be binary or analog. A battery may no longer be able to properly drive an electric vehicle (EV) because of an increase in its internal resistance and/or a decrease in its capacity but may be given a second lease of life in domestic storage (where power peaks are not required or a decreased energy is acceptable) [94].

The assessment of all the above parameters implies that the battery management system communicates with the rest of the vehicle: the communications function of a BMS may be provided though a data link used to monitor the performance of vehicle, log data, diagnostics or set system parameters.

2.2.2. Battery Thermal Management System (BTMS)

The Battery Thermal Management System (BTMS) regulates the temperature inside the battery pack by cooling or heating, and ensures temperature homogeneity throughout the battery pack, keeping it in the optimal operating range. This prevents overheating and optimizes the electrochemical performance of the battery pack. In automotive applications, the BTMS is chosen and designed to be effective in the monitoring described; also aspects such as reliability, low cost, ease of maintenance, light weight and volumetric compactness are considered. According to [125] BTMS functions are:

- *cooling*: battery cells will not only generate electricity but also heat during it's work. Thus, a cooling function is required in order to remove this heat from the battery pack when battery temperature reaches the optimum temperature or even in advance.
- *heating*: a heating function, such as PTC heater, is required to assist the battery pack to reach the proper temperature range, when battery pack temperature probably falls below the lower temperature limit, in cold climates, .
- *ventilation*: is required to exhaust the hazardous gases within battery pack.
- *insulation*: to prevent battery fall or rise out of proper temperature range due to temperature difference between the inside and outside of the battery pack, in extreme cold or hot weather. Good insulation is needed

because can slow down the falling or rising of battery temperature, especially when the vehicle is parked outdoors (most Lithium-ion batteries cannot be charged quickly at a temperature below $5°C$ and cannot be charged at temperatures below $0°C$).

There are different technologies for the heating and cooling of the battery pack; in this work we just list some of them, referring to the specific literature for further information.

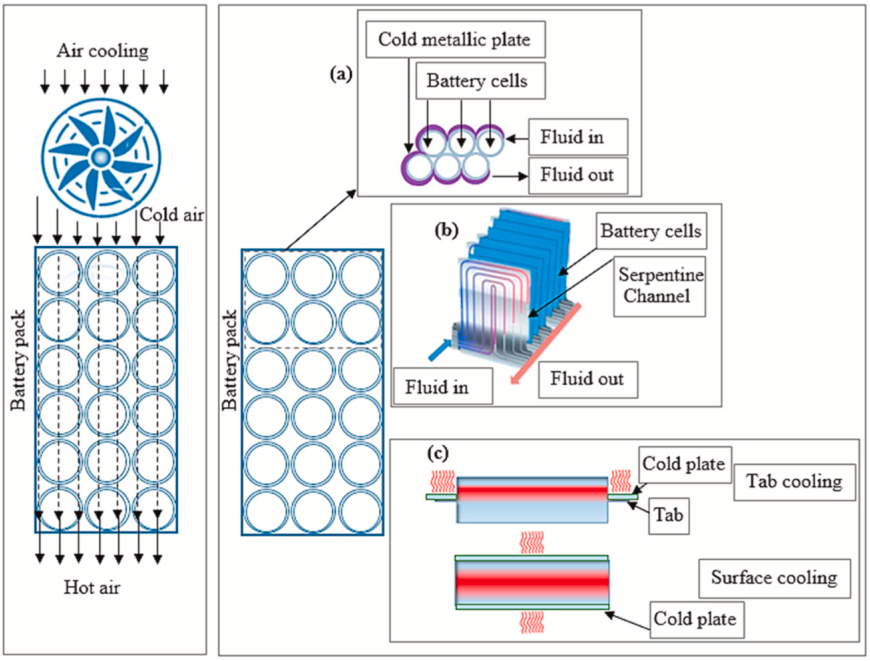

Figure 2.6: Air and liquid thermal management systems (a) layout of the surface cooling by using a cold metallic plate for cylindrical batteries, (b) arrangement of serpentine channels in a pouch and prismatic batteries, and (c) tab and surface cooling of Lithium-ion battery. Reprinted with permission from [28].

Some methods of cooling/heating, according to [126, 127], are (Figure 2.6):

- air-cooled, natural or forced with the use of a fan
- with liquid, with cooling fluids, such as oils, water, glycerol, etc., in direct or indirect contact. The liquid flows inside pipes or cavities that lap the cells; the system is more effective than the one using air because of the greater heat exchange capacity of the liquid compared to air; the risk is that of loss of coolant in case of failure of the refrigerant circuit, which can lead to short circuits of the battery pack.
- with phase change materials
- with heat pipe systems
- combined systems

Regardless of the system used, a logic is integrated in the BTMS that regulates the operating parameters of the system, such as the air flow rate in the case of forced air cooling. The BTMS, besides being intrinsically effective, is all the more effective the more the battery pack has been designed and positioned correctly inside the vehicle. Some years ago, new approaches emerged and studied, including thermoelectric coolers, thermoacoustic refrigeration, magnetic refrigeration, or combining the advantages of different techniques. Therefore, different are the operating strategies of the temperature control system applied at all levels of the storage system. At the same three levels generally also safety devices are installed, depending on the application, which we briefly list: Thermal fuse, to protect against overcurrents; Positive Temperature Coefficient (PTC), also to protect against overcurrents due to external short circuits or other potential Thermal Runaway triggers; Current Interrupt Device (CID), which protects against excessive internal overpressures; Safety Vent, very important that intervenes to release dangerous gases that can form inside the storage system before the housing breaks down [28].

2.3. Battery diagnostics: tests and methodologies

In addition to the management of the cells, modules and packages made on the electric vehicle or in stationary systems in which secondary electrochemical cells are used, in particular Li-ion, a piece of the final safety of these devices is attributable to the design and preliminary testing phase. In fact, if on the one hand the growing demand for energy storage systems has pushed towards obtaining cells with high specific energy, light and compact, at the same time the preliminary test systems have evolved, useful for the engineering of a new electrochemical system that combines a high storage capacity and reliability and safety for its entire life. Starting from the already mentioned quantities (§2.2.1) that provide the "dynamic" operating state, those that from the "static" point of view characterize an electrochemical cell are the capacity, index of energy storage; the internal resistance, index of the delivered current; the self-discharge, indication of the mechanical integrity of the cell. Of undoubted usefulness are, in the prototyping phase of an electrochemical system, all the mathematical modeling techniques that through more or less structured algorithms [128] simulate the behavior of the cell in various configurations, estimating its characteristic properties [25, 129]. Then through various experimental techniques, which from time to time examine the chemical/physical/electrochemical behavior of the cell under study, the theoretical results obtained with the simulations are validated. Some parameters that are usually considered in the main experimental procedures are reported in a summary way; then we list the main types of experimental tests [130], referring to the specific literature for the right insights:

- *Voltage*: Battery voltage reflects state-of-charge in an open circuit condition when rested.

- *Internal Resistance*: identifies corrosion and mechanical defects. There are various methods to measure the internal resistance depending on the type of battery and the quality of the measurement we want to obtain, including the ohmic measurement in which the battery receives a short

discharge lasting a few seconds and at the same time a voltmeter measures the voltage drop and Ohm's law calculates the value of the resistance [131].

- *Voltage Efficiency*: defined as ratio of cell during discharge and charge processes; it's given by:

$$\eta_V = \frac{V_{Dchg}}{V_{Chg}} \tag{2.4}$$

  where V_{Dchg}= average voltage during discharging and V_{Chg}= average voltage during charging.

- *Coulombic Efficiency*: defined as ratio of total electrical charge withdrawn during discharge (Q_{Dchg}, discharge capacity) versus the charge stored after charging (Q_{Chg}, charge capacity) ; it's given by:

$$\eta_C = \frac{Q_{Dchg}}{Q_{Chg}} \tag{2.5}$$

- *Discharge capacity fade over long-term cycling*: important metric in evaluating the stability and robustness of a particular system in delivering the desired output current density; takes into account the degradation of various cellular components, any unwanted side reactions and the precipitation of electroactive species.

Below is a short list of the most commonly used diagnostic techniques [130]:

- *Galvanostatic Charge/Discharge (cycling)*: the most widely-used method for basic characterization of battery performance is constant-current discharge and charge. When charging and discharging curves are executed in series, cycling performance can be assessed.

- *Polarization curves*: illustrate the relationship between cell voltage and charging or discharging current.

- *Cyclic voltammetry (CV)*: used to evaluate the cur- rent response to a linear voltage sweep.

- *Current interruption (CI)*: is an in-situ technique used to relate the transient voltage response from a current interruption event to cell parameters, most commonly ohmic.

- *Electrochemical impedance spectroscopy (EIS)*: EIS requires a small voltage/current perturbation signal of known amplitude and frequency to the cell, forcing the cell to deviate from equilibrium by a very small magnitude. Over a spectrum of frequency, the amplitude and phase of the resultant, measured signal is recorded.

A reliable analysis of an electrochemical system that characterizes its performance and identifies its critical points is not easy; on the contrary, it requires a lot of efforts and different approaches, especially in a panorama as evolving as that of today's batteries, passing from the current generation to the following ones.It is definitely appropriate the comparison between a battery and the

human body by Buchmann [131]: *"battery testing and monitoring is far more complex than outsiders perceive it. As there is no single diagnostic device that can assess the health of a person, so are there no instruments that can quickly check the state-of-health of a battery. Like the human body, batteries can have many hidden deficiencies that no single tester is able to identify with certainly"*. In the following paragraphs we focus on a useful technique from the point of view of testing the materials that make up the cell, with particular reference to electrode materials.

2.3.1. Behavior of electrode materials: *in situ* Dilatometric Analysis

Issues related to battery safety and reliability are of primary importance in the current scenario where there is an exponential growth in demand for energy storage systems as a result of the trend described in previous chapters. The electrochemical cell is a complex system characterized by main parameters and aspects that appear to be secondary but which in reality are not subsidiary. In this paragraph we will briefly talk about one of the techniques [132], the dilatometry analysis that allows to analyze and understand the behavior of the electrodes in an electrochemical cell, in particular a Li-ion cell. While the majority of the electrode material investigations have been focused on electrical and electrochemical properties [133], the mechanical properties, including elastic modulus, maximum allowable deformation, tensile strength and mechanical failure behavior are equally important [134, 135]. As it is well known, the volume variation of the active electrode material in Li-ion batteries is one of the most critical factors for battery stability and can reflect what occurs inside the battery during utilization and aging [136]. In fact, cyclic expansion and contraction due to lithium ion intercalation in the electrodes during charge and discharge cycles can ultimately cause structural damage to the electrode with possible fragmentation of electrode particles; this can potentially be an important cause of battery capacity fade, and thermal runaway.[137]. On the one hand, the study of the materials that make up the electrodes and determine their electrochemical-mechanical performance is investigated through modeling techniques and mathematical simulation. [138, 139]. An important contribution to the study of these materials under working conditions is made using the dilatometric technique: dilatometric experiments provide information on the thickness change of a single electrode during lithiation and delithiation, as the separator is fixed in position. In literature there are some variants of this technique that take into account the fact that the electrode material by varying its volume provides information that can be measured in three dimensions. Hence, it is possible to study only one or more components of this variation [140]. Moreover, this technique can be applied to the whole cell, i.e. taking into account the expansion of all the components of the cell (anode, separator, cathode), or to half a cell, i.e. considering the variation of only one electrode (which will be called *working electrode*, WE) and keeping the other electrode (also called *counter electrode*, CE) and separator out of the expansion measure. The volume variation due to the expansion/contraction of the electrode materials can be measured with different technologies: it goes from the simple one-way measurement obtainable with a comparator to 2D measurements obtained with laser scanner or with interferometric techniques [141]. Before proceeding with

the review of some of the devices that have been built for this type of test, a short historical excursus is presented.

The first measures of thickness variation, of a pyrographite electrode in contact with boron trifluoride in thioxyethane, date back to 1977 [142]: the attention to the time was turned to the study of the intercalation behavior of a certain species in graphite and on the consequent dilatation. Subsequently, the poor resolution of the device used by Metrot in 1977, was improved in Biberacher's studies. With the system described in [143], they arrive up to 25 *nm*. The measurement of the thickness variation is based on the resonance frequency shift of an oscillator circuit whose inductors is constituted by a ferrite coil. This system, schematized in Figure 2.7 was also used for the study of the intercalation of lithium ions in graphite at the industrial level [29].

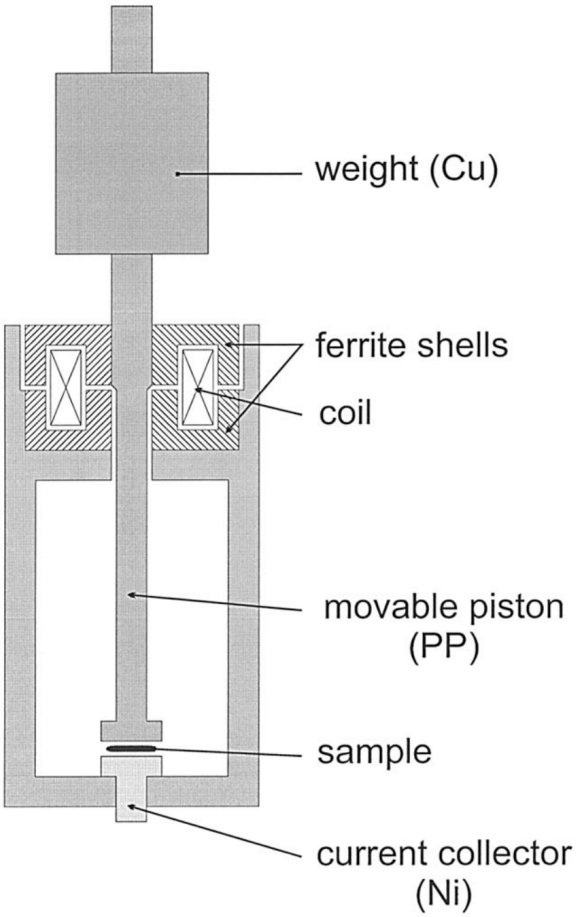

Figure 2.7: Electrochemical Dilatometer layout. Reprinted with permission from [29].

An important development of this instrument was conducted at the Paul Scherrer Institute in the Rüdiger Kötz group [30, 144]. Here, the overall change in volume (i.e. thickness, since it is measured only in the direction orthogonal to the sample surface, neglecting the effects in the other two directions) of the cell

is measured by an inductive displacement transducer. The sample cell consists of a fixed lower electrode acting as a counterelectrode (CE), a separator and an upper electrode acting as a working electrode (WE) and free to move against a constant load (20 N) applied by means of a spring (Figure 2.8). Currently, the instrument described above, in its latest version, is marketed by the company *EL-Cell GmbH*.

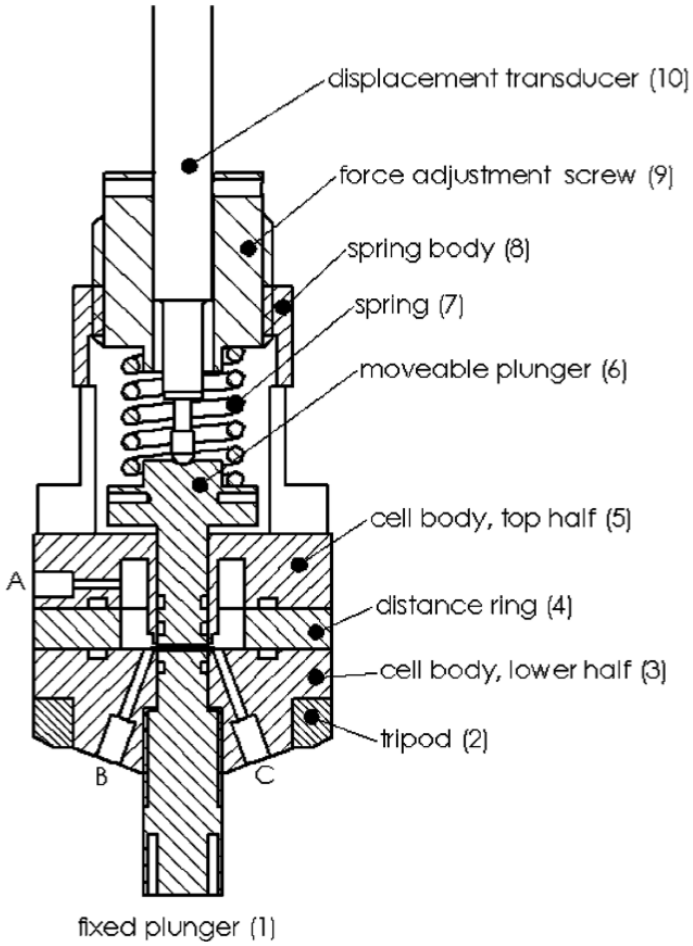

Figure 2.8: Dilatometer in the full cell configuration. Reprinted with permission from [30].

In its latest version the system supplied by EL-Cell (Figure 2.9) the cell sample under test is hermetically sealed in a electrochemical sample holder by external environment. The stack of materials contained in the sample holder consists of a working electrode (WE) which, through a current collector, is connected to a mobile piston and through a membrane to the height transducer. A constant load is applied on the WE through the application of a weight. On the opposite side, to complete the electrochemical cell there is the CE, separated from the WE by a rigid separator called T-frit: it is made of a material that has all the characteristics to work as an electrochemical separator (i.e. to allow the

ionic contact, but prevent the electrical contact) and in addition, being rigid, it separates the contribution of thickness variation of the WE from that of the CE, thus allowing to transducer only the expansion of the upper working electrode. Moreover, given the chemical compatibility characteristics of the fabrication materials (including steel and *polyether ether ketone* ,PEEK) and the small size of the system, it is also possible to test all materials that require handling in a controlled atmosphere, e.g. in absence of oxygen or water. The preparation and setup of the test can be done in a glove box with controlled atmosphere. Then, after the sample is assembled and sealed in the cell, the test can be carried out in ambient atmosphere or in a climatic chamber. The measurement of the thickness variation of the sample under test is transduced through an inductive displacement transducer (*Linear Variable Displacement Transducer*, LVDT).

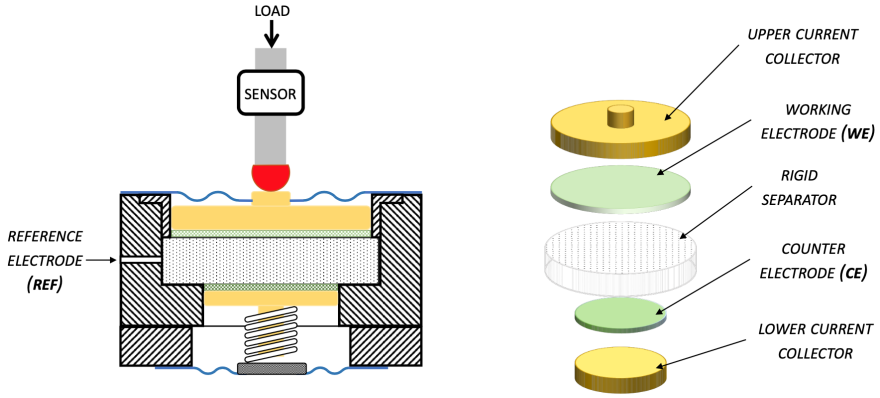

Figure 2.9: Electrochemical Dilatometer: working principle. The principle illustrated is taken from the documentation of the EL-Cell instrument.

Depending on the material that makes up the sample tested, there may be variations of several percentage points. A full Li^+ intercalation in graphite (ideally up to LiC_6) produce a variation of about 10 % of the initial thickness [145] andthe lithiation of $LiFePO_4$ to Li_xFePO_4 produces a variation of about 6.5 % [146].

The system just described is on the one hand the point of arrival of an engineering process that started at the end of the seventies and on the other hand the starting point of the contribution of this thesis work to the improvement of investigation techniques for materials that make up batteries. In addition, there is a plethora of "home-made" systems that are conceptually similar and that meet the needs of the experimenter but do not have all the engineering characteristics of a measuring instrument. Referring to the specific literature for further information, some examples of these home-made systems can be found in ref [147–149].

It is evident at this point that a deeper understanding of the behavior during cycling of the materials that make up the electrodes allows the design phase of an electrochemical cell. The correct choice of the anode/cathode/separator limits problems that would negatively affect the final level of reliability and safety.

In the following chapters we will describe the dilatometric test setup that has been developed in this thesis.

2.3.2. Leak test

Both in the prototype and in the production-industrial phase of a battery, there are numerous tests oriented to obtain a high level of efficiency and reliability according to the specifications and standards required by the application. Among the various tests, the leak test is one of those that can be carried out at several levels, from single cell to the whole battery pack. A loss of electrolyte at the cell level due to mechanical damage could bring to degradation of performance in terms of capacity, to direct contact with humans and trigger several phenomena, including short circuit with consequent increase in temperature and risk of thermal runaway. Moreover, considering that most of the components of the electrochemical system are reactive in the presence of oxygen and water, a possible breakage or perforation of the casing would put in contact with the external environment with high risks of fire. In addition, reactions lead to internal gas evolution. These aspects could bring the level of fire/explosion risk to unacceptable values. The problem is more considerable for big packs, for example in stationary systems [118]. The issue of losses is of primary importance and leakage tests more articulated than the one that is described in this paragraph. Some general aspects of this type of control will be reported below, which are closely related to the controls carried out industrially on the series production of electrochemical cells, modules and battery packs, as well as on the related cooling circuits and plates.

In order to guarantee the widest possible useful life and constant and uniform performance on all cells of the same type, it is necessary to keep under control many production phases of the cells themselves: from the design phase, in which suitable and stable materials are chosen in the appropriate temperature range; to the prototype phase, in which the resistance of the cell in repeated charge/discharge cycles is verified. Once the type of cell has been identified, therefore, all strategies can be adopted to make it work correctly: then a suitable cooling system will be designed, for example, and all the safety precautions mentioned in the paragraph §2.1.2. What is more difficult to predict and therefore requires a specific control method is the occurrence of "statistical" anomalies during the production process. These anomalies may concern, for example, impurities entering the cell, local defects in the material of which the cell casing is made, unwanted air ingress during the closing of the cell casing or module or battery pack, or electrolyte loss. [150–152]. Some defects may also occur immediately or in the short/medium period after the cell has been activated, while others may have their effect over long-term. This aspect considerably complicates the investigation of the defect. Finally, considering that the mere presence of a defective cell in a battery pack can compromise the functioning of the entire battery pack in which it is installed, it is easy to guess that considerable efforts have been invested in finding effective methods to detect defects in the production phases of cells, modules, packages and accessory systems, in particular leak test systems that identify any leaks. Some other considerations should be made:

1. difference between coarse leaks and moderate/small leaks: it is obviously not possible to establish a priori what will be the amount of the loss that will be found, so on the one hand it is necessary to think of a system that is able to identify both the "big" and the "small" leak. In the state of the

art of the leak test techniques there are different methods of investigation preferable according to the entity of the loss (Figure 2.10) [153]:

- in the range of the "*big leaks*", i.e. between 10^2 e 10^{-1} (scc/s, *standard cubic centimeters per second*)), Bubble Test or the Pressure/Flow Drop Test can be performed.
- in the range of "*industrial leaks*", (those most likely to be found in industrial production), i.e. between 10^{-2} e 10^{-7} scc/s, the Pressure/Flow Drop Test can be performed up to 10^{-3}, Bubble Test up to 10^{-4} and leak test with Helium from 10^{-2} to 10^{-7} scc/s.
- in the range of "*small leaks*" that is from 10^{-7} to 10^{-10} scc/s and beyond, the Helium leak test is mostly used.

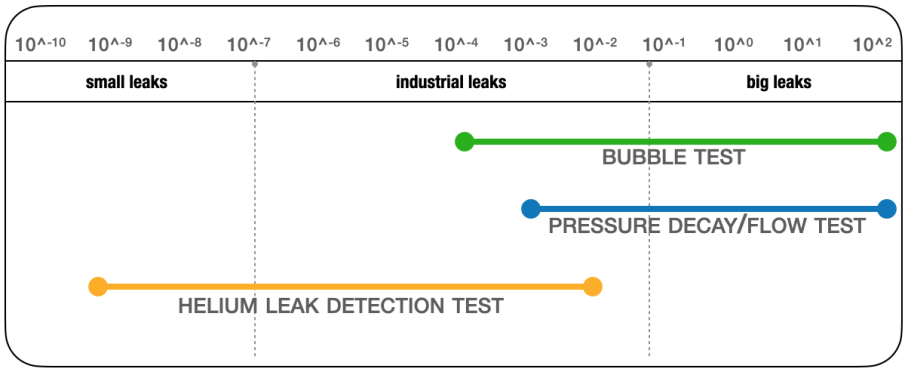

Figure 2.10: Leak Testing Methods. Leak flow in (scc/s)

An in-depth look at leack test techniques can be found in the literature and technical pages of the companies [154, 155] that develop these test systems, for example *http://www.tecnasrl.com*

2. *Master Leak* concept, i.e. defining a known leak to be taken as "reference" so that the leak detection system can be calibrated. For example, as for linear measurements there is the reference sample with the classical characteristics of accuracy, repeatability and reproducibility as well as time stability, it may be necessary to have the same to report gas or liquid leakage. This is a major technical problem that sees numerous studies [156] and prototypes underway by companies: on the one hand because it is not easy to create a "calibrated" leak with the characteristics of a "sample"; on the other hand because the sample must have the characteristics just listed in the measurement range of interest for the application being developed (therefore it must meet the control requirements of the customer who requires it). In this regard, in the field of electrochemical cell controls, the leakage investigation range goes from 10^{-3} to 10^{-7} scc/s. As far as leakage checks on modules and battery packs are concerned, the range goes from 10^0 to 10^{-4} scc/s. Therefore, creating a sample leak in certain measuring ranges complicates its realization quite a bit. The bubble test is not suitable for testing EV battery components.

3. statistical unpredictability of the type of loss: if it is true, as already stated, it is not possible to determine with certainty the amount of the loss that will be detected by the system on the part under examination and it could happen that the system built to detect it is inadequate. For example, to detect the small losses of a cell, in a control station of the production line downstream of the closure of the casing whatever it may be, a method has been implemented that is based on mass spectrometry: therefore the heart of the system is made up of a suitably calibrated spectrometer (therefore the system has been calibrated in a range of scc/s) on the most probable type of loss that is reasonably thought to be found. If an object with a leak outside the calibration range were to appear completely randomly, the spectrometer would present problems of "poisoning", providing an incorrect reading of the leak and therefore an incorrect check of the sample under examination. Moreover, it would be necessary to restore it with consequent "downtime" of the control station. It should be clear at this point the importance of designing a leak detection system that minimizes the possibility of error in the check, ensuring the highest level of effectiveness and reliability.
   Part of the work done in this thesis contributes to increasing the reliability of a system like the one just described in the example.

Marposs S.p.A, the company that hosted this thesis, offers a rather rich range of solutions for the leak testing of automotive EV components. Below a quick overview of the tests offered, please refer to the technical pages (*www.marposs.com*) for further details.

Leak test at Cell level

The integrity of the cell casing is at the basis of the life of a battery: it prevents unwanted and harmful interactions between electrolyte, containing a fluorinated lithium salt and water vapour (hydrofluoric acid can be formed). Preventing the electrolyte from escaping from the case and preventing moisture from entering the case are the fundamental requirements of cell level control. To check the integrity of the cell casing it is necessary:

- the *case* check, before electrode assembly.
- the inspection before filling and sealing the cell.
- the inspection after filling, before and after sealing the cell

This series of control tests are mostly performed using helium as gas tracer and a mass spectrometer as the analysis unit [157].

Leak test at Battery Module & Packs level

Sealed modules and battery packs prevent short circuits deriving from unwanted moisture entry and permit to contain within a certain overpressure any dangerous gas that is formed in case of malfunction. The typical leak rates are defined in order to guarantee the IP67/68 compliance. In case of module huosing,the tests are usually conducted without tracer gas by measuring the absolute pressure decay, or differential pressure, or air flow rate. For battery

pack and its components, it's usually requested to guarantee IP67/68/69K sealing conditions. The tests are done on the housing alone and once the package, with the modules inside, is sealed. To test the battery tray alone the pressure drop or flow test is used with air where possible [154, 156, 158], or with helium in vacuum chamber tests [154, 159]. To test the complete assembly, i.e. the battery pack with the modules inside, a probe is usually used to detect local leaks along the entire sealing perimeter of the battery pack.

Leak test at Cooling Circuits and Plates level

In the modules, in the packs and in the power control system there are cooling circuits or plates for heat exchange with a fluid, keeping the temperature in the correct operating range. A loss of refrigerant fluid, usually a mixture of water-glycol or refrigerant gases, would lead to an uncontrolled rise in temperature with the triggering of potentially disastrous phenomena. Moreover, it could lead to short circuits. In this case, for the test of the plates and components of the circuit, it is possible to use either the measurement of pressure drop or flow drop with air, or the test with helium tracer gas if the refrigerant fluid is a gas. In the latter case the test is done in a vacuum chamber [158] using a mass spectrometer as analyser [154]. Once the refrigeration system has been assembled, it is possible to check the tightness of the entire circuit using probes that sniff near the joints: in this case any leaks are detected, in the order of 10^{-3} to 10^{-5} scc/s, checking for the presence of previous helium injected into the refrigeration system.

2.3.3. Industrial sensors for gas detection

Identification and quantification of traces of substances in small quantities is of particular importance in various technical fields. As mentioned in previous chapters in today's revolution in the automotive sector energy harvesting is a crucial issue that at least at this stage, denotes the outlines of this epochal transition from ICE (*Internal Combustion Engine*) to EV (*Electric Vehicle*). Lithium-ion batteries, in all the variants currently on the market, are the most "precious" parts to take into consideration and for this reason are the objects that technically must have the highest possible performance and require a careful control of its manufacturing process. Often a drop in battery performance is certainly linked to a leak of electrolyte and this can occur both during the production process and during use: therefore detection of electrolyte leaks could optimize the production process minimizing of process waste. Furthermore leak detection during use of the single battery or battery pack could provide a diagnostics giving alarms in order to control efficiency or avoid event failure. Recent researchs show that human health is significantly endangered by the exposure to harmful gases, explosives or Volatile Organic Compounds (VOCs) causing respiratory diseases, skin diseases and SBS (Sick Building Sindrome) [160]. This, in addition to the growing sensitivity to environmental pollution, consolidates the importance of having more or less integrated and integrable systems that are able to detect potential dangers where our senses do not reach us. Gas sensing also plays a crucial part in fire detection, drug delivery, food safety, environmental monitoring, and national defense security [161, 162].

The aim of this paragraph is to illustrate sensors, developed as an extension

of the human senses, that can be used for the detection of leak electrolyte or rather detect VOCs from the leaking electrolyte, both in portable or stationary applications [163].

Gas Sensors: state of art

Given the extensive scientific and technical literature, an attempt will be made to provide an insight, probably not entirely exhaustive, into the main technologies that detect gases, starting with those of more industrial use.
A gas sensor is a device which detects the presence of gases, which might be harmful to humans or animals. The development of gas sensor technology has received considerable attention in recent years for monitoring environmental pollution. It is well known that chemical gas sensor performance features such as sensitivity, selectivity, time response, stability, durability, reproducibility, and reversibility are largely influenced by the properties of the sensing materials used [164].

1. Industrial Gas Sensor
   Several classifications of gas sensors have been made: Liu et al. [162] has classified the gas sensors based on their sensing methods and divided them to two groups: (a) methods based on variation in electrical properties and (b) methods based on variation in other properties. Materials like *Metal Oxides Semiconductor* (MOS), carbon nanotubes and polymers are able to sense gas based on variation in electrical properties. The other variations are optic, acoustic, gas chromatographic and calorimetric. Comini [165] classified the gas sensors according to the measurement methods as: (1) DC conductometric gas sensors (2) Field-Effect-Transistors (FET) based gas sensors (3) Photoluminescence (PL) based gas sensors. Interesting is also the analysis made by Korotcenkov [34] which compares different types of sensor according to certain basic parameters (see Table 2.1).

   According to Hooker [166], you have:

   - *Catalytic Combustion Gas Sensor*: the operating principle of a catalytic combustion sensor is based on the oxidation of the combustible gas in contact with a surface covered by an electrically heated catalyst compound. The oxidation causes an increase in the temperature of the sensitive element (pellistor), generally consisting of a resistor or of the same heating element, depending on the concentration of the gas detected. The resulting change in resistance of the sensitive element can be determined and the control electronics calibrated to provide concentration or alarm measurements. Among the positive aspects of this sensor are its long life, high precision, quick response and versatility. However, for operation it requires a minimum oxygen content and is subject to the poisoning phenomenon [167].
   - *Semiconductor Gas Sensor*: the operation of a semiconductor sensor is determined by the conductivity variation of a semiconductor element (SnO_2), caused by the chemical absorption of the gases in contact with the porous surface of the electrically heated semiconductor at a predetermined temperature. The temperature of the

Parameters	**Types of Gas Sensors**				
	SMO Gas Sensor	**Catalytic Combustion Gas Sensors**	**Electro Chemical Gas Sensors**	**Thermal Conductivity Gas Sensors**	**Infrared Absorption Gas Sensors**
Sensitivity	E	G	G	B	E
Accuracy	G	G	G	G	E
Selectivity	P	B	G	B	E
Response	E	G	P	G	P
Stability	G	G	B	G	G
Durability	G	G	P	G	E
Maintenance	E	E	G	G	P
Cost	E	E	G	G	P
Suitability to portable instruments	E	G	P	G	B

Table 2.1: Comparison of various types of gas sensors. (E=excellent; G=good; P=poor; B=bad). [34].

sensitive element (depending on the type of gas to be detected between 100 and 450°C) is a determining parameter for sensitivity / selectivity. Positive aspects of this sensor are the low cost, long life and versatility [161, 168].

- *Electrochemical Gas Sensor*: the operation of an electrochemical sensor is determined by the variation of the electrical parameters of two electrodes immersed in an electrolyte solution. This variation is caused by the reactions of the gas in contact with the surface of the electrodes. This type of sensor is widespread to detect toxic gases. The advantages of this sensor are the low power consumption and versatility. Unfortunately, it has a long response time and requires frequent calibration operations [169].
- *Infrared Gas Sensor*: the operating principle of an infrared sensor is based on the absorption of energy in the infrared spectrum by the gas analyzed and on the consequent variation of energy absorbed by an infrared receiver chosen for a specific wavelength band. This band corresponds to a specific gas which the sensor is most sensitive to. Therefore the infrared sensor is by its nature selective. Long life, low response time and stability are among the main features of this sensor. Nevertheless it is very sensitive to the environmental conditions [170].
- *Thermal Conductivity Gas Sensors*: the detection principle of thermal conductivity sensors is based on a known temperature difference wich is maintained between a "cold" and a "hot" element. Heat is transferred from the "hot" element to the "cold" element via thermal conduction through the investigated gas. The power needed to heat

the "hot" element therefore is a direct measure for the thermal conductivity. Heat loss due to radiation, convection and heat conduction through the sus- pensions of the "hot" element need to be minimized by sensor design [171]

2. Laboratory gas sensors
   Among the traditional techniques of molecule analysis it is necessary to mention the most widespread, that is:

   - Mass spectrograph
   - Raman spectroscopy

   Referring to the specific literature for further study,for example [172, 173], it is undoubtedly true that both are very effective on a wide range of gases with excellent selectivity. However, they are difficult to use in an industrial environment, unless they are ideally suited for their use. They are also expensive.

3. Nanostructured gas sensors: chemical gas sensor performance can be evaluated in terms of sensitivity, selectivity, time response, stability, durability, reproducibility, and reversibility. It is worth noting that the sensitivity of chemical gas sensors is strongly affected by the specific surface of sensing materials. Higher specific surface of a sensing material leads to a higher sensor sensitivity, therefore many techniques have been adopted to increase the specific surface of sensing films with fine structures, especially to form nanostructures, taking advantage of the large specific surface of nanostructured materials. One of these techniques, among the most smart nanotechnologies that allows the use of polymers, semiconductors, organic / inorganic composites is electrospinning [174–176]. Therefore, using an electrospun material as a sensitive element, an increase in sensitivity and response time is expected. Since 2004 this type of sensor is an excellent alternative, albeit still in a laboratory scale, to gas sensors with a flat film sensitive element. Given the versatility of the technology, different sensing techniques can be implemented [177]. Below are the main ones:

   - *Resistive Gas Sensor*: there are two types of these: the first is based on the use of conductive polymers, in which the charge carriers are free to move along the polymer chain (conductivity). These sensors are suitable for the immobilization of gas molecules (chemical selectivity) and are reversible. The tested gases are: NH_3, H_2O, acetone, ethylacetate. The second one is based on metal oxides: nanowires (starting from oxides and precursors through annealing) or composite nanofibres (polymer + metal oxide, eg TiO_2, SnO_2). Tested gases: NO_2, CO, methanol [178, 179]
   - *Photoelectric Gas Sensor*: They are based on the variation of conductance of zinc oxide. The traditional ones (not nanostructured) operate at high temperatures, and require a very high temperature for their activation, so they are difficult to use. Tested gases: O_2. [164, 180]

- *Optical Gas Sensor*: the nanofibers are used to increase the sensitivity of FTIR equipment (Fourier Transform Infrared Spectroscopy): the absorption spectrum of a particular substance is measured, and nanofibers (composite nanofibers) increases the sensitivity of the measurement [181, 182].
- *Acoustic Wave Gas Sensor*: The nanofibers are laid over a QCM (*Quartz Crystal Microbalances*), increasing their sensitivity: the nanofibers of a certain material interact with the gas by varying its weight. In output there is a variation in the resonance frequency of the quartz crystal proportional to the quantity of gas.Tested gases: NH_3, H_2O, H_2S, CH_3, SH, benzene [177, 183].

Carbon Nanotubes & Conducting Polymers as Gas sensors

Among the characteristics that make CNTs excellent candidates for the realization of sensitive elements of gas detection sensors are certainly the excellent electronic properties and the high surface-volume ratio (after all, they are frequently processed through the electrospinning technique) [184]. Moreover, the good mechanical and chemical stability and the ease with which they can be combined with other materials, such as polymers, make them extremely sensitive as sensors for several gases[185].
Conductive polymers, Polypyrrole (PPy), Polyaniline (PANI), Polythiophene (PTh), Poly(3,4-ethylenedioxythiophene) (PEDOT), are equally attractive materials: given their structure, they offer wide margins of customization that allow to calibrate the response of the sensitive element made with these materials towards the specific response of the gases to be detected [186]. They are therefore particularly useful for the detection of organic vapours [187].

Metal Oxide Gas Sensors

Among the gas detection sensors, Metal Oxide Semiconducors (MOS) are those that have found many industrial applications due to their simplicity. Numerous materials have been reported to be usable as metal oxide sensors including both single (e.g., ZnO, SnO_2, WO_3, TiO_2, and Fe_2O_3) and multicomponent oxides ($BiFeO_3$, $MgAl_2O_4$, $SrTiO_3$, and $Sr_{1-y}Ca_yFeO_{3-x}$) [188] . The strength of this technology is that besides being simple it can be use a wide range of materials as sensitive elements, allowing the fabrication of sensor with precise characteristics and with good selectivity. [162]. The mechanism for gas detection in these materials is based, in large part, on reactions that occur at the sensor surface, resulting in a change in the concentration of adsorbed oxygen [189]. Oxygen ions adsorb onto the material surface, removing electrons from the bulk and creating a potential barrier that limits electron movement and conductivity. When reactive gases combine with oxygen, the height of the barrier is reduced, increasing conductivity. This change in conductivity is directly related to the amount of a specific gas present in the environment, resulting in a quantitative determination of gas presence and concentration. Most sensors of this type are produced through deposition process. In this technique (Figure 2.11), multiple layers (including the sensor material itself) are deposited onto rigid substrates and heated to a relatively low temperature to partially densify the sensor. These substrates are then integrated into modified electronic stacks.

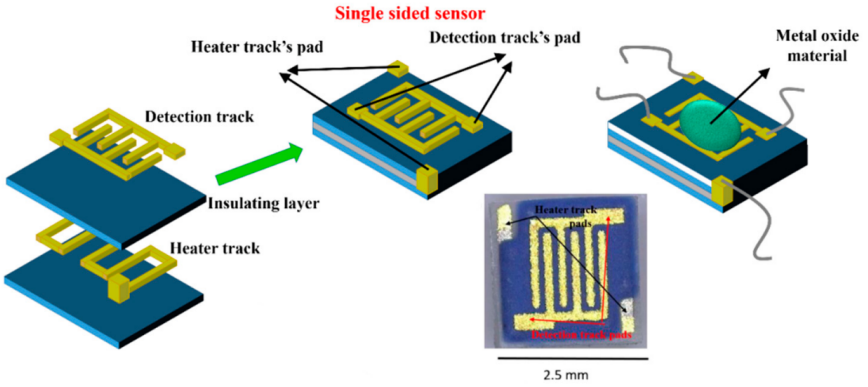

Figure 2.11: Metal-oxide substrate construction. Reprinted with permission from [31]

An interesting application of this type of sensor concerns the integrity verification of a Lithium-ion cell: Wenger et al. [190] detect volatile organic compounds (VOC) from the leaking electrolyte, whereas standard cell monitoring methods can only detect a leak indirectly over premature cell performance degradation.

Photoionization Detectors

Photoionisation is an established detection method originally developed to be used with high-performance, laboratory-sized gas chromatographs (GCs). Photoionisation detectors (PID) of interest to this thesis work are implemented in portable instruments suitable for field detection being battery-powered. They provide a direct response to a wide variety of organic and some inorganic compounds. In particular, they are suitable for detecting VOCs in concentrations that are typically in the range of 0.01 to 10000 ppm (parts per million), with very accurate measurements down to about 2000 ppm. They work very well in applications where, for example, catalytic sensors are at the limit of their effectiveness and where, for example, FID (Flame Ionization Detectors) are too bulky. From their first industrial applications in the early 1970s in soil monitoring and fumes in environmental remediation operations, PIDs have evolved. With the advent of microelectronics and high-power portable batteries, they have become miniaturised and have been integrated *on-board* into portable equipments. This development has favoured the widespread of PID in industrial hygiene, where, a wide range of chemicals can be detected by simply inserting a correction factor (found experimentally by calibrating the sensor in the laboratory against isobutylene gas) which allows the instrument to be calibrated against the chemical species to be detected. The technical evolution of these sensors has recently made it possible to detect organic compounds with resolutions from 1 to 10 ppb (parts per billion), confirming them as powerful tools for measuring ambient levels of organic vapours even in indoor environments such as offices. This need is increasing as regulatory agencies begin to include total VOC limits in their indoor air quality guidelines [160]. Other emerging applications for this type of sensor include the detection of drugs, chemical warfare agents, and the

localisation of microbiologically generated VOCs such as mould in buildings[32].

Working Principle

The PID sensor (Figure 2.12) consists of a short wavelength ultraviolet (UV) lamp shining on a small cell containing the gas sample.

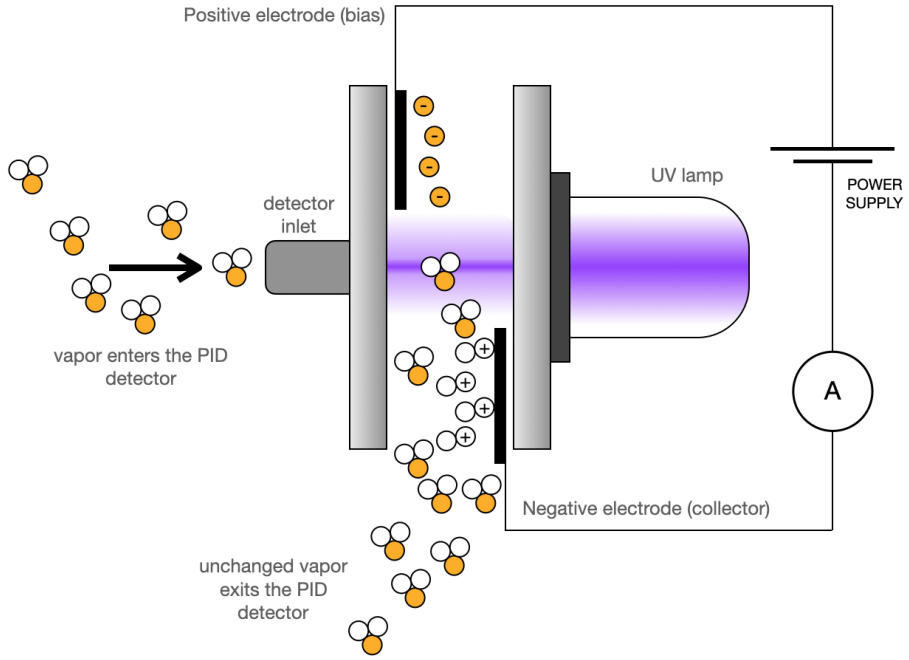

Figure 2.12: General schematic of a PID sensor. Image reconstructed from [32]

Inside the cell are two electrodes with an applied electrical potential. The UV light photo-ionises all organic compounds eventually present in the sample, but not the air, resulting in the ejection of electrons and the formation of positively charged molecules. The electrons and positive ions are attracted to the electrodes and the resulting current is proportional to the concentration of gas or vapour. Theoretically, any compound with an ionisation energy (IE) lower than that of the lamp's photons can be detected, with virtually instantaneous response times (in the order of milliseconds) in the applications mentioned above, which depend heavily on the speed at which the sample is brought into contact with the sensor. [32].
The application of this sensor in a control system for a battery production line will be proposed and described in the following chapters.

Towards the future: Smart Sensors

For all that has been said so far, there can be no doubt that safety is the aspect on which we must concentrate our efforts: batteries will certainly be used more and more intensively, that is they will require higher performance. They will also be used more and more "extensively", that is by more and more people

and in an increasing number of applications. It is therefore necessary to be familiar with available and to know their limits. In the last decade, with the beginning of the spread of the electric vehicle, the level of reliability of the systems that monitor energy storage systems has increased considerably. However, these systems mostly operate "from a remote location". As an example, we consider the temperature a potential trigger of disastrous phenomena: it can be detected either during the design phase of the cell, i.e. in the laboratory, by means of thermocouples or pyrometers. Even if the measurements were precise and the tests replicate as much as possible the real operating conditions of the cell, thery are still laboratory tests. The temperature of the remaining part near the cell can also be measured by the systems installed on the battery pack: these measurements, calculated by the control logic of the Battery Management System (BMS), have the intrinsic defect of being punctual, i.e. not fully representative of all the cells that make up the pack. It is clear that in order to overcome the intrinsic characteristics of current control systems and significantly increase the level of safety, it would be necessary read the temperature as close as possible to the cell during actual operation. In recent years the trend has been to integrate sensors into the battery, aiming at the creation of an "intelligent battery" able to communicate its internal state and interface with the outside world.
Considering not only temperature but also deformation as a monitoring parameter of the correct functioning of a cell, there are several studies in recent years in which these quantities are measured and monitored using *in situ* optical fibre sensors. Bae et al. [191] have embedded *Otical Fiber Bragg Grating* (FBG) within Li-ion battery pouch cells in order to monitor the internal electrode strain during cycling. Thermocouples are difficult to integrate inside the electrochemical cell, so its "sensing" takes place in the laboratory on a sample that is often partially disassembled [192, 193]. Alternatively, thermocouples, FBG sensors and other sensors like *distributed optical fibres* (DFOS) based on Rayleigh diffusion [194] are placed on the external surface [195] and the measurements help the validation of mathematical models that predict the evolution in temperature of the cell during repeated charge/discharge tests. In other interesting studies, both FBG (which translate variations of different nature into deformations) [196] and small sensors such as thermocouples [197, 198] or *Resistance Temperature Detector* (RTD) [199] are integrated in a less invasive way in cells prepared *ad-hoc* in the laboratory. The integration of FBG, thermocouples or other sensors within the battery structure [200, 201], be they cylindrical, prismatic [202], pouch or coin, certainly indicates that the technological efforts that need to be made are aimed at obtaining a monitoring as close as possible to the phenomena that occur inside the cell, whether electrochemical, thermal, mechanical or other, because only in this way can you really grasp the state of operation of the system by intercepting malfunctions at the origin.
This trend has been the one that the European Community has deliberately indicated in the aforementioned initiatives (§1.4). It is worth mentioning a number of existing projects that in the next few years will establish Europe both from a technical and economic point of view as a world nerve centre for the production of new generations of batteries. *INSTABAT*, project focused on embedded physical and virtual sensors and coordinated by CEA, *Commissariat à l'Energie Atomique et aux Energies Alternatives, France*, through in operando reliable monitoring of key parameters (i.e., temperature and heat flow, pressure, strain, Li^+ concentration and distribution, CO_2 concentration, abso-

lute impedance, potential and polarisation) and an enhanced BMS algorithms, allow us to improve the safety and the quality, reliability and life of batteries (*https://battery2030.eu/research/research-projects/instabat*) [203]. *SENSIBAT*, coordinated by the Ikerlan technology centre in Spain, aims to create temperature, pressure, conductivity and impedance sensors inside the batteries to monitor their operating status and extend their life (*https://battery2030.eu/research/research-projects/sensibat*) [204]. *SPARTACUS*, supervised by the Fraunhofer Institute in Würzburg, Germany, will develop integrated acoustic-mechanical and thermal sensors for the diagnosis of reactions leading to battery degradation (*https://battery2030.eu/research/research-projects/spartacus*) [205]. *BAT4EVER*, led by Vrije Universiteit Brussel, is studying a new type of electrochemical cell that uses self-healing polymers made of silicon anodes, nucleo-shell structured cathodes and electrolytes; the desired objective is to compensate for internal micro damage due to repeated charge/discharge cycles by increasing the capacity and durability of the battery (*https://battery2030.eu/research/research-projects/bat4ever*) [206].
The experimental activity carried out in this thesis work, which will be described in the next chapters, certainly takes its inspiration from the last paragraphs of this chapter with the ultimate aim of contributing to the generation of more efficient and safe energy storage systems, such as batteries.

3. Materials, techniques and experiments

Il valore di un'idea
sta nel metterla in pratica.
T.A. Edison - inventore

In the following section a deep overview of the materials, techniques, and experiments adopted in this work is presented.

3.1. Dilatometric Bench

In the design of an electrochemical dilatometer with advanced functionalities, able to effectively measure the expansion/contraction of the electrode materials in an electrochemical cell during charge/discharge cycles, it is necessary to define a series of specifications that will guide the choice of materials and geometries that will constitute the instrument. Below are the starting specifications:

- the system must be able to measure a variation in thickness. This variation is on average 10 % of the initial thickness of the sample to be measured. The typical thickness range for this type of material is from 30 μm to 100 μm for anode and cathode and from 100 μm to 250 μm for separator.
- the measurement of the thickness variation could be made on a sample consisting of the complete cell (*anode-separator-cathode* or an half-cell (*electrode-separator*). This sample must be able to be measured in the correct direction in order to appreciate the maximum contribution of this variation (it actually has three components). The possibility of further implementing the system in order to also allow the measurement of single electrode expansion ias been considered.
- the materials making up the sample cell to be tested must be circular in diameter: ø15 mm for the anode and cathode and ø20 mm for the separator.
- sample preparation must be possible in a controlled environment, such as that of a dry box; the sample holder must also be able to ensure perfect separation of the active materials in the cell from the external environment, given their reactivity in the presence of oxygen and moisture.

- it must be ensured that the holder materials have a good degree of chemical resistance to the electrolytes used, i.e. that the latter can be contained and separated from the external environment, avoiding undesirable reactions due to leaks in the liquid or vapour phase.

- the sample under test must be able of being subjected to a compressive force during repeated charge-discharge cycles; the range of compressive force is from 10 N to 100 N. The possibility of designing a force application system that is able to vary the range of force values available in the initial setup phase is not excluded.

- the electrochemical cell under test must be able to undergo the normal charge-discharge cycles set by existing laboratory equipment, without unwanted short circuits occurring.

- the system will be used in a temperature-controlled environment, guaranteeing a variation of $\pm$ 1°C; however, the possibility of performing tests from -10 °C to 60 °C must be guaranteed.

- activation of the sample cell inside the sample holder will be done by adding liquid electrolyte, that could be aqueous or non aqueous.

- the tests carried out with the instrument will have a duration that may vary from a few hours to a few weeks. During the tests it will be necessary to acquire the thickness measurement (or rather its variations) with an acquisition frequency that varies according to the needs of the experiment, as well as the internal and external temperature values. The data collected during each test shall be saved in a file for further processing.

3.1.1. Materials

Following the listed requirements, the materials chosen to make the dilatometer are:

- X30 Cr13, EN10088 , corrosion-resistant stainless steel, supplied by Interacciai S.p.A for the structural frame of the instrument and the current collectors between which the sample cell will be assembled.

- ASTM B265 6AL-4V Grade 5, high strength and toughness titanium alloy with good welding and fabrication characteristics, provided by Alloy Wire International, for the sample holder structure.

- *Ketron*® 1000 Peek, polyetheretherketone resin with high toughness and impact strenght, high dimensional and temperature stability, supplied by *Quadrant Engineering Plastic Products* (QEPP), for electrical insulation parts and those in direct contact with the electrolyte.

- EN AW 6082 Anticorodal 100, high-hardness aluminium alloy, supplied by CO.ME.F.I. Metalli s.r.l, for the locking ring nut of the specimen holder.

- NBR rubber (50SH), supplied by Stampaggio Gomma s.n.c., for the external gasket.

- perfluoro elastomer DuPont^{TM} *Kalrez*® Spectrum^{TM} 6375, highly resistant to chemicals in the electrolyte, provided by DuPont^{TM}, for the gasket inside.

3.1.2. Techniques

The proposed equipment provides several improvements over the state of the art:

- avoids moving components with friction, minimising its magnitude where relative movement is unavoidable.
- is equipped with an adjustable test pressure system in the specified range. A load cell with a measuring range from 0 to $0.5kN$, supplied by Burster, is used to calibrate a graduated scale to be mounted on the instrument and which can be read and acquired with the same frequency as the main measurement of the bench (thickness variation), providing an instantaneous reading of the force applied to the sample under test.
- has a layout in which the specimen holder can be temporarily separated from the rest of the bench for the necessary setup and recovery operations, which certainly require a suitable controlled atmosphere environment.
- uses a measuring system with adequate resolution with respect to the expected phenomenon (resolution of at least 0.1 μm). In this regard, the use of an inductive meter with sealed measuring head (to avoid contamination) is envisaged, among those available in the Marposs S.p.A. catalogue.
- includes two temperature sensors: one measuring the temperature of the environment around the bench, type Pt100 Marposs with a maximum error of $\pm$ 0.5$^{\circ}C$; the other positioned inside the sample holder very close to the cell under test, type *Pt1000* ohm with ø3x30mm, supplied by Italcoppie Sensori s.r.l, which measures any temperature variations of the sample during charge/discharge cycles.
- for the acquisition and recording of measurements over time, the system is equipped with a purpose-built hardware consisting of: four Marposs DigiCrown2^{TM} modules for transducers acquisition (inductive gauge, thermocouples and load cell), power supply and E9066E^{TM} Marposs industrial PC running the Quick SPC^{TM} package for Windows ® for data logging (manual or automatic) and saving.

In addition at the beginning of the test the distance measurement on the sample itself could be set to zero, after which all subsequent measurements will be recorded as variations of the initial recorded thickness. However, for the calibration of the bench during testing, the use of calibrated "master" thickness gauges is envisaged.

For this, PTC Creo ® 4.0 was used, software for 3D modelling and for the drawing of all the parts that make up the dilatometer. For the production of the parts, after the design process, the well-established CNC machining techniques were used, starting from raw materials in various forms or from semi-finished products. For the assembly and the final adjustment phase before testing, all

good mechanical workshop practices were used, involving the orderly assembly of sub-assemblies and groups and the subsequent assembly using synthetic grease and Prussian blue respectively for the connections and for any interferences to be eliminated manually.

3.1.3. Experiments

Several tests were carried out in order to validate the proposed equipment. Firstly, routine functional checks were carried out to validate the assembly phase: a check-up of all the assembled bench units was carried out to verify their actual functionality. Next, the transducers were tested, namely:

- load cell calibration (Figure3.1): by applying a known weight to the load cell, it is verified that the value of the reading corresponds, in tolerance, with the expected value corresponding to the master weight.

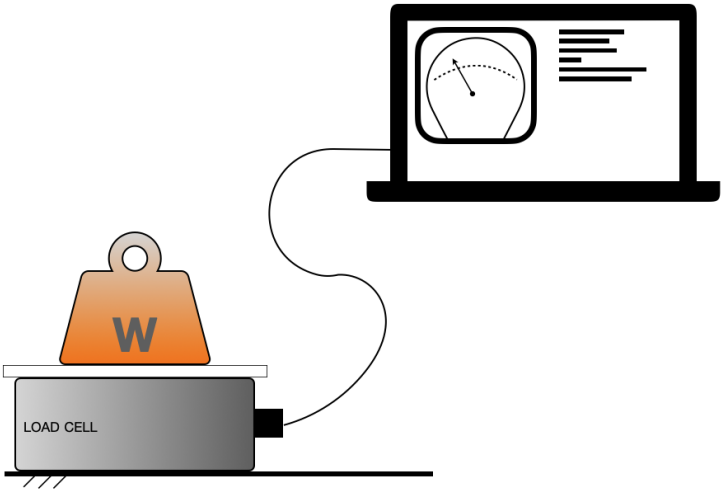

Figure 3.1: Schematic layout of the setup used for load cell calibration.

  In the event of a mismatch, a correction is made by entering appropriate coefficients in the transducer software interface.

- calibration of the Marposs temperature sensor, by means of an internal calibration procedure (the Pt1000 thermocouple from Italcoppie sensori s.r.l is supplied already calibrated and ready for use).

- calibration and thermal drift of the inductive transducer used to measure the change in volume of the sample under test (Figure3.2). This step is necessary in order to verify the thermal stability of the inductive gauge, which will probably have to take a measurement at a certain frequency throughout the duration of the test (even several days). The objective is to find the coefficients which correct the value measured by the gauge when it is in an environment which, although the temperature is controlled, has a certain thermal drift. For this, the inductive gauge under consideration and two other comparator gauges, an LVDT (*Linear Variable Dis-*

placement Transducer) and an HBT (Linear Variable Displacement Transducer) are rigidly mounted on a static C-shaped support (Figure3.2(a)) and connected to the acquisition electronics so as to record their readings in a predefined time range in which the temperature may vary. The holder with the transducers is placed in a thermal chamber, ClimeEvent C/600/40/3, purchased from Weiss Technik Italia Srl(Figure3.2(b)). By recording the temperature and measurement trends for each transducer and monitoring the temperature of the substrate on which the transducers are mounted, it is possible to verify the correctness of the measurement and, if necessary, correct it by entering the appropriate coefficients.

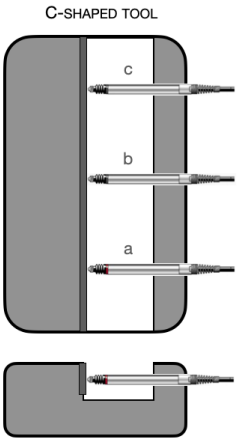

(a) C-shaped rigid tool with mounted transducers: a)inductive transducer; b)LVDT transducer; c)HBT transducer.

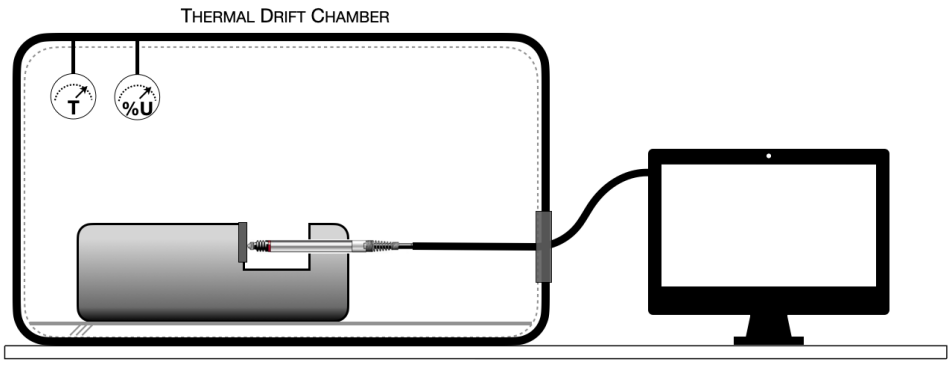

(b) Thermal drift chamber and setup for transducer drift test.

Figure 3.2: Transducers calibration.

Once the calibrated transducers have been definitively tested by connecting them to the electronic hardware, the thermal drift test of the entire instrument is carried out: the aim is to check its behaviour within the temperature range

declared in the specifications, i.e. -10 $°C$ to 60 $°C$ in order to guarantee the correctness of the measurement as the temperature changes. Also in this case, several thermal drift cycles are performed in the climatic chamber. Once the whole measuring system has been placed internally, (Figure3.3) the drift cycle is programmed and the test is started. At the same time, with a certain frequency set on the electronics connected to the dilatometer and placed outside the thermal chamber, the values of all the transducers on the instrument are acquired.

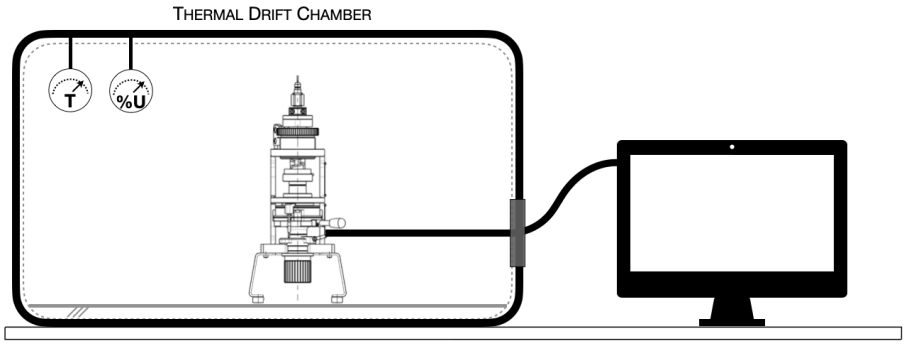

Figure 3.3: Schematic layout of the setup used for dilatometer thermal drift.

In performing the test, it is taken into account that:

- no sample is inserted in the sample holder of the instrument, so the starting condition is with the two current collectors in contact.
- it is necessary to record the temperature at which the sample holder is closed: this is because during the closing process a certain volume of air is trapped inside. As the temperature changes, this volume of air will expand or contract with the temperature according to the perfect gas law. This must be taken into account when calibrating/testing the instrument.
- it is necessary to verify the behaviour of the instrument as the applied force varies in addition to the temperature variation. Therefore applied compression force, temperature and transducer measurement value are the three variables to be correlated.

One of the most important parts of the designed instrument, which requires great attention, is the electrochemical chamber inside which the under test is assembled and sealed. Once the sample electrochemical cell is hermetically sealed inside, this volume must be isolated from the external environment. For this reason, a leak test of the sample chamber alone was carried out using Helium as a tracer gas (Figure 3.4(a)).

Helium is injected into the hermetically sealed sample chamber and the connections between the two parts of the chamber are inspected using an INFICON portable helium detector to detect any leaks from the designed seals. (Figure 3.4(b)). Considering that helium is the gas with the smallest molecular mass after hydrogen, helium leakage test can detect very small losses of up to $10^{-11} mbarL/s$. This should ensure tightness in the presence of gaseous phases derived from the electrolytes currently used in batteries.

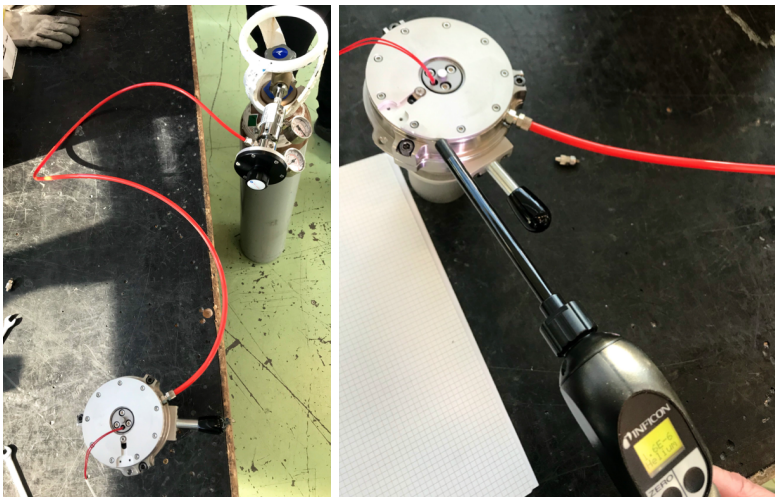

(a) Setup used for the helium leak test: using a tube, helium contained in a tank is injected at a certain pressure into the sample chamber.

(b) Seal inspection with portable sniffer.

Figure 3.4: Helium leak test on sample chamber.

In the next chapter, the results of the tests just described will be illustrated.

Once the functional test phase was completed, the dilatometer was given to the researchers of the Laboratory of Electrochemistry of Materials for Energetics at the Department of Chemistry " Giacomo Ciamician" of the University of Bologna, so that they could test the instrument in its real conditions of use. The tests conducted were essentially of two types:

1. functional tests in the laboratory: i.e. suitable dimensions compatible with the equipment present (dimensions of the sample holder compatible with the glove-box, total dimensions of the dilatometer compatible with the internal volume of a common laboratory oven).

2. electrochemical tests: i.e. repeated charge/discharge cycles on real samples consisting of anode-separator-cathode-electrolyte of which the change in volume due to the intercalation/deintercalation of lithium ions is to be measured.

We refer the description of the materials and equipment, as well as the dilatometer, used to carry out these tests to the relate publication [207], but we would like to point out that after the first tests and their results, which will be summarily illustrated in the next chapter, it was decided to start the design of the sample holder for single-electrode (or rather, half-cell) tests, in which only the contribution of volume variation of the working electrode alone is measured. The results of this new design part will be explained in the relevant section of the next chapter, describing the technical measures taken.

3.2. PID Sensor

The use of a PID sensor, as described above,(§2.3.3) is proposed for the leakage detection in coin cells by setting up a control station in the production line: the aim is to find an alternative way to the established use of spectrometric techniques (§2.3.2). It has been planned to proceed step by step, i.e. first of all to combine this control with that carried out with the mass spectrometer: consequently, the detection of "small" leaks is carried out by the spectrometer, while "big" leaks are detected by the PID sensor. In the next chapter, only the part relating to basic experimentation will be reported, i.e. that aimed at validating the use of the PID sensor for detecting electrolyte leaks. In addition, the proposed layout of a control station on a coin cell production line using PID technology for detecting defective batteries downstream of the sealing process will be described.

3.2.1. Materials

A commercial PID sensor integrated into a VOCs detection instrument was used for initial testing activities, mod. *FALCO Diffused* 1-3000 ppm , purchased by ION Science. The instrument has an integrated PID sensor with Krypton (10.6 eV) lamp and provides an accuracy of $\pm$ 5 % with respect to the calibration point (*isobutylene* gas as reference). The samples used for testing consist of small amounts of dimethyl carbonate (Sigma-Adrich, $\geq$99%), which are poured into a metal vessel and placed in the detector inlet hole.

3.2.2. Techniques

Preliminary tests are conducted using an instrument that works under 'static' conditions, i.e., exploiting the natural diffusion of the substance in the air. In addition, the use of a system such as a penstock with a pump or fan, which allows the molecule to reach the instrument's nose more quickly, thus minimising the sensor's response time, is immediately considered.

3.2.3. Experiments

Tests are conducted under various experimental conditions (Figure 3.5), including:

- sample in air, at different distances from the instrument inlet hole connecting the PID sensor to the external environment (Figure 3.5(a)).
- sample inside a closed cup and sensor connection pipe (Figure 3.5(b)).
- sample consisting of a *coin cell* on which a hole is drilled with a diameter of 0.3 mm (Figure 3.5(c)).

3.3. Smart Colorimetric Sensor

Following the European trend of improving the degree of efficiency and safety in batteries, an innovative approach is proposed to monitor the proper functionality of a Li-ion cell, e.g. as part of a battery pack for electric vehicles. The

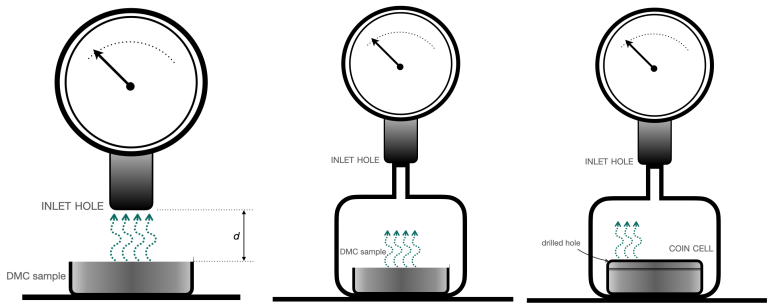

(a) PID open-air test setup.

(b) PID closed-chamber test setup.

(c) PID closed-chamber with coin cell.

Figure 3.5: PID tests setup.

focus is on this application despite the fact that in theory the new sensor concept is also perfectly suited to stationary applications for example. In addition, although the concept is developed and tested from a lithium-ion cell, it theoretically also applies to subsequent generations of batteries. Thus, two fundamental aspects must be considered:

1. a system must be created that monitors the quantities as close as possible to the electrochemical cell so as to give a warning signal in case of malfunction in a shorter time than the current systems used in electric vehicles (e.g. BMS, *Battery Management System*); to increase the level of security, a monitoring and control system with a shorter response time than the systems currently used would certainly be needed.

2. both in the Li-ion batteries, currently the most used, and in those of future generations, the normal electrochemical reactions that occur at the two electrodes are flanked by secondary reactions that potentially pose a risk to the efficiency and safety of the battery. These secondary reactions give rise to reaction products that, harmless and tolerable within certain limits, negatively affect the operation of the cell if present in large quantities.

The aim is to prove that by monitoring the concentration of molecules by colorimetric technique in particular areas inside the cell (Figure 3.6), it is possible to determine the amount of reaction by-products and thus intercept malfunctions much earlier than with current systems. The goal is to create a system able to detect the presence of chemical species at one of the two electrodes of the cell, fully integrable within the cell and reversible, i.e. able to switch from the initial state to the activated state and vice versa, more than once.

Insertion materials used in lithium-ion batteries, change their color upon electrochemical insertion of lithium ions [208]. On this basis, it is attempted to construct a sensor which will intercept the colour in the vicinity of the electrodes, or in other areas inside the electrochemical cell which may vary their colour. It is highly probable that the positioning of such a sensor will change depending on the type of cell and its materials. In any case, the basic architecture of the proposed sensor is simple (Figure 3.7(a)). A miniaturised commercial RGB sensor detects colour variations that are highlighted by a micro-LED placed close

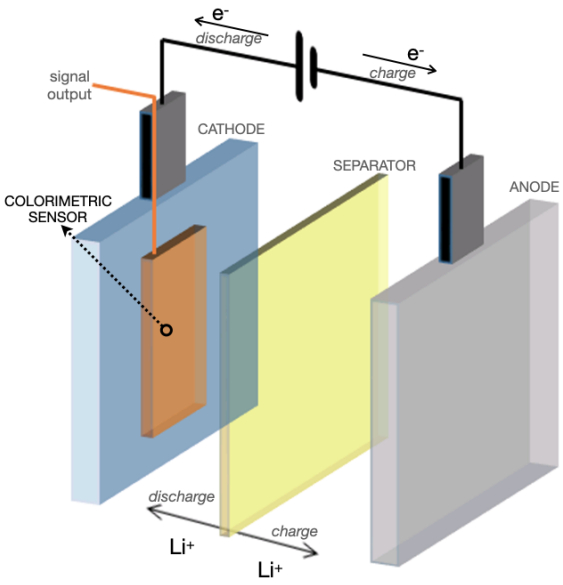

Figure 3.6: Colorimetric sensor "idea": possible layout inside the cell.

to the RGB sensor: the RGB sensor and micro-LEDs, mounted on a support and encased in a material that chemically protects them from the substances contained in the electrolyte, transmit any detected colour variations to the outside world that can be traced back to malfunctions or their initial stages. If the colour change is small and possibly undetectable, or if the reaction compounds are weakly coloured, it is proposed to integrate an 'amplification layer' into the sensor (Figure 3.7(b)) consisting of a material that colours itself in the presence of reaction compounds. This material could be a thin layer of nanometric fibres 'doped' with appropriate additives that are sensitive to the expected reaction compound and that become strongly coloured in its presence, causing the sensor detection.

3.3.1. Materials

A colorimetric sensor prototype, as outlined in Figure 3.7, has been realised using *ISL29125 digital RGB color light sensor* with IR blocking filter, purchased by Renesas; an *evaluation board*, ISL29125EVAL1Z, purchased by Renesas, was used to interface the sensor with a PC so that information from the sensor could be displayed and recorded. In order to provide light to the sensor, which would otherwise remain in the dark once inserted into the cell, *an LED* TOPLED E1608, mod. KW DELPS2.RA, purchased by Mouser Electronics has been mounted on the RGB sensor holder close to it. A *transparent encapsulant* from DOW® was used to isolate the sensor and protect it from chemicals once inside the battery, the SILGARD^{TM} 184 Silicone Elastomer, purchased as two-part liquid component kits.

The first laboratory tests were performed using coloured aqueous solutions consisting of:

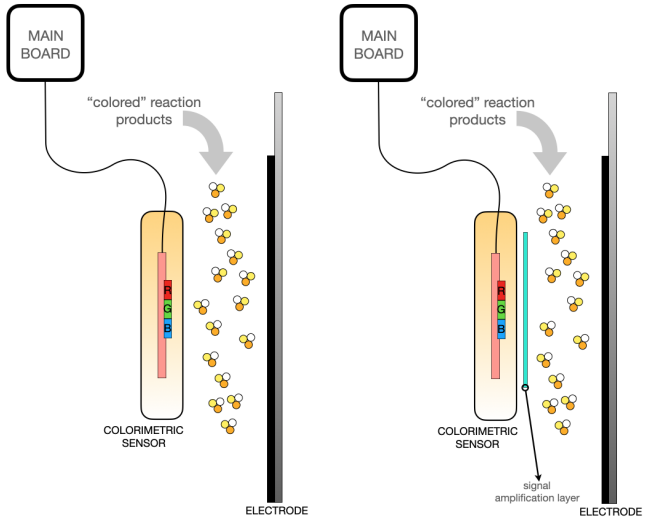

(a) Conceptual layout of the colorimetric sensor.

(b) Layout of the colorimetric sensor with amplification layer.

Figure 3.7: Colorimetric sensor setup.

- Nickel(II) acetate tetrahydrate 99.0+% (Sigma Aldrich, Germany) in distilled water (green solution).
- Copper(II) acetate monohydrate 99.01+% (Sigma Aldrich, Germany) in distilled water (blue solution).
- rose bengal dye content 95.0% (Sigma Aldrich, Germany) in distilled water (purple solution).

Finally, the sensor was tested inside an electrochemical cell that was specifically build to accommodate the sensor. The cell was constructed using:

- Silgard ^{TM} 184 for resining and attaching Microscope slides
- Container: hermetically sealed glass chamber
- the cell was assembled in a dry box (LabMaster SP, MBraun) with argon atmosphere (H_2O <0.1 ppm, O_2 <0.1 ppm), with LNMC working electrode (80% of $Li(Ni_{1/3}Mn_{1/3}Co_{1/3})O_2$ (Gelon), 10% polyvinylidene difluoride (PVDF) , 10% Super P on Al current collector) and lithium metal as counter electrode and reference electrode.
- the electrolyte was 1 M $LiBF_4$ ($\geq$ 99%, Fluka) in propylene carbonate (PC, $\geq$ 99%, Fluka) and the two electrodes were separated by a Teflon® spacer. The electrochemical tests were carried out with a multi-channel VMP (Perkin Elmer, Waltham, MA, USA) potentiostat/galvanostat.
- the electrochemical characterization started with three charge/discharge cycles between 2.8 and 4.6 V *vs* Li^+/Li, with a charge at C/5 constant current (CC).

3.3.2. Techniques

In the sensor prototyping phase, the LED is first soldered to the board on which the light RGB sensor is mounted (Figure3.8(b). The resulting assembly is then connected to the main board using a 6 mm pentapolar cable, approximately 25 cm long, to allow the sensor/illuminator to be used close to the sample cell 3.8(a).

(a) Colorimetric sensor assembly.

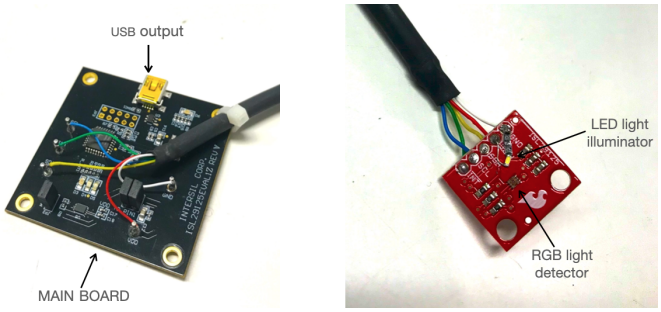

(b) Connection of pentapolar cable on main board side and sensor side. Detail of RGB sensor and LED illuminator.

Figure 3.8: Colorimetric sensor assembly phase.

The assembly is then encapsulated in the silicone-based encapsulant using a polypropylene mould (Figure 3.9).

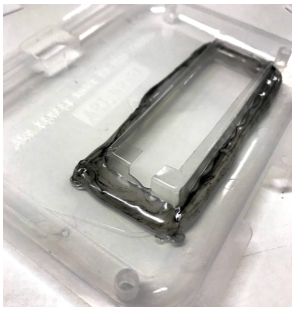

(a) Mould for casting encapsulant.

(b) Casting assembly.

Figure 3.9: Colorimetric sensor moulding phase.

After 12 hours, the dried encapsulant has perfectly encapsulated the support

where the RGB sensor and illuminator are mounted (Figure 3.10).

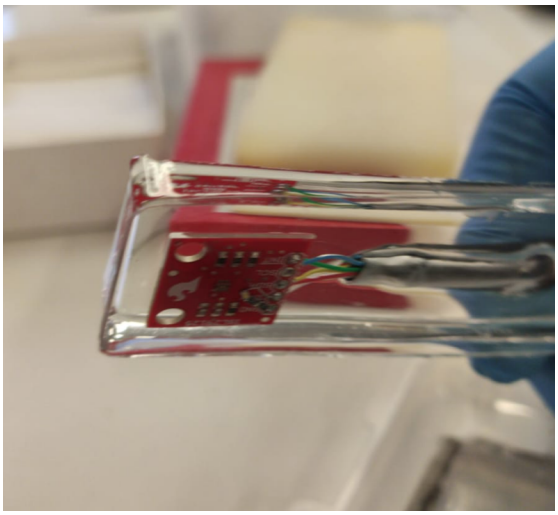

Figure 3.10: Encapsulated and dry assembly.

For the electrochemical cell test, a container is constructed with the colorimetric sensor at its base (Figure 3.11(a)). Once assembled, the container was brought inside the dry box and the electrochemical cell safely assembled inside the container. When the cell is mounted inside the container, the whole assembly is sealed inside a glass cylinder with a sealed cap that allows the passage of cables for charge/discharge tests and for connecting the sensor to the main board (Figure 3.11(b)).

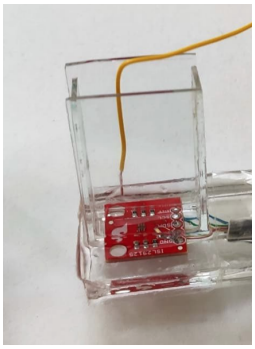

(a) Assembled "tumbler" with colorimetric sensor at base.

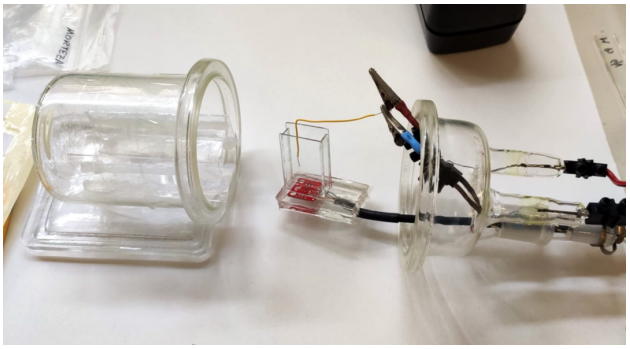

(b) Glass container and sensor assembly.

Figure 3.11: Experimental setup with electrochemical cell and colorimeter sensor.

3.3.3. Experiments

In a first step, tests are carried out using coloured aqueous solutions: the aim is to investigate the behaviour of the sensor in a non-aggressive environment such as the inside of an electrochemical cell. Aqueous solutions were prepared by dissolving a certain amount of dye in water Figure 3.12. Different colour gradations were obtained to investigate the behaviour of the sensor under different conditions.

Figure 3.12: Coloured aqueous solutions tested.

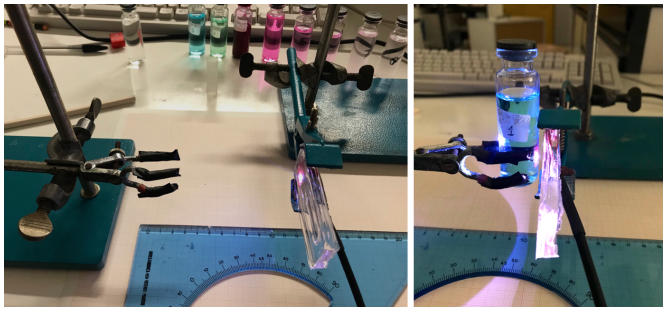

(a) Colorimetric sensor close to coloured solution: test setup.

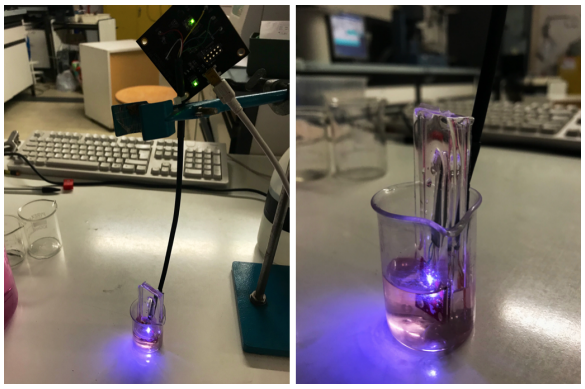

(b) Colorimetric sensor immersed.

Figure 3.13: Colorimetric sensor tests with coloured aqueous solutions.

First the test is carried out by placing the sensor close to the container with the coloured solution (Figure 3.13(a)). Then repeat the test by immersing the sensor in the coloured solution (Figure 3.13(b)).

In the second step, the prototyped sensor is tested in a real electrochemical cell. The system Figure 3.11 allows the assembly of the cell and the sensor to detect the colour changes during cycling. Sample electrochemical cell is assembled (Figure 3.14(a))and placed inside the container (Figure 3.14(b)).

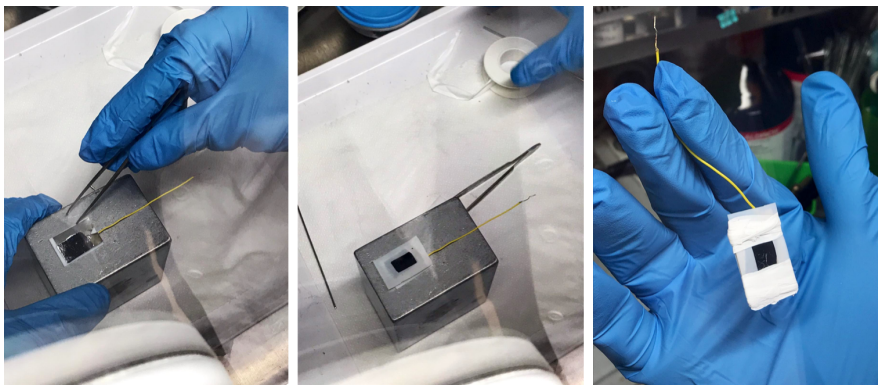

(a) Cell sample assembly: raw materials.

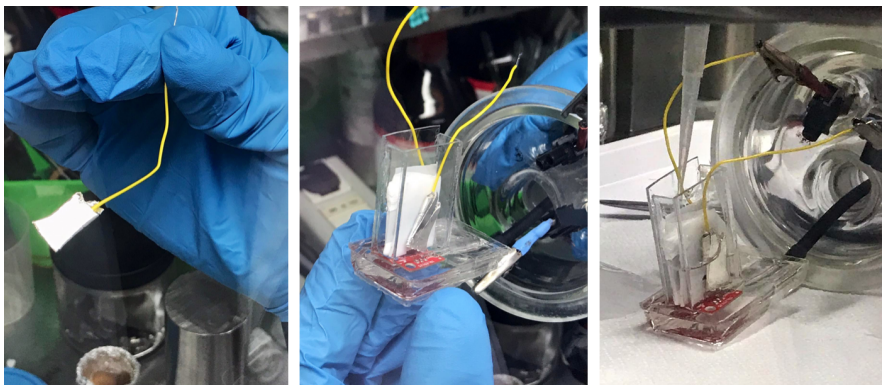

(b) Full cell sample assembly.

Figure 3.14: Electrochemical cell tested with colorimetric sensor.

After the assembly phase is completed, the glass container is sealed (Fig. 3.15(a)) in order to isolate the electrochemical cell inside the external environment. In order to create the right test conditions, we close the glass container inside a box (Figure 3.15(b)), preventing light variations during the test from influencing the measurement of the colorimetric sensor. At this point, having closed the box and connected the main board to the PC, it is possible to set the parameters for repeated charge/discharge cycles.

(a) Final sealed assembly

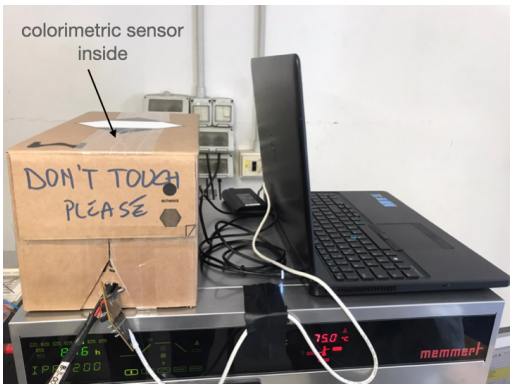

(b) containment box for isolating the sensor from external light

Figure 3.15: Electrochemical cell test setup with colorimetric sensor.

4. Results and discussion

One cannot plan for the unexpected.
Human curiosity, the urge to know is a powerful force
and is perhaps the best secret weapon of all
in the struggle to unravel the workings of the natural world.
A. Klug - chimico e biofisico

4.1. Dilatometric bench Testing

Following the specifications introduced in §3.1, a bench for measuring the expansion of electrode materials during charge/discharge cycles has been realised (Figure 4.1), with the following main features:

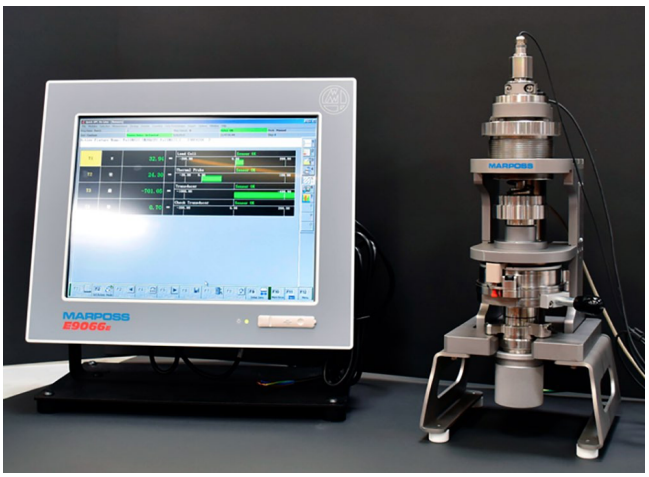

Figure 4.1: Dilatometric Measurement Bench.

- possibility of applying a compressive force to the sample under test, even during the test, from 10 N to 100
- possibility of changing the range of force applied, during the retooling of the instrument.

- possibility of conducting "*whole cell*" (anode-separator-cathode) (Figure 4.2(a))or "*half cell*" (only the working electrode, WE)(Figure 4.2(b)) tests.

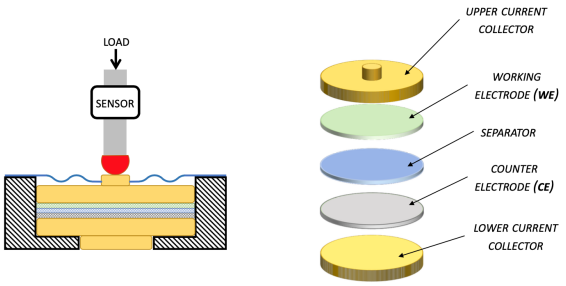

(a) "*Whole cell*" test working principle.

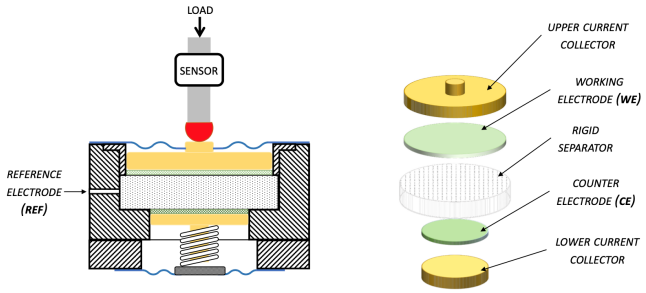

(b) "*Single cell*" test working principle.

Figure 4.2: Test configurations available on the bench

The designed measurement bench (Figure 4.3), consisting of:

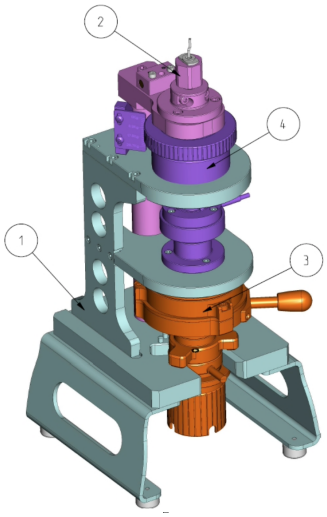

Figure 4.3: Main parts of the measuring bench.

1. a frame consisting of a base and two support: the vertical development of the measuring bench makes it possible to respect Abbe's Principle [209, 210], one of the fundamental guidelines for the design of measuring instruments. This principle states that "to improve measurement accuracy, the target and the scale of the instrument must be aligned in the direction of measurement". In this case it is possible to have both the measuring device (scale) and the sample to be measured (target) vertically aligned. When designing an instrument that works on a laboratory bench, it is important to consider weight and size as binding aspects: for this reason a *main frame* (Figure 4.4(a)) is designed with three support planes necessary to support the sample holder (*lower plane support*), the lower part of the system that imparts the force on the sample (*intermediate plane support*) and the upper part of the system in which the applied force is adjusted (*upper plane support*).

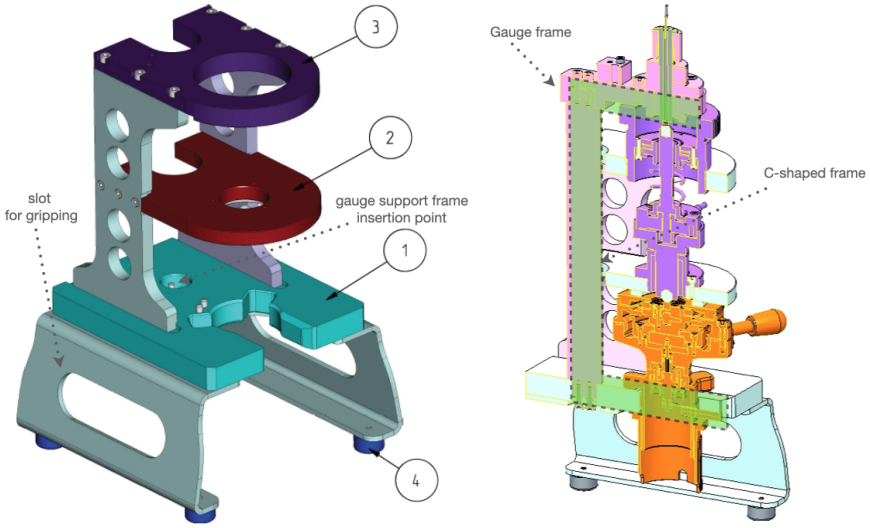

(a) Parts of bench main frame. (1: support of electrochemical chamber; 2: suppport of lower part of load adjustment system; 3: support of upper part of load adjustment system; 4:ground support with electrical insulation;)

(b) Gauge frame (pink) and resulting *C*-frame

Figure 4.4: Frame of measuring bench

Various parts of the frame have been lightened to minimise weight while maintaining mechanical rigidity: in particular, the two slots on the base not only act as lighteners but also allow the instrument to be gripped from below. It should be noted that the frame supporting the measuring system is connected to the main frame in only one area, that of the lower plane: as this is the most rigid, a mechanically stable support for the gauge frame is guaranteed; furthermore, as the latter is not linked to other parts of the main frame, the best condition for correct operation of the measuring system is achieved, i.e. the "C" support (Figure 4.4(b)), such as that of the micrometers for external diameters.

2. a non-contact measurement system so as not to influence the natural dilation of the sample during the tests. Among the gauges that can be used for this application and that are available in the Marposs S.p.a. catalogue, a non-contact one is chosen. In fact, if a phenomenon such as electrode expansion is resolved in a few microns, it is expected that the use of a contact measuring system, with a measuring head that physically touches the sample to be measured, could negatively affect the metrological performance of the system. The gauge used is an inductive magnetic sensor that measures a linear variation by calculating the magnetic reluctance of an air gap formed between the gauge and a target made of a ferritic material (Figure 4.5). The measuring range is 500 μm, the resolution 0.01μm and the maximum non-linearity error 0.1 μm.

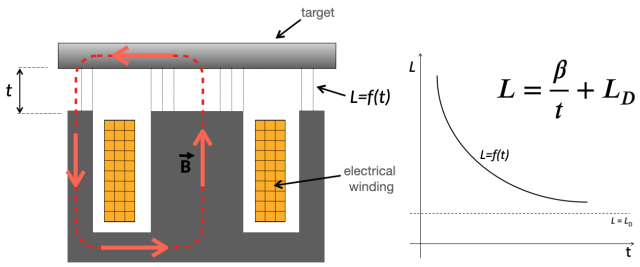

Figure 4.5: Inductive magnetic gauge working principle.L_D: leakage inductance ;β:form factor ;t: air gap.

Each linear measuring device must also be placed "in the field", i.e. in the centre of its measuring range. This is why the designed measuring system has a manual adjustment ring nut (Figure 4.6) with which the relative position of the measuring device in relation to the reference can be varied during measurement setup.

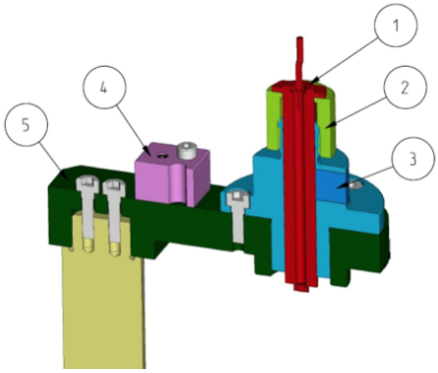

Figure 4.6: Measuring system assembly on the dilatometer bench.(1: contactless, magnetic inductive gauge, connected to E9066 Marposs electronics; 2: gauge adjustement ring; 3: gauge fixture ; 4: room thermal probe; 5: frame.

In addition, a *Marposs Pt100 ambient temperature probe* is positioned close to the gauge: this allows us to monitor the temperature of the environment

in which the bench is working but also to have a precise temperature reference close to the gauge. On the other hand, the designed bench will give the best response in stationary temperature conditions.

3. an electrochemical chamber composed of an upper electrical contact, a lower electrical contact and an electric and chemical insulation system. The chamber receives the sample to be tested and can be transported in glove-box for assembly and setup operations of the samples to be tested (Fugure 4.7).

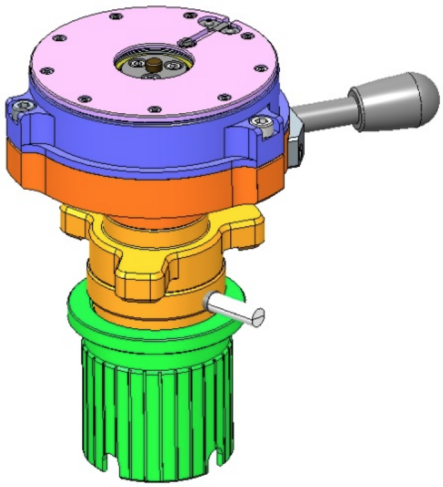

Figure 4.7: Sample holder

Given the importance of the component, as it accommodates the sample to be tested, quite a lot of work was carried out, starting with:

- choice of materials, particularly in the part in contact with the cell sample. The adoption of materials with a high chemical and electrical resistance allows a safe containment of the sample to be analysed. In addition, being a component of the bench, it must fit into it in a repeatable manner so as to guarantee the correct positioning of the sample under the measuring system. Also in this case, the choice of material has made it possible to create a rigid object, with solid reference parts and at the same time with a limited weight (about 1.5 kg).
- definition of the geometries. Specifically, the one that allow the coupling of the sample holder to the static part of the bench, the one of the internal components, and the one defining the final external dimensions. To ensure rapid and repeatable coupling of the sample holder to the main frame of the instrument, a star-shaped coupling was chosen, which allows repeatable positioning and secure tightening in two movements (Figure 4.8). To avoid accidental electrical contact, the internal components were shaped to create an isolation "shell" between the powered cell and the external structure. Finally,

the optimisation of the external geometry was aimed at achieving a footprint suitable for the dimensions of the access chambers, the smallest of the glove-boxes usually used in laboratories.

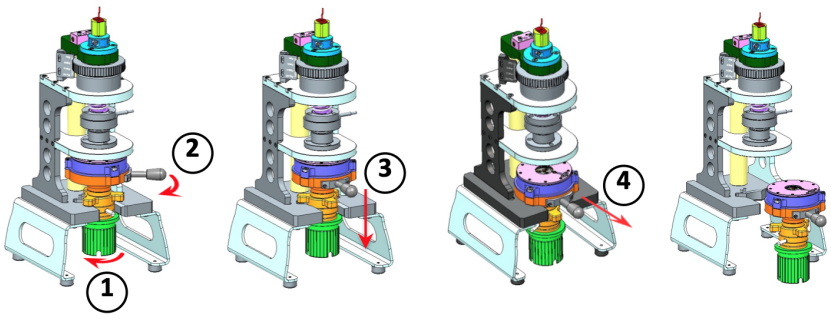

Figure 4.8: Unmounting chamber from bench

The resulting structure of the sample holder is compact and suitable for easy handling. In the setup phases of the experiment (Figure 4.9) it can be easily introduced into the glove-box.

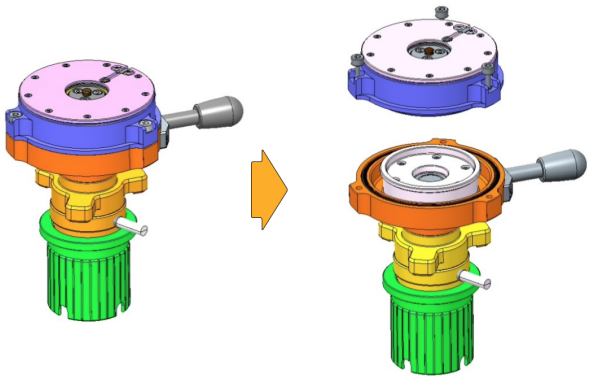

Figure 4.9: Sample holder setup operation.

Here, through simple operations, the sample holder can be opened, allowing the preparation and assembly of the sample inside; each internal part can also be disassembled for cleaning and restoration. Once preparation is complete, the sample holder can be closed and sealed, isolating the sample from the external environment.
The technical details described are purposely hidden in the images for reasons of intellectual property.
In order to enable the instrument to test in the two modes described in Figure 4.2, two sample holders with the same geometry and external dimensions were designed. In designing the sample holder for "single cell" tests, particular attention was paid to the choice of the material of the rigid separator. In addition to all the characteristics of a conventional separator, it must be non-deformable under the action of the compression force applied to the sample, allowing only the expansion of the working

electrode to be measured. Another important aspect has been considered: in single-electrode dilatometric measurements, it is necessary to have a reference electrode inside the sample cell which allows to evaluate the electrode potentials (WE-reference and CE-reference). For this purpose, a reference electrode integrated in the rigid separator has been developed, the technical details of which are omitted due to intellectual property issues (patent application pending by Marposs S.p.a).

4. a force regulation system which allows tests to be carried out at different pressing force on the cell. The peculiarity of the force regulation system (Figure 4.10) is that it has a "*variable range*".

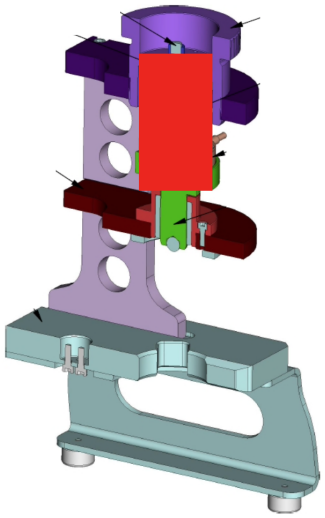

Figure 4.10: Load Setting System

While in the manufactured version the compression force on the sample can vary from 10 to 100N, which can be adjusted manually by means of a ring nut, by reconfiguring a part of the system it is possible with almost all the same components to deliver a compression force in a different range, for example from 50 to 150N or from 5 to 10N.

Following, a brief description of bench working principle. After setting the electrochemical sample chamber in position, the two current collectors, one for the upper electrode (WE) and one for the lower electrode (CE) are electrically connected to the potentiostat, with the reference of teh potentiostat short circuited with the CE. Then adjustement ring are used to lead the desired load above the electrode stack. The value of the load applied can be read from the graduated scale placed near the ring nut or, as an option, by reading the load cell through the dedicated electronic module. Once the desired load has been reached, the test can start and the gauge, connected to dedicated electronic will monitors the expansion. During the charging and discharging cycles of the cell, the measurement system will rise and fall following the cyclic expansion of the electrodes in the sample under test, without adding force components that would alter the measurement.

Sample volume variation measurements are acquired and recorded together with ambient temperature, sample temperature, and applied compression force values through the Marposs E9066, a configurable industrial computer for logging data from the gauges. Acquisition of the probes on the instrument can be either *frequency-set* or *one-shot*.

The aim is to correct any errors in the response of the test bench to changes in temperature. Although the test should be carried out under static temperature conditions as specified, i.e. away from transients, a tolerance must be associated with the set temperature value, within which the true value may vary: therefore, understanding the behaviour of the measuring bench at temperature is fundamental to achieving a good level of reliability of the measurement obtained from the test. The results obtained during the thermal validation tests for both the linear gauge (Figure3.2) and the full bench (Figure 3.3)are summarised below.

4.1.1. Thermal drift test on inductive magnetic gauge

In this section a full description of what happens when the inductive gauge works in an environment where the temperature varies is presented. As explained in the previous chapter, the inductive gauge is used as the main transducer in the designed bench and according to the specification, should work at constant temperature $T \pm 1°C$. Despite this, the test was carried out in the air-conditioned room of the Marposs test laboratory, where a maximum temperature range of $\pm 2°C$ is guaranteed.

The temperature variation and measurement variation curves from the thermal drift test are detailed presented in Figure 4.11.
In Table 4.1 the metrological-thermal parameters extracted from the curves are listed. From the tests carried out it has been observed that all three transducers have good temporal stability characteristics, and that the variations in the measurement are mainly due to the variation in temperature. In fact, comparing the trend of the three transducers with the trend of the temperature probe, it can be seen that there is good consistency between the curves.

	Temperature Probe ($°C$)	**IMG** (μm)	**LVDT** (μm)	**HBT** (μm)
max-min	4.1	0.75	0.6	0.3
thermal drift ($\mu m/°C$)		0.18	0.15	0.07

Table 4.1: Gauge thermal drift test.

The IMG transducer is, of the three tested, the one with the greatest thermal drift. It must be considered, however, that placing all the transducers at the centre of the measuring field, different conditions are obtained between IMG and the differential transducers: while LVDT and HBT at the centre of the field are in the position where the thermal drift has the least effect as they have an electrical zero due to the way they are constructed, the magnetic inductive transducer does not have an electrical zero and is placed in the middle between the most favourable zone (beginning of the field) and the most unfavourable zone (end of the field). The thermal drift test of the magnetic inductive transducer

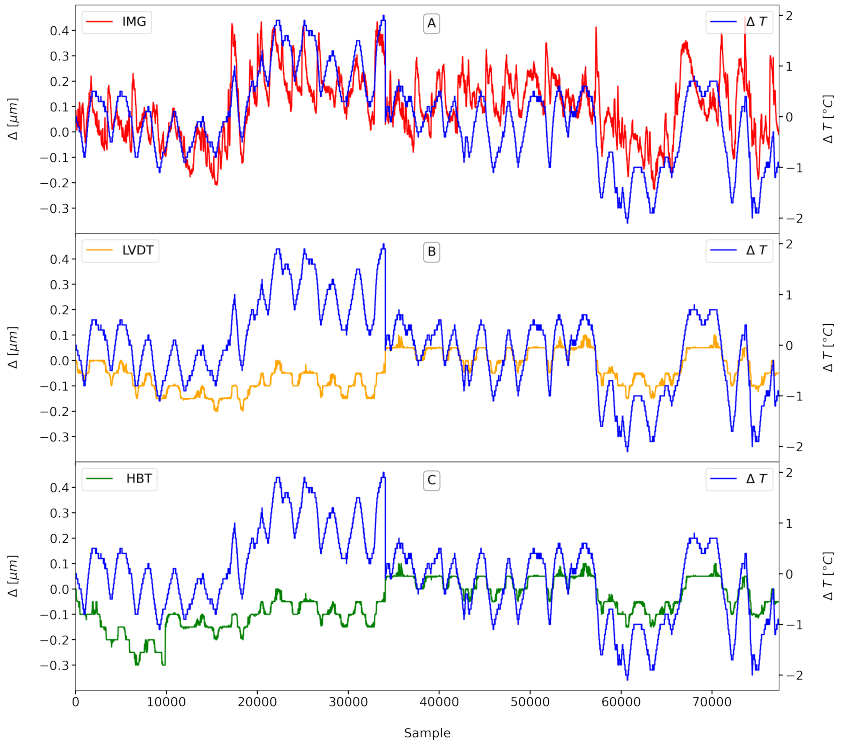

Figure 4.11: Gauge thermal drift test: A) Inductive Magnetic Gauge (*IMG*) variation vs. Temperature variation. B)*LVDT* variation vs. Temperature variation. C) *HBT* variation vs. Temperature variation.

alone was then repeated, no longer in the thermal chamber but in air at room temperature, monitoring the daily temperature range with a thermal probe.

As can be seen in the Figure 4.12, the trend of the measurement variation curve follows with good approximation the temperature variation curve. This variation (Table 4.2) also reflects what was found during the stability test. By compensating for the temperature variation, excellent thermal stability results are obtained (green symbols in Figure 4.12).

	Temperature Probe ($°C$)	**IMG** (μm)	**IMG** comp. (μm)
max-min	6.7	1.1	0.5
thermal drift ($\mu m/°C$)		0.17	0.08

Table 4.2: Daily thermal drift test: the effect of compensation.

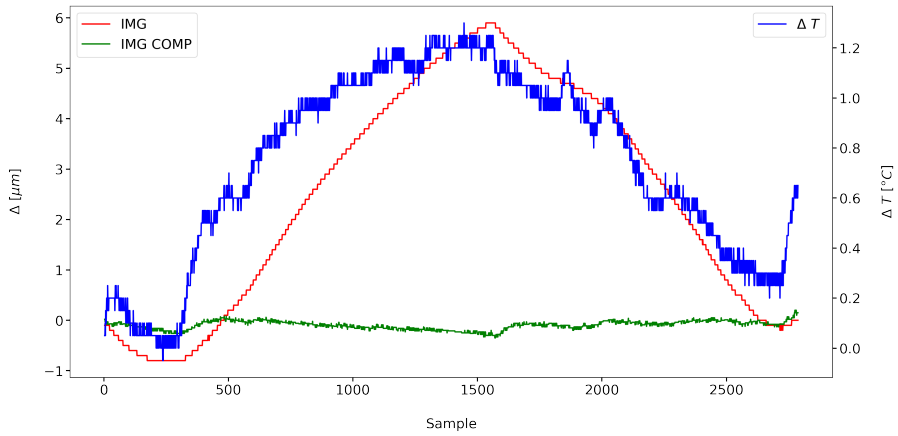

Figure 4.12: IMG daily thermal drift test. Temperature Variation *deltaT* (blue line); Gauge drift (orange line); Compensated gauge (green line)

It is confirmed that the gauge chosen to transduce the measurements on the dilatometer bench is suitable for working even in conditions of slight thermal transient, all the more so in a temperature controlled environment within the limits already specified.

4.1.2. Thermal drift test on whole bench

This section shows the results of the drift tests performed on the measuring bench with the aim of verifying the behaviour of the measurement as the temperature changes over the specified range. In the first part of the experimental campaign, although a certain deviation of the measurement due to the expansion of the instrument components was expected, an unexpected result is found.

Figure 4.13, the drift cycle set in the thermal chamber. In Figure 4.13(A), the blue line represents the temperature and the green line the thickness. In proximity of the temperature rise from 30 to 60°C and from 60 to 40°C there is an anomalous trend of the measurement given back by the IMG: there is an asymptotic growth of the measured value up to a saturation. An equally unusual trend is that of the compression force recorded by the load cell. In this case too, in addition to the normal drift of the measurement caused by the temperature, something unexpected is added, always in the same temperature range (Figure 4.13(B)). In consideration of the results obtained from the tests on the gauge alone, the cause of this "strange" drift is to be found in the mechanical aspects of the bench. Other tests are repeated which, both with the same thermal cycle and with different sequences of thermal jumps, confirm this anomaly. After ruling out settlements due to the coupling of the various parts that make up the instrument frame, the conclusion is reached that the cause of the unexpected phenomenon has to be found in the sample holder.
The air trapped inside the sample holder following the closing of the upper part on the lower part (this operation is necessary as it allows the battery sample

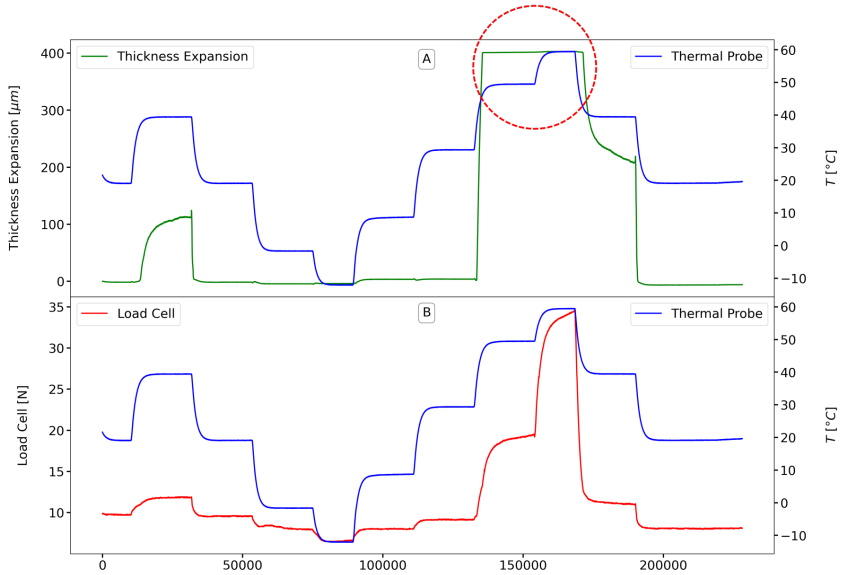

Figure 4.13: Thermal drift test on the whole bench: the anomalous trend of the measure (green line) is evident in the stretch circled (A).In (B), load cell *vs* temperature trend.

to be isolated from the external environment), expands and contracts as the temperature varies (Figure 4.14). As a result, at a certain temperature, the trapped air expands, causing the entire measuring crew to rise and the resulting loss of electrical contact between the electrode and the upper current collector. A careful analysis of the problem revealed that:

- The volume of gas trapped inside the sample holder should be minimised, thus reducing the unwanted phenomenon. This consideration offers certain insights for future design phases but is hardly feasible in the immediate future.
- The expansion/contraction of the gas inside the sample holder is not related to the temperature value at a given time but to the difference between the temperature at which the sample is prepared and the temperature at which the test is carried out.
- The only force that opposes this phenomenon is the compression force that the operator manually imposes on the cell under test.

For this reason it has been decided to overcome the problem by correcting the value of the applied compression force in order to counteract the phenomenon linked to the internal gas. In order to find the relationship that links the temperature jump between the sample preparation temperature T_{prep} and the test temperature T_{test} to the variation of the compression force, we plan tests at different temperatures in which we note:

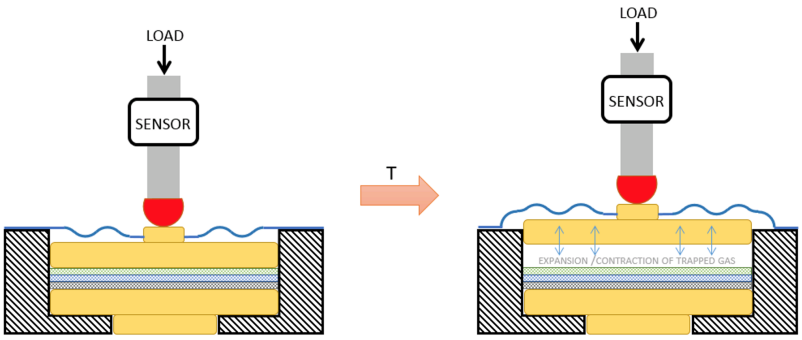

Figure 4.14: Expansion/contraction of the gas trapped inside the sample holder: this is the cause of the anomaly in the measurement result on the bench.

1. the closing temperature of the sample holder T_{prep}.
2. the temperature at which the test will be carried out, T_{test}.
3. the compression force at which the electrical contact between the two current collectors, initially in contact, is lost.

Using the thermal chamber set at a constant temperature, the bench is allowed to reach thermal equilibrium. Initially, the applicable compression force is adjusted to its maximum value. Then, the force is varied by moving the adjustment ring and the value of the force at which the electrical contact between the lower and upper current collectors is lost, is simultaneously measured with a digital multimeter(Figure 4.15).

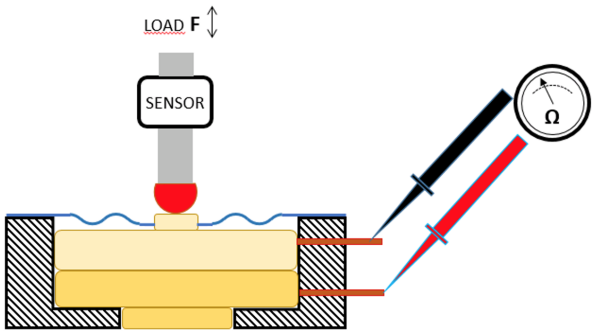

Figure 4.15: Schematic representation of the test for compensation of the compression force value.

By correlating the values obtained from the various tests carried out (Figure 4.16), a coefficient K_{ex} is obtained which allows the correct compression force to be set on the battery to be tested, knowing the sample preparation and test temperatures.

The relationship between the above quantities is as follows:

$$F_{set} = P_0 + F_N - (K_{ex}\Delta T \tag{4.1}$$

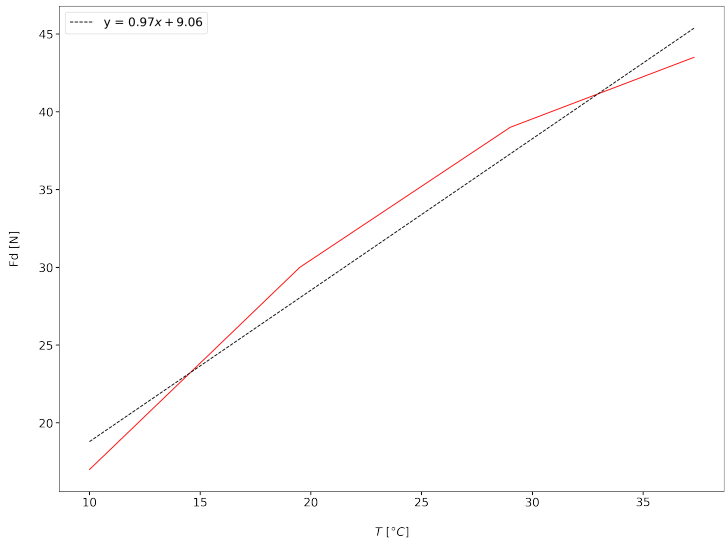

Figure 4.16: Detachment force vs. temperature. Interpolating the experimental values gives the correction coefficient of the force to be applied during the dilatometer tests.

were:
F_{set}= value of the force to be set on the instrument
P_0= weight of unloaded measuring system, constant
F_N= value of the nominal force to be applied during the test
ΔT= T_{test}-T_{prep}

Some tests are conducted in order to verify the effect of compression force compensation. Below, an example of the results obtained, conducting the tests in a thermal chamber with different thermal cycles set.

As can be seen:

- the temperature trend (blue curve) and the gauge trend (orange curve) are now consistent.
- at temperature transients the response of the measuring device varies.
- at constant temperature the response of the meter varies within the declared tolerance range.
- the green curve represents the response of the gauge, corrected taking into account the imposed temperature variation. The formula for this adjustment, which is necessary for the instrument to function correctly and which will be included in the control software supplied with the measuring station, is as follows:

$$M_{comp} = M_{raw} - (k_b \Delta T_b) \tag{4.2}$$

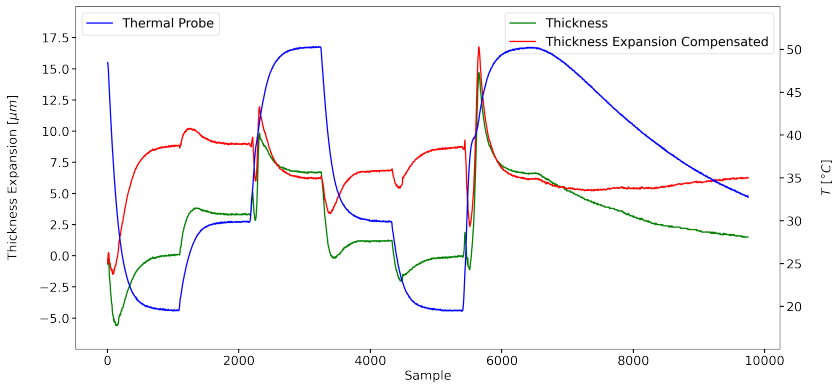

Figure 4.17: Thermal drift test on complete instrument, with compensated compression force.

were:
M_{comp}= adjusted transducer measurement
M_{raw}= raw transducer measurement
k_b= bench compensation coefficient, $(\mu m/°C)$
ΔT_b= temperature variation during the test

As can be seen, the measurement deviation due to temperature fluctuations is reduced once the correction is applied. It can be noted that this is not perfectly evident in the extreme zones of the graph, i.e. at the beginning and at the end of the imposed thermal cycle: this is due to the fact that at the beginning and at the end of the tests the acquisition was started/stop before the thermal stabilisation of the bench was completed. Therefore, for the purposes of evaluating the instrument's corection strategy, these zones were not considered.

4.1.3. Leak test on sample holder

In this section the results obtained from the leak test on the instrument sample holder are presented. The leak test was conducted using helium as a tracer gas as described in §3.1.3. The starting value of the helium overpressure to be injected into the sealed sample holder is obtained by knowing:

- free volume inside the sample holder, calculated by CAD, $5.25 \cdot 10^{-5} m^3$.
- theoretical maximum pressure due to the expansion of the trapped air, calculated from the equilibrium of the forces acting on the sample holder and considering the maximum temperature drop, $\Delta T_{max} = 70°C$, $1167.78 mbar$.
- overpressure in relation to atmospheric pressure $P_{atm} = 1013.25 mbar$, $154.53 mbar$.

Table 4.3 shows the values of internal overpressure and leakage detected by the sniffer during the tests.

Temperature	**Internal helium overpressure**	**Detected leakage**
$(°C)$	$(mbar)$	$(mbar \cdot l/sec)$
21	150	*not detected*
21	160	*not detected*
21	500	$1 \cdot 10^{-7}$
21	750	$1 \cdot 10^{-6}$

Table 4.3: Results of helium leak test on sample holder

The helium test shows a good seal of the sample holder: this result confirms the use of the sample holder as a safe and reliable "container" for the assembly of cells with materials sensitive to air and moisture.

4.1.4. Functional and Electrochemical validation tests

In this section the results of the tests performed at Laboratory of Electrochemistry of Materials for Energetics at the Department of Chemistry "Giacomo Ciamician" of the University of Bologna are summarized and discussed. For a more detailed description of the test activity carried out for the electrochemical validation of the instrument, please refer to the related publication [207].
For the experimental validation of the measuring bench, it was chosen to use graphite as working electrode, since this material is widely used in lithium-ion batteries and therefore widely studied. For this reason it can be taken as "model" electrode and comparison of the characteristics obtained with the measuring bench. The chosen working electrode is studied in two different electrochemical systems,in order to have different answers of the instrument:

1. 1M LiPF6 in EC (ethylene carbonate):DMC (dimethyl carbonate), 1:1 w%:w% (known as LP30).

2. 1M LiTFSI in PC (propylene carbonate); the PC as solvent was selected as a bad example of solvent to graphite.

EC-based electrolytes are well-known for their good compatibility with graphite. EC shows excellent filming capabilities that ensure the formation of a good and stable SEI and DMC decreases the viscosity of the solvent mixture. EC-DMC containing LiPF6 salt is a standard electrolyte (LP30) due to the broad electrochemical stability and high ionic conductivity. On the contrary, the cointercalation of PC with lithium ions in graphite leads to an exfoliation of the electrode that occurs at less than 0.9 V vs Li+/Li without wrecking the bulk structure completely but bringing progressive changes in surface structure. This degradation makes this electrolyte unsuitable for most graphite-based LIBs.
The cell used for the test is made up as follows:

- WE: 90 wt% graphite MAGE (Hitachi), 7 wt% PVDF-Solef (Solvay) S130 (Solvay), 2wt% Super C-65 (Timcal), 1 wt% SF66L graphite (Timcal); (active material= 35 μm)

- Separator: Whatman GF-A (thickness= 184 μm)

- CE: 83,9 wt% carbon PICACTIF (2315 m^2/g), 4.6 wt% of carbon Super P (Erachem Comilog N.V.), 4.8 wt% of carboxyimethylcellulose sodium salt (Na-CMC, Sigma-Aldrich), 6,7 wt% PTFE suspension in water (Teflon®, DuPont, 60.2 wt%),500 μL absolute ethanol (Sigma-Aldrich, $\leqslant$99,8 wt%).

The electrodes and separators used for the electrochemical measurements were cut into discs of 9 mm for the electrodes and 10 mm for the separator by roll punching and were dried under dynamic vacuum in an oven at 120 $°C$ for 12 h. Two experimental setups were carried out: the first one, performed in order to record the potential of the single electrodes versus an internal lithium metal reference electrode and the potential of the whole cell, a Teflon^{TM} T-shaped cells (BOLA, Bolehnder GmBH) and a multimeter was used, as usual in laboratory tests. The recorded values were taken as reference for the dilatometer tests, to first elucidate the electrochemical potential of the processes.
Results of preliminary tests performend in a T shaped cell are following reported Figure 4.18. The test performed with DMC-EC electrolyte show that the *open circuit potentials* (OCP) was -40 mV that corresponds to 3.40 V vs Li^+/Li for the WE and 3.433 V vs Li_+/Li for the CE, then the potential limit value for the measurements with dilatometer, is set to -4.00 V.

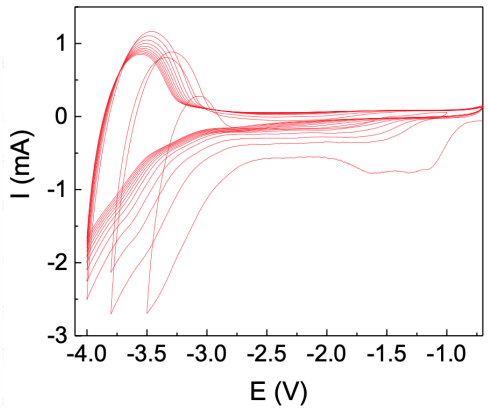

Figure 4.18: Preliminary CV experiment in a T-shaped cell in LP30 at 2 mVs^{-1} in two electrode mode.

The voltammograms was acquired with a scan rate of 2 $mV \cdot s^{-1}$ using the graphite as WE and a capacitive electrode as CE. The electrode potentials were checked with a multimeter vs a lithium metal internal reference electrode. The electrode potential values recorded during CVs in PC-1M LiTFSI are very similar.

In the second setup, the dilatometer was used. The dilatometer cell assembly was performed under argon atmosphere in an *MBraun Labmaster SP* dry box (H_2O and O_2 < 0.1 *ppm*) and the measurements started 2 h after the assembly. Once this time has elapsed, the dilatometer was connected to a *Solartron SI 1255* frequency response analyser interfaced with the *PAR273A potentiostat/galvanostat*, and the tests were performed. In the potential window identified with the previous tests the dilatometric measurement was conducted under a force applied of 10 N (157 kPa for 9 mm disc and 127 kPa for 10 mm

disk) by adding LP30 electrolytic solution or PC-1 M LiTFSI (150 μL for the full cell and 75 μL for the cell components) and the and the results are as follows. In Figure 4.19(a), 4.19(b) are reported the thickness variation (red) and the current (grey) during the first two CVs with the cell voltage on the top axis. The grey vertical lines indicate the cut-off voltages of the CV. The dilatometric profile is characterized by small expansion/shrinking peaks (less than 1 μm) originated from the reduction/oxidation of the graphite electrode and the corresponding insertion/deinsertion of lithium ions within the graphitic layers.

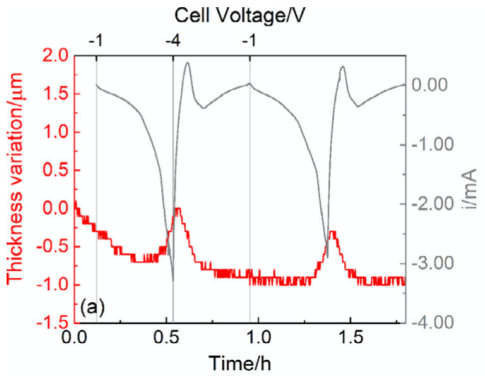

(a) Tickness variation (red) and current (grey) during the first two CVs of the graphite CE in dilatometer cell (2 mV s^{-1}).

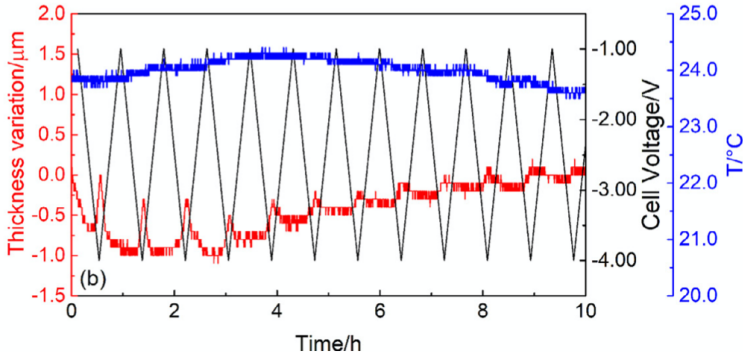

(b) Thickness variation (red), voltage (black) and temperature (blue) during 10 continuous CVs of the graphite CE in dilatometer cell (2 mV s^{-1}).

Figure 4.19: Dilatometric experiment plot during the during the first two CVs cycles in LP30 electrolyte system. *WE*: graphite, *CE-RE*: activated carbon, *separator* Whatmann: GF/A, 150 μL LP30.

The thickness of the different cell components under the same conditions as above was also monitored (Figure 4.20).
Under the applied pressure, all the materials respond with a deformation that leads to a fast decrease of thickness in the first 2 h. The separator and the CE showed the smallest thickness decrease around 13.0 μm (-9.2%) and 2.6 μm (-0.7%) after 14 h, respectively. This behaviour was expected for CE. The

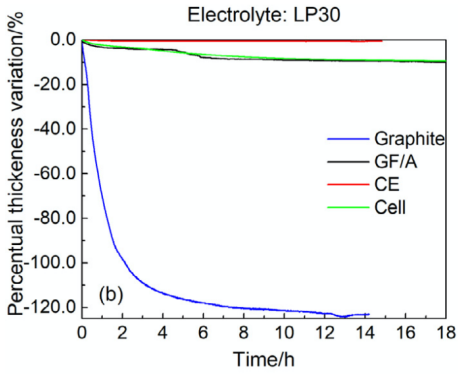

Figure 4.20: Percentual deformation of cell components and of the whole cell under 10 N force with LP30 electrolyte.

selection of a CE based on activated carbon, indeed, was done on the basis of its capacitive properties. It accumulates charge without ion insertion in the electrode bulk active mass, limiting the electrode deformation. On the other hand, the graphite electrode showed higher deformation that stabilizes after 14 h (-123% with respect to the dry electrode). Such a high thickness variation could be justified by the increased thickness of the wet electrode taken as starting reference value. The electrode wetting and related thickness change deserve further investigation. In LP30, indeed, both DMC evaporation and graphite deformation act on swelled materials. The cell deformation (52 μm, -9.2%) was smaller than the sum of the variation of the individual components. It is reasonable that the stress induced by the applied force was distributed on the varous components and causes the deformation mostly on the weakest material.

PC-based electrolyte tests was also conducted and results summarized below (Figure 4.21). The potential window of the electrode materials in 1 M LiTFSI in PC has been set by monitoring the electrode potentials vs Li reference electrode in the same configuration reported above and the values were very similar to those reported for LP30.

The experiments in PC-1 M LiTFSI were performed in two different potential ranges with the lower graphite potential limited to 0.9 V vs Li^+/Li to restrains the exfoliation of the graphite, or set to $\approx 50mVvsLi^+/Li$ for reaching the exfoliation condition. Figure 4.21(a) demonstrates the thickness variation (red) and the curent (grey) during the first two CVs with the cell voltage on the top axis. The dilatometric profile shows bigger expansion/shrinking peaks than those in LP30. The expansion/shrinking peaks aligned with the insertion/deinsertion of lithium-ion in the layered material are reversible in accordance with the imposed cell voltage that prevents the complete exfoliation of the material. The progressive decrease of the baseline observed (Figure 4.21(b) retraces the temperature variation (blue line) during the experiments carried out at room temperature. As in the previous experiment with the LP30 electrolyte, the change in thickness of the whole cell and individual components is monitored. (Figure 4.22).

In PC-based electrolyte, the less deformable materials (after 14 h) were again the separator and the CE with 3.7 μm (2.9%) and 7.3 μm (1.8%), and the graphite electrode showed the highest deformation, around 11.8 μm(25%).

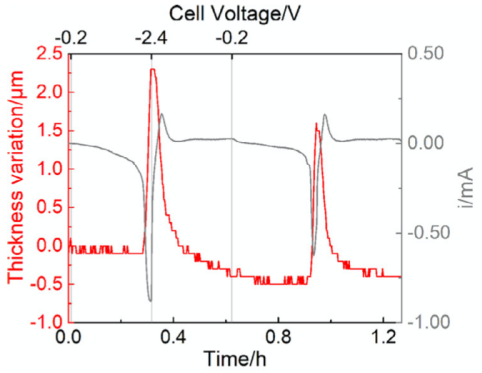

(a) Tickness variation (red) and current (grey) during the first two CVs of the graphite CE in dilatometer cell (2 mV s^{-1}).

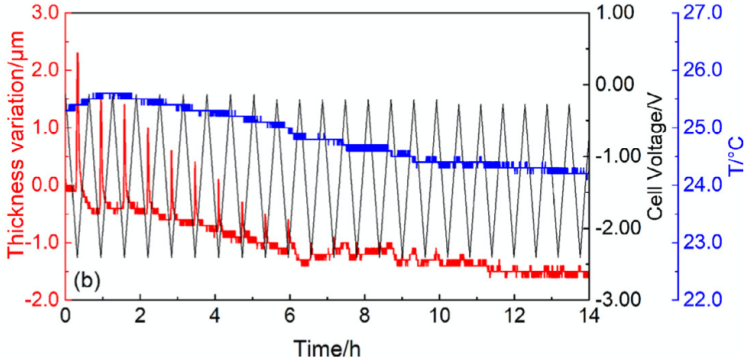

(b) Thickness variation (red), voltage (black) and temperature (blue) during 10 continuous CVs of the graphite CE in dilatometer cell (2 mV s^{-1}).

Figure 4.21: Dilatometric experiment plot during the during the first two CVs cycles in PC electrolyte system. *WE*: graphite, *CE-RE*: activated carbon, *separator* Whatmann: GF/A, 150 μL PC- 1 M LiTFSI.

The thickness variation observed in LP30 electrolyte compared with that of the same components in PC suggests that the recorded compression could depend both on the deformation of the materials and on the presence of DMC that evaporates, evidenced by salt traces in the cell holder. Indeed, in the PC-based electrolyte, the magnitude of the deformation of all materials is three up to five times lower. With the PC-based electrolyte, it is possible to assume that the response observed is entirely due to the compression of the examined materials. The highest deformation in graphite results also predictable if correlated to the softness of the materials itself due to the weak $\pi - \pi$ stacking interactions between the graphitic layers.

Some tests was also conducted at a different level of force imposed on the instrument, with the aim of seeing that it actually responded consistently with the level of increasing force imposed and also to test the ability of the designed instrument to detect other phenomena that occur during the tests such as those

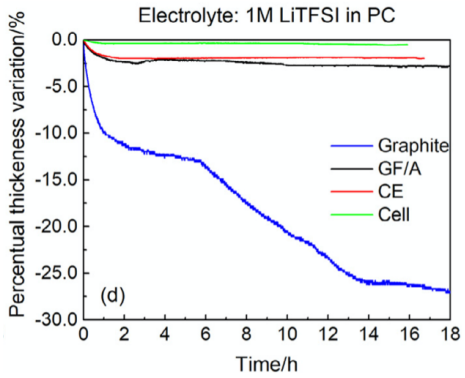

Figure 4.22: Percentual deformation of cell components and of the whole cell under 10 N force with PC-1 M LiTFSI electrolyte.

related to gas formation.

Referring to the cited publication ([207]) for the results of a chronoamperometric test conducted to assess the sensitivity of the instrument to two levels of applied force (10 and 20 N) on a sample that develops a certain amount of hydrogen when cycling, the following are the results of the application of the two mentioned force levels on graphite sample in PC-1 M LiTFSI.

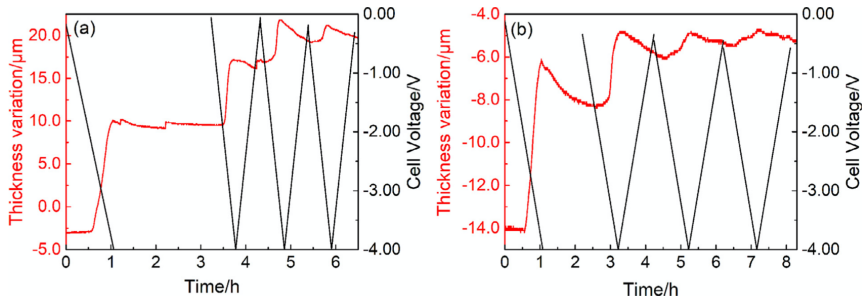

Figure 4.23: Thickness variation (red) and cell voltage (black) during electrochemical experiments under *(a)* 10 N and *(b)* 20 N applied force. *WE:* graphite, *CE-RE:* activated carbon, *separator* Whatman: GF/A, 150 μL PC-1 M LiTFSI.

Graphite was then tested in PC-1 M LiTFSI in exfoliation condition with 10 N and 20 N applied. The dilatometer cell underwent a linear sweep voltammetry experiment from -0.1 V (open circuit potential) to -4 V. The cell was discharged later and after a few hours underwent three CV cycles. The thickness variation was continuously monitored during the whole experiment as shown in Figure 4.23. At the cell voltage of -2.5 V ($\approx$0.9 V vs Li^+ /Li) co-intercalation of Li^+ $(PC)_n$ occurs. The dilatometric curve records a large expansion in electrode thickness (10-12 μm) that represents a 35% change in thickness upon intercalation. This variation, consistent with the co-intercalation of Li^+ $(PC)_n$ and contemporary PC degradation, that leads to the formation of propylene gas, causes crack and exfoliation of the graphite layers. The resultant dilatometric

curve (Figure4.23a) is given by the combination of the exfoliation and the gas evolution. The force adjustment system and the control of the applied pressure allow to get insight into the contribution of the gas formation during the expansion as shown before for H_2 evolution, and Figure4.23b displays the thickness variation of the cell operating in exfoliation condition with 20 N applied force. The expansion decrease was observed, as expected. The first cycle expansion corresponds to 13 μm and 8 μm for 10 N and 20 N experiments, respectively. The pore volume filled by the evolved gas is smaller when external high force is applied and, in turn, the recorded expansion. To support the mechanism of interaction between graphite and PC just explained, the SEM images of graphite in the three states tested with the instrument, i.e. virgin, after cycling in LP30 and after the experiment with the PC, are shown in the Figure 4.24.

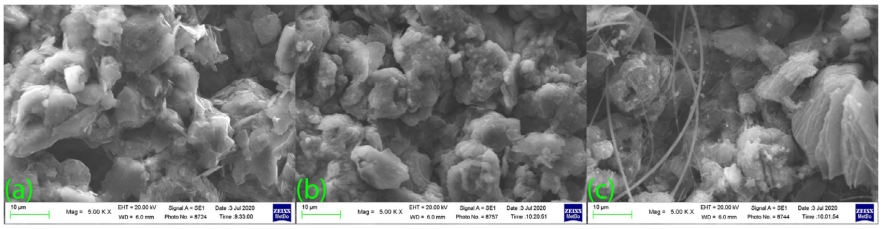

Figure 4.24: SEM images of *(a)* pristine graphite electrode, *(b)* graphite electrode cycled in LP30 and *(c)* graphite electrode cycled in exfoliation condition in PC-1 M LiTFSI.

It is easy to see the state of the graphite following the interaction with the PC under exfoliation conditions. Tests carried out under different conditions of force applied to the test specimen show the good response of the instrument and that the force is an interesting parameter to keep monitored.

4.1.5. Re-design of sample holder

The intense use of the instrument in the electrochemical laboratory tests, has highlighted the need to measure the expansion of the individual materials that make up the battery.
So to complete the series of tests that can be done with the instrument it has been decided to design a new sample holder able of measuring the volume variation of the working electrode individually, without the influence of the other materials making up the cell under test. In Figure 4.25, in which some internal parts have been deliberately hidden for intellectual property reasons, is represented the result of the design of the new sample holder for "*half-cell*" measurement.
Having succeeded in redesigning the internal part that includes a rigid separator necessary to measure only the single electrode, maintaining the same external dimensions, the instrument has the same functionality and usability already tested in the "*whole cell*" experiments. So both sample holders can be easily removed from the instrument and introduced in glove-box for restoration and maintenance operations.

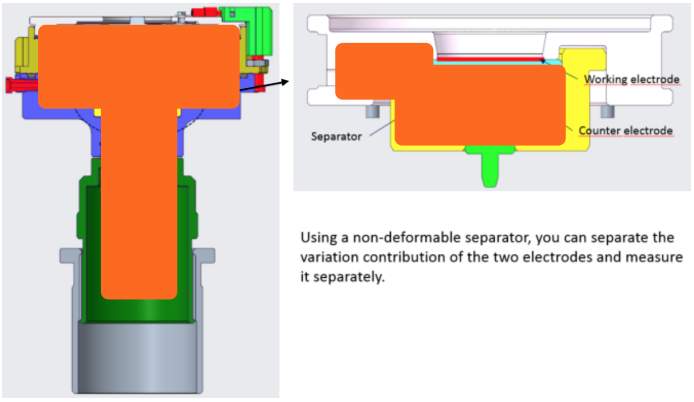

Figure 4.25: "*Half-cell*" measurement sample holder.

The design and construction of the new layout of the sample holder will undoubtedly make it possible to extend, improve and complete the electrochemical characterisation of the instrument designed: in fact, while experiments carried out using silicon and sulphur, for example, which are materials with large volume variations over time during charge-discharge cycles, could have produced more significant results from the point of view of measurement, it should be borne in mind that with the current configuration of the dilatometer (whole-cell sample holder), it would in any case have been difficult to attribute this variation to the electronic material alone. For this reason it was decided to postpone tests with this type of material to future experimental campaigns, when the new "half-cell" sample holder will be available.

4.2. Preliminary evaluation of the PID sensor

In this section, the results of preliminary tests for the detection of dimethyl carbonate using PID technology are presented. As explained in the chapter §3.2, this technology is of interest in combination with the analysis made with a mass spectrometer that detects "small" losses: in this configuration the PID sensor acts as a "fuse" for the spectrometer, avoiding poisoning problems caused by gross leaks.

The results of the qualitative survey conducted with the commercial PID sensor (Figure 4.26), are shown in Table4.4. The test configuration is the same as already shown in Figures 3.5.

(a) PID commercial sensor. (b) PID sensor during preliminary tests.

Figure 4.26: PID *VOCs* sensor by ION Science.

Configuration Test	**Detection Time** (sec)	**Temperature** ($°C$)
Figure 3.5(a)	10	22
Figure 3.5(b)	60	22
Figure 3.5(c)	180	22

Table 4.4: Results of helium leak test on sample holder

Preliminary test results indicate:

- the capability of integrating this technology within in-line battery control systems
- the importance of an accurate design in the integration process. In fact it can be easily deduced that for an on-line control a detection time of 10 seconds is certainly not very advantageous.

For these reasons, we propose an architecture for an in-line control station for battery production, e.g. coin cells, in which a PID sensor works close to a mass spectrometer (Figure 4.27).

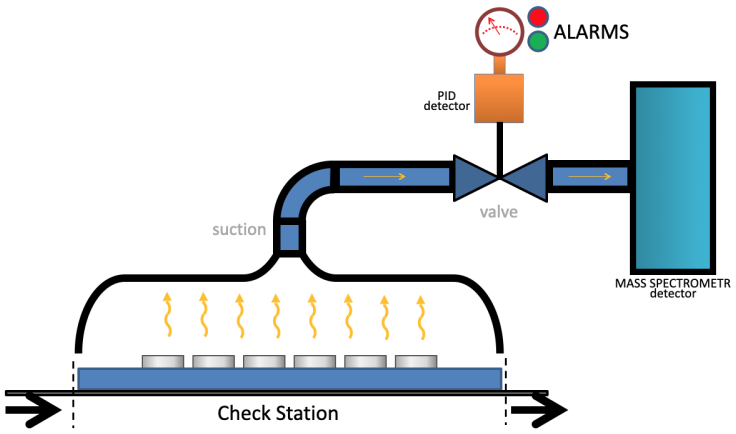

Figure 4.27: PID integration in a *in-line* control station.

If a leak is detected that exceeds the detection range set on the mass spectrometer, the PID sensor triggers an alarm and closes an inlet valve upstream of the spectrometer, thus protecting it from poisoning.
As a further step in the development of an in-line control based on PID technology, the design of a multi-sensor system was considered: a matrix of sensors mounted on a grid support that "floats" on the battery production line (Figure 4.28).

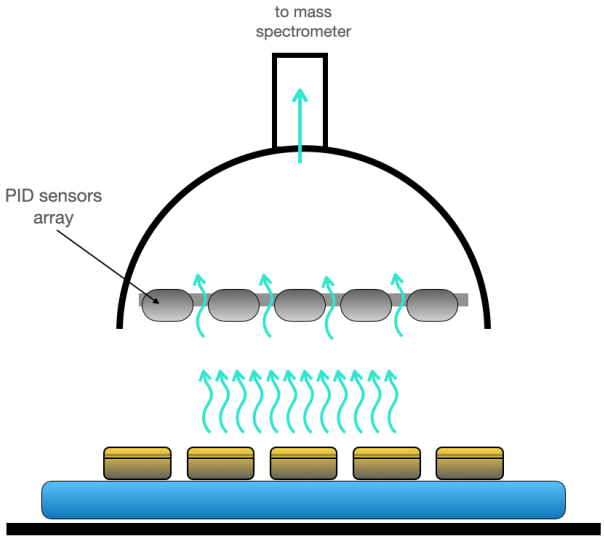

Figure 4.28: Alternative layout of the control station on the battery production line control station.

This solution could partially solve the sensor response time problem in a

system where the gas to be detected moves by natural diffusion. Details of the engineered solution layout are omitted for reasons of intellectual property.

4.3. Colorimetric sensor: first evaluations and assessments

In this section a full description of the results of validation tests of the working principle of the colorimeter sensor shown in §3.3 is presented.
The purpose of these preliminary tests is to demonstrate the feasibility of an alternative method for battery monitoring based on a colour sensor.
It should be taken into account that:

- The tests carried out are "comparative", i.e., the signals coming from the sensor are compared with a sensor signal taken as a reference. The colour detected and transduced in RGB coordinates does not claim, at least at this stage, to be the absolute exact colour detected. What underlies this preliminary assessment is the colour variation and not the colour itself.
- The colorimetric sensor is uncalibrated, i.e. it has no definite response when compared to the fundamental reference colours Red, Green and Blue. Although there is a standard calibration procedure for this type of sensor, it is chosen to bypass it as this stage evaluates the relative response of the sensor, i.e. the colour change from an initial reference state.
- the illumination coming from the led mounted next to the colorimetric sensor is not adjustable at this preliminary stage: this definitely alters the response of the sensor as the best conditions are not created to obtain the most precise response from the sensor.

The evaluation of the potential of this new survey method can disregard the aspects listed, leaving all observed improvements to the next development phase.

4.3.1. Tests with aqueous solutions

For sake of clarity purposes, the test methods performed, shown above in §3.3.3, are once again schematized (Figures 4.29).
Table 4.5 presents the composition of the tested solutions and below are the signals detected by the sensor in the two experimental sessions: in Table 4.6 those of the Figure 4.29(a) test and in Table 4.7 those of the Figure 4.29(b) test.

Solution	**Content**	**Concentration**	
		g/L	mol/L
1	Nickel Acetate (NA)	23	0.01
2	Copper Sulphate (CS)	35	0.03
3	Bengal Rose (BR)	15	$1 \cdot 10^{-3}$
4	(BR) #3 diluted 1 : 30	0.5	$3 \cdot 10^{-5}$
5	(BR) #4 diluted 1 : 15	30	$2.2 \cdot 10^{-5}$
6	(BR) #5 diluted 1 : 10	3	$2.2 \cdot 10^{-6}$
7	(BR) #6 diluted 1 : 10	0.3	$2.2 \cdot 10^{-7}$
8	(BR) #7 diluted 1 : 10	0.03	$2.2 \cdot 10^{-8}$

Table 4.5: Summary of solutions tested.

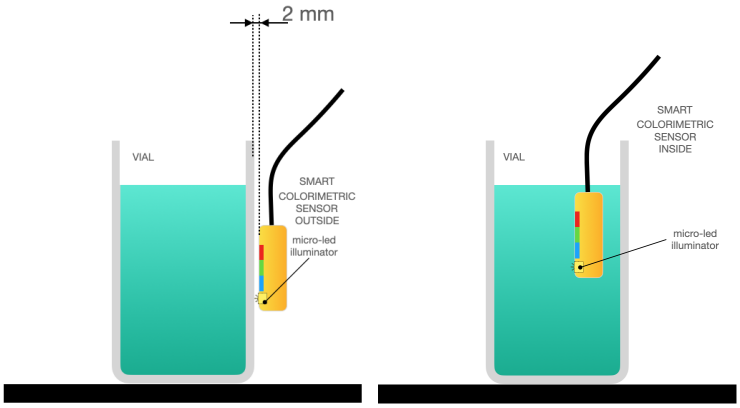

(a) Colorimetric sensor outside the vial.

(b) Colorimetric sensor inside the vial.

Figure 4.29: Setup of tests with aqueous solutions.

Vial n°	**Coordinata RGB**		
	Red	Green	Blue
1	268.82	344.52	196.78
2	252.78	323.44	156.04
3	268.04	332.85	182.58
4	267.8	334.15	178.68
5	275.32	344.12	194.97
6	258.95	325.78	163.71
7	258.2	325.57	162.85
8	253.2	320.15	154.5

Table 4.6: RGB coordinates relative to the test with sensor positioned outside the vial at a distance of 2 mm

Vial n°	**Coordinata RGB**		
	Red	Green	Blue
1	78.13	238.73	334.13
2	96.93	227.86	226.5
3	60.86	69.83	24.33
4	130.7	154.76	236.46
5	142.56	210.93	298
6	99.7	185.33	211.56
7	126.8	223.63	281
8	108.76	186.06	212.26

Table 4.7: RGB coordinates relative to the test with sensor immersed in vial

The data shown are the average of 7 measurements made on the same aqueous solution. The graphs in Figure 4.30 represent the three RGB coordinates for the two experiments conducted.
It is therefore clear that the best configuration is the one with the sensor im-

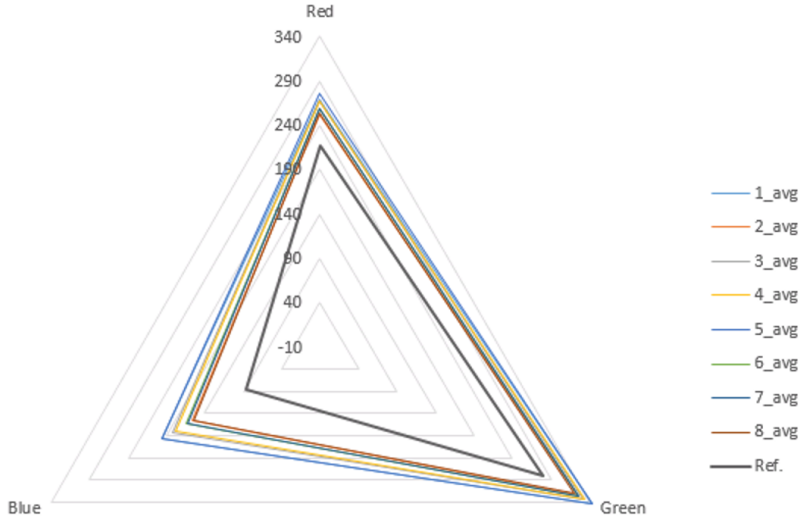

(a) RGB coordinates for external sensor.

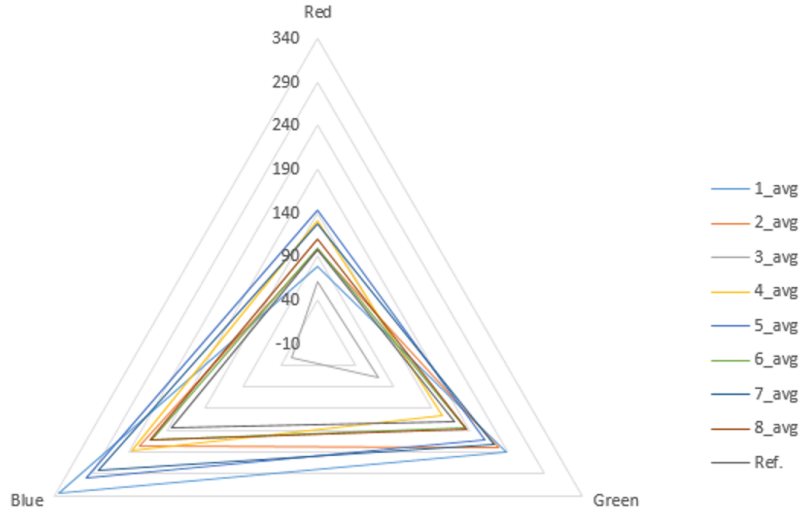

(b) RGB coordinates for internal sensor

Figure 4.30: RGB coordinate graphs

mersed in the aqueous solution, as it is able to distinguish the differences in colour (Figure 4.30(b). Moreover, it is easy to understand how, in the configuration with the sensor close to the vial (Figure 4.30(a)), the colour detected by the sensor is affected by reflection phenomena due to the presence of the glass layer of the solution container. The thickness of the glass acts as a filter, smoothing out the colour signal arriving at the sensor. This configuration has to be avoided because, although tests are carried out by comparison, it does not give the opportunity to discriminate small variations in colour.

4.3.2. Tests with electrochemical sample cell

The experimental setup used is shown in Figure 4.31.

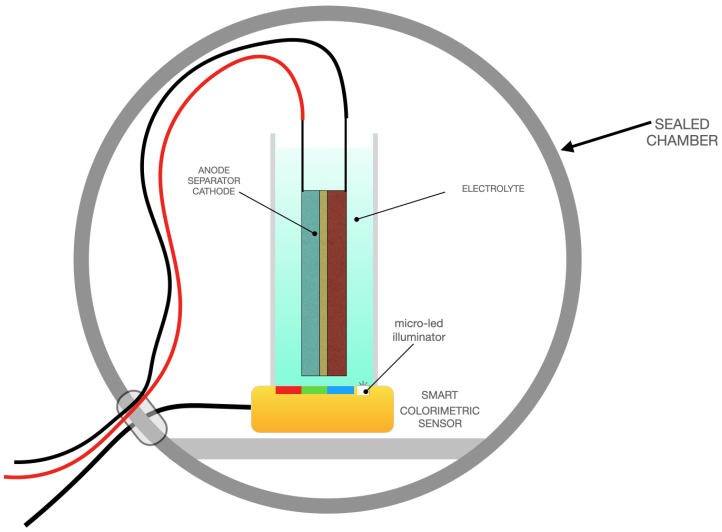

Figure 4.31: Experimental test setup with colourimetric sensor and battery sample

After assembling and closing the cell inside the glass container,as described in §3.3.3, the terminals are connected to the potentiostat and proceed with the charge/discharge test as described above, programming the acquisition of the signal from the sensor. The graph in Figure 4.32 shows the results obtained.

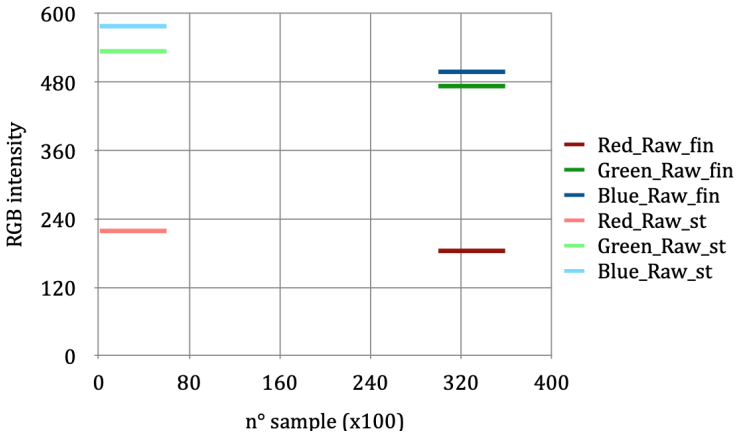

Figure 4.32: Colour variation during the battery test: acquisition of RGB coordinates at the beginning and end of the test

There is a clear transition of the colour coordinates from the initial to the final state. This is also confirmed by the final state of the battery after the test (Figure 4.33).

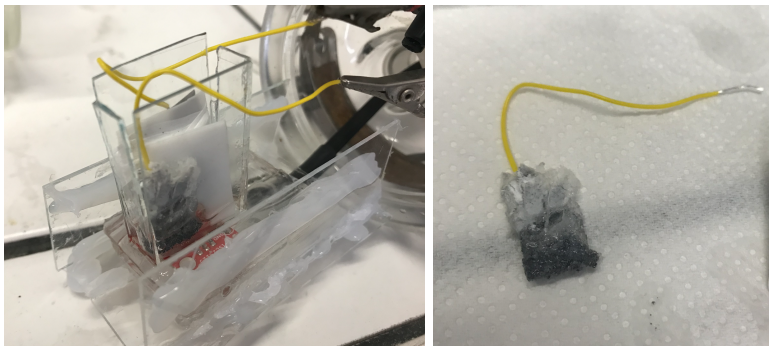

(a) Cell still assembled.

(b) Disassembled lithium electrode.

Figure 4.33: Sample battery at the end of the test.

The detected colour variation corresponds to the observed lithium oxidation, caused by exposure of the lithium electrode to air, which probably entered the glass container. The response of the sensor is consistent with the observed phenomenon: there is a decrease in the intensity of the colour, i.e. a change from a lighter to a darker colour.
Although the recorded colour change is not related to the formation of secondary reaction products but to a test failure, it is nevertheless a noteworthy result that provides a preliminary validation of the colorimetric approach proposed for monitoring the integrity and proper functioning of an electrochemical cell.

4.3.3. Future developments: integration in a real electrochemical cell

Although preliminary, the tests conducted and reported above support the case for developing this system. Obviously, development work is in its infancy here, and will certainly require more detailed modelling of the operation of such a detection method under different conditions and at different points in the electrochemical cell space. The ambition is first of all to develop an effective communication system between the inside and outside of each cell in which the sensor will be installed; in this respect, the extremely small size of the sensor in itself lends itself to favourable integration within the various cell architectures currently present. Once the system for translating the signal from all the cells that make up the battery pack of a vehicle, for example, has been designed, it is necessary to implement this information in the architecture of the BMS: one possibility, for example, is that when a signal from a single cell exceeds the set thresholds, the BMS is able to know which cell is working in abnormal conditions in order to "disable" it, preventing all the other cells from being affected by this anomaly. The tests of this sensor planned for the near future will certainly outline its potential and limits.

5. Conclusion

Io non ho fallito 5000 esperimenti.
Ho avuto successo 5000 volte,
gli insuccessi mi hanno insegnato che
quei materiali non funzionavano.
T. A. Edison - inventore ed imprenditore

The overall aim of this dissertation is to understand how to improve the efficiency and safety of a Lithium-ion cell. The relevance of batteries is increasing day by day even in everyday life and many efforts have been made to improve their performance. In the last decades, energy storage systems have assumed a central role in all states with a booming economy as the trend is to reduce *greenhouse gas* (GHG) emissions in favor of clean energies such as renewables: undoubtedly the implementation of cleaner fuels and passenger vehicles can bring significant health benefits, with positive impacts on the overall quality of life of citizens. However, for effective use of energy from the sun and wind, stationary storage systems are needed. The advancement of consumer electronics has also favored the spread of portable devices powered by batteries, which must therefore be increasingly high performance. The battery has thus become an object of daily use and although there are considerable efforts to improve its efficiency, some aspects still need to be improved: one of the most important is safety. In order to face this problem, many researches have been carried out and the most promising approaches concern the use of different combinations of materials for the construction of electrodes and the use of alternative electrolytes to those currently used. From the point of view of the monitoring and control systems of the batteries, considerable efforts are made to improve the efficiency of the *Battery Management System* (BMS) and to find alternative ways that lead to the intelligent battery of the future. In this context, this thesis work was carried out with the aim of contributing to the advancement of battery safety.
The purpose of the work was achieved through 3 steps:

1. the design and validation of an instrument for measuring the expansion of electrodes during charge/discharge cycles. Three main features characterize the designed dilatometer: the ability to vary the compression force acting on the sample under test according to the experimental needs; the possibility to test the electrode materials in a wide temperature range, from -10 to 60 $°C$; the capability to change the test configuration on the instrument, i.e., test on "whole cell" or "half-cell". Each feature plays

its own role in the success of the test. Preliminary activities validated the design of the instrument, both from a mechanical and electrochemical point of view, to ensure the best possible measurement with this system.

2. the preliminary investigation into the use of a commercial photoionization detector (PID) for leak testing on batteries. Simplicity and low cost are from the industrial point of view the most attractive features of this technique for the detection of *volatile organic compounds* (VOCs). The experimental work explored the potential reliabilityof this approach for detecting dimethyl carbonate electrolyte leakage in the battery production line. In addition, a possible working strategy of a PID sensor in combination with a mass spectrometer has been indicated.

3. the proposal of an innovative method for monitoring the integrity and health of Lithium-ion batteries. We explore the possibility of transducing the goodness of electrochemical processes occurring within a cell through a color signal. Preliminary experiments evaluated the opportunity to develop a sensor based on this principle, fully integrable into the cell that can monitor the state of the cell throughout its useful life.

Each steps lead to important considerations, summarized in the following.

5.1. Dilatometric bench design

The process that allowed the design of the instrument has revealed the importance of many aspects that contribute to the realization of a system capable of measuring correctly: from the choice of materials, able to provide the right stiffness and stability over time and at the same time to resist the chemical agents of the cell samples under test, to the mechanical and thermal testing phases. Through an accurate process of calibration of the force applied on the sample and correction of the thermal drift, it is possible to test the samples in a wide range of temperatures. The thermal drift tests have highlighted the points that can be improved in the future: for sure, the optimization of the dead volume inside the sample holder that represents a drawback when testing at a temperature different from the sample preparation temperature. After all, to obtain the maximum precision from the measurement it is necessary to carry out the test in static temperature conditions, providing a time of "thermostatting of the instrument" before starting the test. The electrochemical validation phases have confirmed that the instrument is able to measure the phenomenon of expansion of the electrodes due to the insertion/deinsertion of lithium ions into the structure of the material. However, the difficulties that emerged in the attribution of this phenomenon to each of the components of the battery tested with the "whole cell" sample holder initially available, has allowed to expand the range of tests that can be performed on the instrument. Starting from the whole cell sample holder, it was designed a second one able to perform the half-cell test. Finally, the instrument is equipped with two sample holders for two different tests on the same instrument. In addition to this, it is also possible to vary the compression force range applicable on the sample battery, during the retooling of the measuring bench. In the planned development activity the improvement of the measuring equipment will be considered in order to make

it as light as possible, giving the opportunity to apply a compressive force in a lower range than currently possible also through retooling.

5.2. PID leak test method

It is evident from preliminary tests that a sensor based on this technology is able to detec electrolyte leakage. However, the high response times, at least if compared with those that can be expected in a production line, suggest the need to design a more complex system than the simple sensor facing the leak. In this regard, the concept that is proposed is to design a control station in which a PID sensor can work in combination with a mass spectrometer. While the latter detects *small leaks*, the PID intercept *gross leaks* in order to prevent mass spectrometer poisoning and the consequent downtime to restore the instrument. During the dissertation some aspects related to the development of the system based on this technology have been omitted for intellectual property issues since an architecture like the one described could be implemented in a real control station on a battery production line. The development will be planned in order to minimize the response time of the system, for example building a penstock that sucks the volume of air to be analyzed and brings it quickly to the sensor.

5.3. Smart Colorimetric Sensor

The experimental activity carried out in this area has permitted to consider an alternative way of battery monitoring techniques starting from their weaknesses. Thinking about a sensor that could be integrate inside the electrochemical cell, we try to solve the problem of the response time of the battery management system that, in some cases, is too high to prevent degradation phenomena or potential danger of battery packs. Having proposed the monitoring of the coloration in some internal points of the electrochemical cell, preliminary tests have been conducted to validate this approach. The results obtained are encouraging, in fact both in the tests with colored aqueous solutions and in those on sample battery, the response of the proposed sensor has been consistent with that expected.
Also from the results it emerges that:

- the best way to detect a color change proportional to the concentration of secondary reaction products, indicative of a malfunction, is by putting the sensor in intimate contact with the battery components.

- although the results give the impression that a control made with the proposed sensor is entirely qualitative, the adjustment of the light that allows the sensor to detect colors and a robust initial calibration procedure, lead with good probability to a quantitative and accurate measurement of the concentration of these reaction products. As a consequence we could also think to set trigger thresholds that if exceeded send an alarm signal to the BMS that at that point intervenes, protecting the cell individually or the set of cells where the defective battery is inserted.

- the time of detection and intervention by the security systems that integrate this sensor, is likely to be lower because the onset of an unwanted

phenomenon is more easily detectable by an in situ sensor able to detect electrochemical phenomena rather than by a macroscopic and extensive physical quantity such as voltage, current or temperature of the cell recorded by BMS.

In any case, the results obtained are preliminary. Consequently, an intensive development phase is planned leading to:

- quantify the signal coming from the sensor in an absolute way.
- managing the parameters that affect the response of the sensor, such as light intensity.
- engineering the hardware of the sensor with the aim of miniaturizing it, obtaining the maximum integrability inside the batteries.
- Identify the strategic points of insertion of the sensor inside the electrochemical cells.
- investigate an effective system of signal transduction that avoids the use of cables.
- design a system to manage the signals coming from the sensors of the cells that compose a battery pack.
- implement the sensor within the architecture of current management systems.
- Make the colorimetric sensor useful in all types of batteries currently on the market and in those of future generations.

5.4. Concluding remark

At the end of this work, let me make some considerations with respect to the issues addressed. From the materials point of view, the development and engineering of the dilatometer offers the opportunity of a more accurate investigation of the behavior of the materials that constitute the electrodes, recreating more easily the real working conditions. In addition, the accessories provided with the instrument, i.e. the two types of sample holders and the possibility of retooling are unique in the state of the art of this inspection technique.
Moreover, from the sensor point of view, at the current state of the art there is no control on the battery production line based on photoionization technology; this certainly demonstrates the wide margin for improvement in this area of technology and the gap that currently exists between the aspect of efficiency and that of safety.
The same is true for the proposed colorimetric sensor: in this case, the gap between the object to be monitored and the monitoring system is even wider. This is confirmed by the numerous initiatives being promoted and funded by Europe and by all the Countries in recent years. The study of the colorimetric sensor fits perfectly into this research trend and offers undoubtedly food for thought for the exploration of increasingly intelligent monitoring systems that aim to obtain safer systems for energy storage, safe and efficient electric vehicles

and ultimately a better quality of life and the environment in which we live. In the very end, this work successfully achieved its goals and some interesting steps were taken in the process of improving battery control and monitoring techniques.

References

[1] Bernhard Bereiter, Sarah Eggleston, Jochen Schmitt, Christoph Nehrbass-Ahles, Thomas F. Stocker, Hubertus Fischer, Sepp Kipfstuhl, and Jerome Chappellaz. Revision of the EPICA Dome C CO2 record from 800 to 600-kyr before present. *Geophysical Research Letters*, 42(2):542–549, 2015.

[2] Andy Haines and Kristie Ebi. The Imperative for Climate Action to Protect Health. *New England Journal of Medicine*, 380(3):263–273, 2019.

[3] Sebastian Wolff, Matthias Brönner, Maximilian Held, and Marcus Lienkamp. Transforming automotive companies into sustainability leaders: A concept for managing current challenges. *Journal of Cleaner Production*, 276, 2020.

[4] Sabine Fuss, Josep G. Canadell, Glen P. Peters, Massimo Tavoni, Robbie M. Andrew, Philippe Ciais, Robert B. Jackson, Chris D. Jones, Florian Kraxner, Nebosja Nakicenovic, Corinne Le Quéré, Michael R. Raupach, Ayyoob Sharifi, Pete Smith, and Yoshiki Yamagata. COMMENTARY: Betting on negative emissions. *Nature Climate Change*, 4(10):850–853, 2014.

[5] ESA European Space Agency. ESA - Coronavirus lockdown leading to drop in pollution across Europe. *Coronavirus lockdown leading to drop in pollution across Europe*, 2020.

[6] Siang Fui Tie and Chee Wei Tan. A review of energy sources and energy management system in electric vehicles. *Renewable and Sustainable Energy Reviews*, 20:82–102, 2013.

[7] Gianfranco Pistoia and Boryann Liaw. *Behaviour of Lithium-Ion Batteries in Electric Vehicles*. Number July. 2018.

[8] Marco Münster, Michael Schäffer, Gerhard Kopp, Gundolf Kopp, and Horst E. Friedrich. New Approach for a Comprehensive Method for Urban Vehicle Concepts with Electric Powertrain and their Necessary Vehicle Structures. *Transportation Research Procedia*, 14:3686–3695, 2016.

[9] Nick Albanese. Presentation - Electric Vehicle Outlook 2020. Technical report, 2020.

[10] Bloomberg. Electric Vehicle Outlook 2020-Executive Summary. Technical report, 2020.

[11] Bloomberg. Electric Vehicle Outlook 2019-Executive Summary. Technical report, 2019.

[12] Deloitte Insight. Electric vehicles- Setting a course for 2030. Technical report, 2020.

[13] Christian Julien, Alain Mauger, Ashok Vilh, and Karim Zaghib. *Lithium batteries*, volume 15. 2016.

[14] Harry L Tuller. *Solid State Batteries: Materials Design and Optimization*. 1994.

[15] Jang Wook Choi and Doron Aurbach. Promise and reality of post-lithium-ion batteries with high energy densities. *Nature Reviews Materials*, 1, 2016.

[16] Antti Väyrynen and Justin Salminen. Lithium ion battery production. *Journal of Chemical Thermodynamics*, 46:80–85, 2012.

[17] Tobias Elwert, Daniel Goldmann, Felix Römer, Matthias Buchert, Cornelia Merz, Doris Schueler, and Juergen Sutter. Current developments and challenges in the recycling of key components of (Hybrid) electric vehicles,

2016.

[18] Bruce Dunn, Haresh Kamath, and Jean Marie Tarascon. Electrical energy storage for the grid: A battery of choices. *Science*, 334(6058):928–935, 2011.

[19] Da Deng. Li-ion batteries: Basics, progress, and challenges. *Energy Science and Engineering*, 3(5):385–418, 2015.

[20] Dominic Bresser, Kei Hosoi, David Howell, Hong Li, Herbert Zeisel, Khalil Amine, and Stefano Passerini. Perspectives of automotive battery R&D in China, Germany, Japan, and the USA. *Journal of Power Sources*, 382(February):176–178, 2018.

[21] Bruce Dunn, Haresh Kamath, and Jean Marie Tarascon. Electrical energy storage for the grid: A battery of choices. *Science*, 334(6058):928–935, 2011.

[22] Arumugam Manthiram, Yongzhu Fu, Sheng-heng Chung, Chenxi Zu, and Yu-sheng Su. Rechargeable Lithium-Sulfur Batteries. *Chemical Reviews*, 114(23):11751–11787, 2014.

[23] M Steen, N Lebadeva, F Di Persio, and L Boon-Brett. EU Competitiveness in Advanced Li-ion Batteries for E-Mobility and Stationary Storage Applications - Opportunities and Actions. *Publications Office of the European Union*, page 44, 2017.

[24] Ilka von Dalwigk, Patrick Clerens, and Edel Sheridan. European Technology and Innovation Platform, Status April 2019. Technical Report April, 2019.

[25] W.A. Schalkwijk and B. Scrosati. *Advances in Lithium-Ion Batteries*. 2002.

[26] Xiangkun Wu, Kaifang Song, Xiaoyan Zhang, Naifang Hu, Liyuan Li, Wenjie Li, Lan Zhang, and Haitao Zhang. Safety issues in lithium ion batteries: Materials and cell design. *Frontiers in Energy Research*, 7(JUL):1–17, 2019.

[27] V. Ruiz, A. Pfrang, A. Kriston, N. Omar, P. Van den Bossche, and L. Boon-Brett. A review of international abuse testing standards and regulations for lithium ion batteries in electric and hybrid electric vehicles. *Renewable and Sustainable Energy Reviews*, 81(July 2017):1427–1452, 2018.

[28] Pius Victor Chombo and Yossapong Laoonual. A review of safety strategies of a Li-ion battery. *Journal of Power Sources*, 478(July):228649, 2020.

[29] Martin Winter, Gerhard H. Wrodnigg, Jürgen O. Besenhard, Werner Biberacher, and Petr Novák. Dilatometric Investigations of Graphite Electrodes in Nonaqueous Lithium Battery Electrolytes. *Journal of The Electrochemical Society*, 147(7):2427, 2000.

[30] M. Hahn, O. Barbieri, F. P. Campana, R. Kötz, and R. Gallay. Carbon based double layer capacitors with aprotic electrolyte solutions: The possible role of intercalation/insertion processes. *Applied Physics A: Materials Science and Processing*, 82(4 SPEC. ISS.):633–638, 2006.

[31] Rachel L. Wilson, Cristian Eugen Simion, Christopher S. Blackman, Claire J. Carmalt, Adelina Stanoiu, Francesco Di Maggio, and James A. Covington. The effect of film thickness on the gas sensing properties of ultra-thin TiO2 films deposited by atomic layer deposition. *Sensors (Switzerland)*, 18(3), 2018.

[32] RAE Systems Inc. *The PID Handbook*. 2013.

[33] Gianfranco Pistoia. *Lithium-Ion Batteries Advances and Applications Gianfranco*. 2014.

[34] G. Korotcenkov. Metal oxides for solid-state gas sensors: What determines our choice? *Materials Science and Engineering B: Solid-State Materials for Advanced Technology*, 139(1):1–23, 2007.

[35] Lee Chapman. Transport and climate change: a review. *Journal of Transport Geography*, 15(5):354–367, 2007.

[36] Suzana Kahn Ribeiro, Maria Josefina Figueroa, Felix Creutzig, Carolina Dubeux, Jane Hupe, Shigeki Kobayashi, Luiz Alberto de Melo Brettas, Theodore Thrasher, Sandy Webb, and Ji Zou. Energy End-Use: Transport. In *Global Energy Assessment (GEA)*, pages 575–648. 2012.

[37] Ottmar Edenhofer, Ramon Pichs-Madruga, Youba Sokona, Ellie Farahani, Susanne Kadner, Kristin Seyboth, Anna Adler, Ina Baum, Steffen Brunner, Patrick Eickemeier, Benjamin Kriemann, Jussi Savolainen, Steffen Schlömer, Christoph von Stechow, Zwickel Timm, and Jan C. Minx. Climate Change 2014: Mitigation of Climate Change. Contribution of Working Group III to the Fifth Assessment Report of the Intergovernmental Panel on Climate Change. Technical report, 2014.

[38] Andrew A. Lacis, Gavin A. Schmidt, David Rind, and Reto A. Ruedy. Atmospheric CO2: Principal control knob governing earth's temperature. *Science*, 330(6002):356–359, 2010.

[39] Bjorn H. Samset, Jan Sigurd Fuglestvedt, and Marianne T. Lund. Delayed emergence of a global temperature response after emission mitigation. *Nature Communications*, 11(1):1–10, 2020.

[40] Daniel Mitchell, Clare Heaviside, Sotiris Vardoulakis, Chris Huntingford, Giacomo Masato, Benoit P Guillod, Peter Frumhoff, Andy Bowery, David Wallom, and Myles Allen. Attributing human mortality during extreme heat waves to anthropogenic climate change. *Environmental Research Letters*, 11(7), 2016.

[41] WHO. Quantitative risk assessment of the effects of climate change on selected causes of death, 2030s and 2050s. (April), 2014.

[42] Kristie L. Ebi, Tomoko Hasegawa, Katie Hayes, Andrew Monaghan, Shlomit Paz, and Peter Berry. Health risks of warming of 1.5 Â°c, 2 Â°c, and higher, above pre-industrial temperatures. *Environmental Research Letters*, 13(6), 2018.

[43] United States Environmental Protection Agency. The Plain English Guide to the Clean Air Act. page 28, 2007.

[44] Lars Friberg and Marie Vahter. Lead in Petrol. *The Lancet*, 322(8343):220, 1983.

[45] United Nations. United Nations Framework Convention on Climate Change. Technical report, 1992.

[46] United Nations. KYOTO PROTOCOL TO THE UNITED NATIONS FRAMEWORK CONVENTION ON CLIMATE CHANGE. 1998.

[47] European Parliament and Council of the European Union. Regulation (EC) no. 443/2009. *Official Journal of the European Union*, 140(1):1–15, 2009.

[48] European Council. European Council (23 and 24 October 2014) Conclusions, EUCO 169/14, CO EUR 13, CONCL 5. *European Council*, (October):1–15, 2014.

[49] Paris Agreement, 2015.

[50] Global Warming of 1.5Â°C. An IPCC Special Report on the impacts of global warming of 1.5Â°C above pre-industrial levels and related global greenhouse gas emission pathways, in the context of strengthening the global response to the threat of climate change . Technical report, 2018.

[51] European Commission. A Clean Planet for all. A European long-term strategic vision for a prosperous, modern, competitive and climate neutral economy. *Com(2018) 773*, page 114, 2018.

[52] European Union. Regulation (EU) 2019/631 of the European Parliament and of the Council of 17 April 2019 setting CO2 emission performance standards for new passenger cars and for new light commercial vehicles, and repealing Regulations (EC) No 443/2009 and (EU) No 510/201. *Official Journal of the European Union*, 62(L111):13–53, 2019.

[53] Georgios Fontaras, Biagio Ciuffo, Nikiforos Zacharof, Stefanos Tsiakmakis, Alessandro Marotta, Jelica Pavlovic, and Konstantinos Anagnostopoulos. The difference between reported and real-world CO 2 emissions: How much improvement can be expected by WLTP introduction? *Transportation Research Procedia*, 25:3933–3943, 2017.

[54] Uwe Tietge (ICCT), Sonsoles Díaz, Peter Mock, Anup Bandivadekar, Jan Dornoff, and Norbert Ligterink (TNO). From Laboratory to Road - A 2018 update of official and 'Real-World' fuel consumption and CO2 values for passenger cars in Europe. *ICCT - White Paper*, (January), 2019.

[55] Joeri Rogelj, Drew Shindell, Kejun Jiang, and Solomone Fifita. IPCC 2018, cap2. Technical report, 2018.

[56] Michael R. Raupach, Steven J. Davis, Glen P. Peters, Robbie M. Andrew, Josep G. Canadell, Philippe Ciais, Pierre Friedlingstein, Frank Jotzo, Detlef P. Van Vuuren, and Corinne Le Quéré. Sharing a quota on cumulative carbon emissions. *Nature Climate Change*, 4(10):873–879, 2014.

[57] Piers M. Forster, Harriet I. Forster, Mat J. Evans, Matthew J. Gidden, Chris D. Jones, Christoph A. Keller, Robin D. Lamboll, Corinne Le Quéré, Joeri Rogelj, Deborah Rosen, Carl Friedrich Schleussner, Thomas B. Richardson, Christopher J. Smith, and Steven T. Turnock. Current and future global climate impacts resulting from COVID-19. *Nature Climate Change*, 10(10):913–919, 2020.

[58] Runsen Zhang and Shinichiro Fujimori. The role of transport electrification in global climate change mitigation scenarios. *Environmental Research Letters*, 15(3), 2020.

[59] Chris Busch. China ' s All In On Electric Vehicles : Here ' s How That Will Accelerate Sales In. *Forbes*, 2018.

[60] Charles Riley. The race to the electric car is just getting started. *CNN Business*, 2019.

[61] C. C. Chan. The state of the art of electric and hybrid vehicles. *Proceedings of the IEEE*, 90(2):247–275, 2002.

[62] Filippo Einaudi. Perché il motore elettrico è più efficiente.

[63] Rebecca Matulka. The History of the Electric Telegraph, nov 2014.

[64] Mary Bellis. The {{History}} of {{Electric Vehicles Began}} in 1830. pages 1899–1901, 2019.

[65] Ancitel Energia e Ambiente S.p.a. Linee guida per la mobilità elettrica. Technical report, 2016.

[66] Dmitry V Pelegov and José Pontes. Main drivers of battery industry changes: Electric vehicles: A market overview, 2018.

[67] Guido Ala, Gabriella di Filippo, Fabio Viola, Graziella Giglia, Antonino Imburgia, Pietro Romano, Vincenzo Castiglia, Filippo Pellitteri, Giuseppe Schettino, and Rosario Miceli. Different scenarios of electric mobility: Current situation and possible future developments of fuel cell vehicles in Italy. *Sustainability (Switzerland)*, 12(2), 2020.

[68] V. Tinelli. *Veicoli ibridi elettrici : modelli numerici e confronto tra diverse architetture*. PhD thesis, Politecnico di torino, 2018.

[69] Ahmed F. Zobaa. *Energy Efficiency and Renewable Energy Handbook*. CRC Press, sep 2015.

[70] Haisheng Chen, Thang Ngoc Cong, Wei Yang, Chunqing Tan, Yongliang Li, and Yulong Ding. Progress in electrical energy storage system: A critical review. *Progress in Natural Science*, 19(3):291–312, 2009.

[71] Corte dei Conti Europea. Il sostegno dell ' UE per lo stoccaggio di energia. Technical report, 2019.

[72] David Linden and Thomas B Reddy. *Handbook of batteries*, volume 33. 1995.

[73] John M. Miller. Energy storage system technology challenges facing strong hybrid, plugin and battery electric vehicles. *5th IEEE Vehicle Power and Propulsion Conference, VPPC '09*, pages 4–10, 2009.

[74] G. J. Offer, D. Howey, M. Contestabile, R. Clague, and N. P. Brandon. Comparative analysis of battery electric, hydrogen fuel cell and hybrid vehicles in a future sustainable road transport system. *Energy Policy*, 38(1):24–29, 2010.

[75] John M. Miller, Ted Bohn, Thomas J. Dougherty, and Uday Deshpande. Why hybridization of energy storage is essential for future hybrid, plug-in and battery electric vehicles. *2009 IEEE Energy Conversion Congress and Exposition, ECCE 2009*, pages 2614–2620, 2009.

[76] G.A. Nazri and G. Pistoia. *Lithium Batteries: science and technology*. 2009.

[77] Laurence Kavanagh, Jerome Keohane, Guiomar Garcia Cabellos, Andrew Lloyd, and John Cleary. Global lithium sources-industrial use and future in the electric vehicle industry: A review. *Resources*, 7(3), 2018.

[78] Jakobus Groenewald, Thomas Grandjean, and James Marco. Accelerated energy capacity measurement of lithium-ion cells to support future circular economy strategies for electric vehicles. *Renewable and Sustainable Energy Reviews*, 69(November 2016):98–111, 2017.

[79] Yan Wang, Qing Gao, Guohua Wang, Pengyu Lu, Mengdi Zhao, and Wendi Bao. A review on research status and key technologies of battery thermal management and its enhanced safety. *International Journal of Energy Research*, 42(13):4008–4033, 2018.

[80] Mogalahalli V. Reddy, Alain Mauger, Christian M. Julien, Andrea Paolella, and Karim Zaghib. Brief history of early lithium-battery development. *Materials*, 13(8):1–9, 2020.

[81] John B. Goodenough. How we made the Li-ion rechargeable battery: Progress in portable and ubiquitous electronics would not be possible without rechargeable batteries. John B. Goodenough recounts the history of the lithium-ion rechargeable battery. *Nature Electronics*, 1(3):204, 2018.

[82] Heng Zhang, Chunmei Li, Gebrekidan Gebresilassie Eshetu, Stéphane Laruelle, Sylvie Grugeon, Karim Zaghib, Christian Julien, Alain Mauger,

Dominique Guyomard, Teófilo Rojo, Nuria Gisbert-Trejo, Stefano Passerini, Xuejie Huang, Zhibin Zhou, Patrik Johansson, and Maria Forsyth. From Solid-Solution Electrodes and the Rocking-Chair Concept to Today's Batteries. *Angewandte Chemie - International Edition*, 59(2):534–538, 2020.

[83] Wu Xu, Jiulin Wang, Fei Ding, Xilin Chen, Eduard Nasybulin, Yaohui Zhang, and Ji Guang Zhang. Lithium metal anodes for rechargeable batteries. *Energy and Environmental Science*, 7(2):513–537, 2014.

[84] F. Orsini, A. Du Pasquier, B. Beaudoin, J. M. Tarascon, M. Trentin, N. Langenhuizen, E. De Beer, and P. Notten. In situ Scanning Electron Microscopy (SEM) observation of interfaces within plastic lithium batteries. *Journal of Power Sources*, 76(1):19–29, 1998.

[85] Tetsuya Osaka and Toshiyuki Momma. Lithium metal/polymer battery. *Journal of Power Sources*, 97-98(December 2000):765–767, 2001.

[86] M. Lazzari and B. Scrosati. A Cyclable Lithium Organic Electrolyte Cell Based on Two Intercalation Electrodes. *Journal of The Electrochemical Society*, 127(3):773–774, 1980.

[87] K. Mizushima, P.C. Jones, P.J. Wiseman, and J.B. Goodenough. LixCoO2 (0<xˆl): A NEW CATHODE MATERIAL FOR BATTERIES OF HIGH ENERGY DENSITY. *Materials Research Bulletin*, 15(6):783–789, 1980.

[88] D Guyornard and J M Tarascon. Rocking-Chair or Li thium-Ion Rechargeable Lithium Batteries. *Advanced Materials*, 6(5):408, 1994.

[89] Ralph J Brodd and Henderson Nv. Comments on the History of Lithium-Ion Batteries. page 89074, 2005.

[90] Yuqi Li, Yaxiang Lu, Philipp Adelhelm, Maria Magdalena Titirici, and Yong Sheng Hu. Intercalation chemistry of graphite: Alkali metal ions and beyond. *Chemical Society Reviews*, 48(17):4655–4687, 2019.

[91] Martin Winter, Jürgen O. Besenhard, Michael E. Spahr, and Petr Novák. Insertion electrode materials for rechargeable lithium batteries. *Advanced Materials*, 10(10):725–763, 1998.

[92] Kang Xu. Nonaqueous liquid electrolytes for lithium-based rechargeable batteries. *Chemical Reviews*, 104(10):4303–4417, 2004.

[93] Sheng Shui Zhang. A review on electrolyte additives for lithium-ion batteries. *Journal of Power Sources*, 162(2 SPEC. ISS.):1379–1394, 2006.

[94] C. Glaize and S. Genies. *Lithium Batteries and Other Electrochemical Storage Systems*. 2013.

[95] J. M. Tarascon and M. Armand. Issues and challenges facing rechargeable lithium batteries. *Nature*, 414, 2001.

[96] The European Commision. Science for Environment Policy Future Brief : green behaviour. Technical Report 20, 2018.

[97] Mats Zackrisson, Lars Avellán, and Jessica Orlenius. Life cycle assessment of lithium-ion batteries for plug-in hybrid electric vehicles-Critical issues. *Journal of Cleaner Production*, 18(15):1519–1529, 2010.

[98] J P Breen, F C Meunier, M Haneda, W Sun, Y Kindaichi, H Hamada, Y Yu, J Saussey, M Daturi, C Hedouin, T Seguelong, a Simon, J M Weil, G W Harris, H Frei, B Weckhuysen, San Diego, E Fridell, M Wolf, D a King, Z P Liu, H Arnolds, I M Lane, D C Papageorgopoulos, a Rushton, M Gill, P Fox, a Daunois, M Yamaguchi, I Goto, M Kumagai, K C Patil, M S Hegde, S J Jenkins, P Bazin, O Marie, D Astruc, T Yoshinari, Y Kintaichi, Yun Jung Lee, Hyunjung Yi, Woo-Jae Kim, Kisuk Kang, Dong Soo

Yun, Michael S Strano, Gerbrand Ceder, and Angela M Belcher. versus Al. *Sciences-New York*, 324(May):1051–1055, 2009.

[99] Won Jin Kwak, Rosy, Daniel Sharon, Chun Xia, Hun Kim, Lee R. Johnson, Peter G. Bruce, Linda F. Nazar, Yang Kook Sun, Aryeh A. Frimer, Malachi Noked, Stefan A. Freunberger, and Doron Aurbach. Lithium-Oxygen Batteries and Related Systems: Potential, Status, and Future. *ACS Applied Materials and Interfaces*, 2020.

[100] Peter G. Bruce, Stefan A. Freunberger, Laurence J. Hardwick, and Jean Marie Tarascon. LigO2 and LigS batteries with high energy storage. *Nature Materials*, 11(1):19–29, 2012.

[101] T H E Juncker, Commission Delivers, O N Its, and Energy Union. The Juncker Commission Delivers Energy Union Priority. (April):2019–2020, 2019.

[102] European Battery Alliance. What is the European Battery Alliance and why does it matter?, 2020.

[103] European Comission. Europe on the move - Annex 2: strategic Action Plan on Batteries. *Journal of Retailing and Consumer Services*, pages 1–10, 2018.

[104] The European Commision. Directive 2007/64/EC of the European Parliament and of the Council on batteries and accumulators and waste batteries and accumulators, 2006.

[105] The European Commision. Towards an Integrated Strategic Energy Technology (SET) Plan: Accelerating the European Energy System Transformation EN, 2015.

[106] European Battery Alliance. What is the European Battery Alliance and why does it matter? 2020.

[107] Energy storage: European Commission, 2020.

[108] SETIS. Integrated SET-Plan Action 7 "Become competitive in the global battery sector to drive e-mobility and stationary storage forward". pages 1–70, 2016.

[109] Battery 2030 - about us, 2020.

[110] Peter Cohan and Peter Cohan. Boeing, Dell Technologies, Samsung, Tesla and Burning Lithium Ion Batteries. *Forbes Magazine*, (January):1–3, 2016.

[111] Dan Doughty and E. Peter Roth. A general discussion of Li Ion battery safety. *Electrochemical Society Interface*, 21(2):37–44, 2012.

[112] Zhonghao Rao, Shuangfeng Wang, Maochun Wu, Zirong Lin, and Fuhuo Li. Experimental investigation on thermal management of electric vehicle battery with heat pipe. *Energy Conversion and Management*, 65:92–97, 2013.

[113] James Michael Hooper and James Marco. Characterising the in-vehicle vibration inputs to the high voltage battery of an electric vehicle. *Journal of Power Sources*, 245:510–519, 2014.

[114] Shashank Arora, Weixiang Shen, and Ajay Kapoor. Review of mechanical design and strategic placement technique of a robust battery pack for electric vehicles. *Renewable and Sustainable Energy Reviews*, 60:1319–1331, 2016.

[115] Samuel C. Levy. Safety and reliability considerations for lithium batteries. *Journal of Power Sources*, 68(1):75–77, 1997.

[116] Jianwu Wen, Yan Yu, and Chunhua Chen. A review on lithium-ion bat-

teries safety issues: Existing problems and possible solutions. *Materials Express*, 2(3):197–212, 2012.

[117] Lianbo Ma, Renpeng Chen, Yi Hu, Wenjun Zhang, Guoyin Zhu, Peiyang Zhao, Tao Chen, Caixing Wang, Wen Yan, Yanrong Wang, Lei Wang, Zuoxiu Tie, Jie Liu, and Zhong Jin. Nanoporous and lyophilic battery separator from regenerated eggshell membrane with effective suppression of dendritic lithium growth. *Energy Storage Materials*, 14(February):258–266, 2018.

[118] Samuel C. Levy and Per Bro. *Battery Hazards and Accident Prevention*. Springer US, 1994.

[119] P Notten, H Bergveld, and W Kruijt. *Battery management systems: design by modeling*. Number December. 2002.

[120] Yujie Wang, Jiaqiang Tian, Zhendong Sun, Li Wang, Ruilong Xu, Mince Li, and Zonghai Chen. A comprehensive review of battery modeling and state estimation approaches for advanced battery management systems. *Renewable and Sustainable Energy Reviews*, 131(July):110015, 2020.

[121] Seyed Mohammad Rezvanizaniani, Zongchang Liu, Yan Chen, and Jay Lee. Review and recent advances in battery health monitoring and prognostics technologies for electric vehicle (EV) safety and mobility. *Journal of Power Sources*, 256:110–124, 2014.

[122] Wladislaw Waag, Christian Fleischer, and Dirk Uwe Sauer. Critical review of the methods for monitoring of lithium-ion batteries in electric and hybrid vehicles. *Journal of Power Sources*, 258:321–339, 2014.

[123] Shun Xiang, Guangdi Hu, Ruisen Huang, Feng Guo, and Pengkai Zhou. Lithium-ion battery online rapid state-of-power estimation under multiple constraints. *Energies*, 11(2):22–26, 2018.

[124] Xintian Liu, Yao He, Guojian Zeng, Jiangfeng Zhang, and Xinxin Zheng. State-of-Power Estimation of Li-Ion Batteries Considering the Battery Surface Temperature. *Energy Technology*, 6(7):1352–1360, 2018.

[125] Ahmad Pesaran. Battery Thermal Management in EVs and HEVs : Issues and Solutions. *Advanced Automotive Battery Conference*, (January):10, 2001.

[126] Yan Wang, Qing Gao, Guohua Wang, Pengyu Lu, Mengdi Zhao, and Wendi Bao. A review on research status and key technologies of battery thermal management and its enhanced safety. *International Journal of Energy Research*, 42(13):4008–4033, 2018.

[127] Zhoujian An, Li Jia, Yong Ding, Chao Dang, and Xuejiao Li. A review on lithium-ion power battery thermal management technologies and thermal safety. *Journal of Thermal Science*, 26(5):391–412, 2017.

[128] Manh Kien Tran and Michael Fowler. A review of lithium-ion battery fault diagnostic algorithms: Current progress and future challenges. *Algorithms*, 13(3), 2020.

[129] Parthasarathy M. Gomadam, John W. Weidner, Roger A. Dougal, and Ralph E. White. Mathematical modeling of lithium-ion and nickel battery systems. *Journal of Power Sources*, 110(2):267–284, 2002.

[130] Y. Ashraf Gandomi, D. S. Aaron, J. R. Houser, M. C. Daugherty, J. T. Clement, A. M. Pezeshki, T. Y. Ertugrul, D. P. Moseley, and M. M. Mench. Critical Review-Experimental Diagnostics and Material Characterization Techniques Used on Redox Flow Batteries. *Journal of The Electrochemical Society*, 165(5):A970–A1010, 2018.

[131] Isidor Buchmann. *Batteries in a portable world - A Handbook on Rechargeable Batteries for Non-Engineers*. 2000.

[132] Jun Lu, Tianpin Wu, and Khalil Amine. State-of-the-art characterization techniques for advanced lithium-ion batteries. *Nature Energy*, 2(3), 2017.

[133] Chang Liu, Feng Li, Ma Lai-Peng, and Hui Mmg Cheng. Advanced materials for energy storage. *Advanced Materials*, 22(8):28–62, 2010.

[134] Keyan Li, Hui Xie, Jun Liu, Zengsheng Ma, Yichun Zhou, and Dongfeng Xue. From chemistry to mechanics: Bulk modulus evolution of Li-Si and Li-Sn alloys via the metallic electronegativity scale. *Physical Chemistry Chemical Physics*, 15(40):17658–17663, 2013.

[135] Giovanna Bucci, Tushar Swamy, Yet Ming Chiang, and W. Craig Carter. Modeling of internal mechanical failure of all-solid-state batteries during electrochemical cycling, and implications for battery design. *Journal of Materials Chemistry A*, 5(36):19422–19430, 2017.

[136] F. Grimsmann, F. Brauchle, T. Gerbert, A. Gruhle, J. Parisi, and M. Knipper. Impact of different aging mechanisms on the thickness change and the quick-charge capability of lithium-ion cells. *Journal of Energy Storage*, 14:158–162, 2017.

[137] S. Grugeon, S. Laruelle, R. Herrera-Urbina, L. Dupont, P. Poizot, and J-M. Tarascon. Particle Size Effects on the Electrochemical Performance of Copper Oxides toward Lithium. *Journal of The Electrochemical Society*, 148(4):A285, 2001.

[138] Sumitava De. *Effect of Design Parameters and Intercalation Induced Stresses in Lithium Ion Batteries*. PhD thesis, Washington University in St. Louis, 2014.

[139] Sulin Zhang. Chemomechanical modeling of lithiation-induced failure in high-volume-change electrode materials for lithium ion batteries. *npj Computational Materials*, 3(1):1–10, 2017.

[140] B. Rieger, S. Schlueter, S. V. Erhard, J. Schmalz, G. Reinhart, and A. Jossen. Multi-scale investigation of thickness changes in a commercial pouch type lithium-ion battery. *Journal of Energy Storage*, 6:213–221, 2016.

[141] Alok M. Tripathi, Wei Nien Su, and Bing Joe Hwang. In situ analytical techniques for battery interface analysis. *Chemical Society Reviews*, 47(3):736–751, 2018.

[142] A. Metrot, P. Willmann, and A. Herold. Insertion electrochimique du complexe BF3,(C2H5)2O dans un pyrographite. *Materials Science and Engineering*, 31(C):83–86, 1977.

[143] W. Biberacher, A. Lerf, J. O. Besenhard, H. Möhwald, and T. Butz. A high resolution dilatometer for in situ studies of the electrointercalation of layered materials. *Materials Research Bulletin*, 17(11):1385–1392, 1982.

[144] M. Hahn, O. Barbieri, R. Gallay, and R. Kötz. A dilatometric study of the voltage limitation of carbonaceous electrodes in aprotic EDLC type electrolytes by charge-induced strain. *Carbon*, 44(12):2523–2533, 2006.

[145] J.R. Dahn, Rosamaria Fong, and M. J. Spoon. Suppression of staging in lithium-intercalated carbon by disorder in the host. *Physical Review B*, 42(10), 1990.

[146] A.K. Padhi, K.S. Nanjundaswamy, and J.B. Goodenough. Phospho olivines as positive electrode materials for recheargeable Lithium Batteries. *Journal of Electrochemical Society*, 144(4):1188–1194, 1997.

[147] Daniel Sauerteig, Svetlozar Ivanov, Holger Reinshagen, and Andreas Bund. Reversible and irreversible dilation of lithium-ion battery electrodes investigated by in-situ dilatometry. *Journal of Power Sources*, 342:939–946, 2017.

[148] Bernhard Bitzer and Andreas Gruhle. A new method for detecting lithium plating by measuring the cell thickness. *Journal of Power Sources*, 262:297–302, 2014.

[149] Tsutomu Ohzuku, Naoki Matoba, and Keijiro Sawai. Direct evidence on anomalous expansion of graphite-negative electrodes on first charge by dilatometry. *Journal of Power Sources*, 97-98:73–77, 2001.

[150] Patricia Handel, Gisela Fauler, Katja Kapper, Martin Schmuck, Christoph Stangl, Roland Fischer, Frank Uhlig, and Stefan Koller. Thermal aging of electrolytes used in lithium-ion batteries - An investigation of the impact of protic impurities and different housing materials. *Journal of Power Sources*, 267:255–259, 2014.

[151] Cheng Lin, Aihua Tang, Hao Mu, Wenwei Wang, and Chun Wang. Aging mechanisms of electrode materials in lithium-ion batteries for electric vehicles. *Journal of Chemistry*, 2015, 2015.

[152] Martin Grützke, Vadim Kraft, Björn Hoffmann, Sebastian Klamor, Jan Diekmann, Arno Kwade, Martin Winter, and Sascha Nowak. Aging investigations of a lithium-ion battery electrolyte from a field-tested hybrid electric vehicle. *Journal of Power Sources*, 273:83–88, 2015.

[153] R.S. Katarkar, P.P. Bhosale, K.S. Kumbhar, A.K. Mahajan, and Anil Yachkal. Study on Leak Testing Methods. *International Journal for Scientific Research & Development—*, 5(1), 2017.

[154] Hans Rottländer, Walter Umrath, and Gerhard Voss. Fundamentals of leak detection. Technical Report 199, 2016.

[155] EMRP IND 12 consortium. Metrology of the leak detection - Practical guide. (October):69, 2015.

[156] Eva Schlick-Hasper, Marcel Neitsch, and Thomas Goedecke. Industrial leak testing of dangerous goods packagings. *Packaging Technology and Science*, 33(7):273–286, 2020.

[157] Daniel Wetzig and Maximillian Reismann. Methods for Leak Testing Lithium-Ion Batteries to Assure Quality with Proposed Rejection Limit Standards. *SAE Technical Papers*, (April):1–9, 2020.

[158] Jr. Ralph R. Roe. NASA-STD-7012. Technical report, 2019.

[159] VTech. Leak Detection Methods : A Comparative Study of Technologies and Techniques. Technical report, 2006.

[160] Thad Godish. *Sick Buildings*. 1995.

[161] Andreas Schütze, Tobias Baur, Martin Leidinger, Wolfhard Reimringer, Ralf Jung, Thorsten Conrad, and Tilman Sauerwald. Highly sensitive and selective VOC sensor systems based on semiconductor gas sensors: How to? *Environments - MDPI*, 4(1):1–13, 2017.

[162] Xiao Liu, Sitian Cheng, Hong Liu, Sha Hu, Daqiang Zhang, and Huansheng Ning. A survey on gas sensing technology. *Sensors (Switzerland)*, 12(7):9635–9665, 2012.

[163] Davion Hill, Ben Gully, Arun Agarwal, Ali Nourai, Lora Thrun, Scott Swartz, Mark Koslowske, Steve Cummings, John Butkowski, and Brad Moore. Detection of off gassing from Li-ion batteries. *2013 IEEE Energytech, Energytech 2013*, 2013.

[164] Ghenadii Korotcenkov. *Handbook of Gas Sensor Materials*, volume 2. 2014.

[165] Elisabetta Comini. Metal oxide nano-crystals for gas sensing. *Analytica Chimica Acta*, 568(1-2):28–40, 2006.

[166] Stephanie A Hooker. Nanotechnology Advantages Applied to Gas Sensor Development. *The Nanoparticles 2002 Conference Proceedings*, pages 1–7, 2002.

[167] Claus-Dieter Kohl and Thorsten Wagner. *Gas Sensing Fundamentals*. 2014.

[168] Ananya Dey. Semiconductor metal oxide gas sensors: A review. *Materials Science and Engineering B: Solid-State Materials for Advanced Technology*, 229(December 2017):206–217, 2018.

[169] Rafaela S. Andre, Rafaela C. Sanfelice, Adriana Pavinatto, Luiz H.C. Mattoso, and Daniel S. Correa. Hybrid nanomaterials designed for volatile organic compounds sensors: A review. *Materials and Design*, 156:154–166, 2018.

[170] Jane Hodgkinson and Ralph P. Tatam. Optical gas sensing: A review. *Measurement Science and Technology*, 24(1), 2013.

[171] Isolde Simon and Michael Arndt. Thermal and gas-sensing properties of a micromachined thermal conductivity sensor for the detection of hydrogen in automotive applications. *Sensors and Actuators, A: Physical*, 97-98:104–108, 2002.

[172] Lee Mike S. *Mass Spectrometry Handbook*. 2012.

[173] Ian R. Lewis and Howell G.M Edwards. *Handbook of Raman Spectroscopy*. 2001.

[174] A. Macagnano, E. Zampetti, and E. Kny. Electrospinning for High Performance Sensors. *NanoScience and Technology*, page 340, 2015.

[175] Antonella Macagnano, Emiliano Zampetti, and Erich Kny. *Electrospinning for High Performance Sensors*. 2015.

[176] Jyoti V. Patil, Sawanta S. Mali, Archana S. Kamble, Chang K. Hong, Jin H. Kim, and Pramod S. Patil. Electrospinning: A versatile technique for making of 1D growth of nanostructured nanofibers and its applications: An experimental approach. *Applied Surface Science*, 423:641–674, 2017.

[177] Bin Ding, Moran Wang, Jianyong Yu, and Gang Sun. Gas sensors based on electrospun nanofibers. *Sensors*, 9(3):1609–1624, 2009.

[178] Ji Sun Im, Seok Chang Kang, Sei Hyun Lee, and Young Seak Lee. Improved gas sensing of electrospun carbon fibers based on pore structure, conductivity and surface modification. *Carbon*, 48(9):2573–2581, 2010.

[179] Il Doo Kim, Avner Rothschild, Byong Hong Lee, Dong Young Kim, Seong Mu Jo, and Harry L. Tuller. Ultrasensitive chemiresistors based on electrospun TiO 2 nanofibers. *Nano Letters*, 6(9):2009–2013, 2006.

[180] Min Yang, Tengfeng Xie, Liang Peng, Yiyang Zhao, and Dejun Wang. Fabrication and photoelectric oxygen sensing characteristics of electrospun Co doped ZnO nanofibres. *Applied Physics A: Materials Science and Processing*, 89(2):427–430, 2007.

[181] R Viter, A Abou Chaaya, I Iatsunskyi, G Nowaczyk, K Kovalevskis, D Erts, P Miele, V Smyntyna, and M Bechelany. Tuning of ZnO 1D nanostructures by atomic layer deposition and electrospinning for optical gas sensor applications. *Nanotechnology*, 26(10), 2015.

[182] R. Luoh and H. Thomas Hahn. Electrospun nanocomposite fiber mats as

gas sensors. *Composites Science and Technology*, 66(14):2436–2441, 2006.

[183] A. Z. Sadek, W. Wlodarski, K. Shin, R. B. Kaner, and K. Kalantar-Zadeh. A layered surface acoustic wave gas sensor based on a polyaniline/In 2O3 nanofibre composite. *Nanotechnology*, 17(17):4488–4492, 2006.

[184] Joseph Wang. Carbon-nanotube based electrochemical biosensors: A review. *Electroanalysis*, 17(1):7–14, 2005.

[185] Paolo Bondavalli, Pierre Legagneux, and Didier Pribat. Carbon nanotubes based transistors as gas sensors: State of the art and critical review. *Sensors and Actuators, B: Chemical*, 140(1):304–318, 2009.

[186] Hyeonseok Yoon. Current Trends in Sensors Based on Conducting Polymer Nanomaterials. *Nanomaterials*, 3(3):524–549, 2013.

[187] Mianqi Xue, Fengwang Li, Dong Chen, Zhanhai Yang, Xiaowei Wang, and Junhui Ji. High-Oriented Polypyrrole Nanotubes for Next-Generation Gas Sensor. *Advanced Materials*, 28(37):8265–8270, 2016.

[188] Chengxiang Wang, Longwei Yin, Luyuan Zhang, Dong Xiang, and Rui Gao. Metal oxide gas sensors: Sensitivity and influencing factors. *Sensors*, 10(3):2088–2106, 2010.

[189] Philip J.D. Peterson, Amrita Aujla, Kirsty H. Grant, Alex G. Brundle, Martin R. Thompson, Josh Vande Hey, and Roland J. Leigh. Practical use of metal oxide semiconductor gas sensors for measuring nitrogen dioxide and ozone in urban environments. *Sensors (Switzerland)*, 17(7):1–25, 2017.

[190] M. Wenger, R. Waller, V. R.H. Lorentz, M. Marz, and M. Herold. Investigation of gas sensing in large lithium-ion battery systems for early fault detection and safety improvement. *IECON Proceedings (Industrial Electronics Conference)*, pages 5654–5659, 2014.

[191] Chang Jun Bae, Ashish Manandhar, Peter Kiesel, and Ajay Raghavan. Monitoring the Strain Evolution of Lithium-Ion Battery Electrodes using an Optical Fiber Bragg Grating Sensor. *Energy Technology*, 4(7):851–855, 2016.

[192] Pamina Bohn, Gerd Liebig, Lidiya Komsiyska, and Gunther Wittstock. Temperature propagation in prismatic lithium-ion-cells after short term thermal stress. *Journal of Power Sources*, 313:30–36, 2016.

[193] Shengxin Zhu, Jindong Han, Tai Song Pan, Yi Min Wei, Wei Li Song, Hao Sen Chen, and Daining Fang. A novel designed visualized Li-ion battery for in-situ measuring the variation of internal temperature. *Extreme Mechanics Letters*, 37:100707, 2020.

[194] Elena Vergori and Yifei Yu. Monitoring of Li-ion cells with distributed fibre optic sensors. *Procedia Structural Integrity*, 24:233–239, 2019.

[195] Gang Yang, Catia Leitão, Yuhong Li, João Pinto, and Xuefan Jiang. Real-time temperature measurement with fiber Bragg sensors in lithium batteries for safety usage. *Measurement: Journal of the International Measurement Confederation*, 46(9):3166–3172, 2013.

[196] Joe Fleming, Tazdin Amietszajew, Euan McTurk, Dave Greenwood, and Rohit Bhagat. Development and evaluation of in-situ instrumentation for cylindrical Li-ion cells using fibre optic sensors. *HardwareX*, 3:100–109, 2018.

[197] Dean Anthony, Derek Wong, David Wetz, and Ankur Jain. Non-invasive measurement of internal temperature of a cylindrical Li-ion cell during high-rate discharge. *International Journal of Heat and Mass Transfer*,

111:223–231, 2017.

[198] Panding Wang, Xinyi Zhang, Le Yang, Xingyu Zhang, Meng Yang, Haosen Chen, and Daining Fang. Real-time monitoring of internal temperature evolution of the lithium-ion coin cell battery during the charge and discharge process. *Extreme Mechanics Letters*, 9:459–466, 2016.

[199] Chi Yuan Lee, Shuo Jen Lee, Yi Ming Hung, Chien Te Hsieh, Yu Ming Chang, Yen Ting Huang, and Jyun Ting Lin. Integrated microsensor for real-time microscopic monitoring of local temperature, voltage and current inside lithium ion battery. *Sensors and Actuators, A: Physical*, 253:59–68, 2017.

[200] Joe Fleming, Tazdin Amietszajew, Jerome Charmet, Alexander John Roberts, David Greenwood, and Rohit Bhagat. The design and impact of in-situ and operando thermal sensing for smart energy storage. *Journal of Energy Storage*, 22(February):36–43, 2019.

[201] Micael Nascimento, Susana Novais, Markus S. Ding, Marta S. Ferreira, Stephan Koch, Stefano Passerini, and João L. Pinto. Internal strain and temperature discrimination with optical fiber hybrid sensors in Li-ion batteries. *Journal of Power Sources*, 410-411(October 2018):1–9, 2019.

[202] Micael Nascimento, Marta S. Ferreira, and João L. Pinto. Simultaneous sensing of temperature and bi-directional strain in a prismatic li-ion battery. *Batteries*, 4(2), 2018.

[203] European Commission. INSTABAT, 2020.

[204] European Commission. SENSIBAT, 2020.

[205] European Commission. SPARTACUS, 2020.

[206] European Commission. BAT4EVER, 2020.

[207] Giampaolo Lacarbonara, Morteza Rahmanipour, Juri Belcari, Lorenzo Lodi, Andrea Zucchelli, and Catia Arbizzani. Electrodilatometric analysis under applied force : a powerful tool for electrode. *Electrochimica Acta*, 375:137938, 2020.

[208] Pascal Maire, Anna Evans, Hermann Kaiser, Werner Scheifele, and Petr Novák. Colorimetric Determination of Lithium Content in Electrodes of Lithium-Ion Batteries. *Journal of The Electrochemical Society*, 155(11):A862, 2008.

[209] G. X. Zhang. A Study on the Abbe Principle and Abbe Error. *CIRP Annals - Manufacturing Technology*, 38(1):525–528, 1989.

[210] Richard Leach. CIRP Encyclopedia of Production Engineering. *CIRP Encyclopedia of Production Engineering*, (January), 2020.

Acknowledgment

Author would like to acknowledge:

- professor *Andrea Zucchelli*[1], man and scientist from who I learned to think beyond the evidence and outside the box;
- professor *Catia Arbizzani*[2] for her competence, her availability, her always intelligent help and for the constant incentives to work better and better;
- *Giampaolo Lacarbonara*[3] for his invaluable work, for his support throughout the experimental phase of electrochemical validation, and for his calm and patience shown with a crude mechanical engineer into a electrochemistry laboratory;
- *Roberto Baruchello*[4], *Andrea Bergami*[5] and *Nicola Scandola*[6] for giving me the opportunity to continue my education in the doctoral school and for supporting me during my first three years at Marposs S.p.A.
- *Antonio De Renzis*[7] for sharp suggestions and support in the realization of the sensor prototype;
- *Lorenzo Lodi*[8], *Marco Buoso*[9], *Antonio Mengoli*[10], *Franco Stanghellini*[11], *Giuseppe Vollaro*[12], *Chiara Dal Porto*[13], *Enrico Mansini*[14] and all office colleagues for their important help and support with daily problems and for all the funny time spent together;
- *Marposs S.p.A company*[15] for its important help and support during throughout the PhD program;

[1] Associate professor, Department of Industrial Engineering, University of Bologna.
[2] Associate professor, Department of Chemistry *"Giacomo Ciamician"*, University of Bologna.
[3] Ph.D. student, Department of Chemistry *"Giacomo Ciamician"*, University of Bologna.
[4] Division Development Center Manager, Marposs S.p.A .
[5] Special Applications Division Manager, Marposs S.p.A .
[6] HR, Organization and Information Systems Manager, Marposs S.p.A .
[7] R&D Embedded Systems Development Manager, Marposs S.p.A .
[8] Division Development Center Manager, Marposs S.p.A .
[9] R&D Measuring Systems - Senior Hardware Designer, Marposs S.p.A .
[10] R&D Measuring Systems - Senior Hardware Designer Marposs S.p.A .
[11] Electric Vehicles - Industry Manager, Marposs S.p.A .
[12] Assembly and Leak Test Systems - Corporate Manager, Marposs S.p.A .
[13] Special Applications - Product Development Engineer, Marposs S.p.A .
[14] R&D Leak-Test Lab. Manager, Marposs S.p.A .
[15] via Saliceto 13, 40010 Bentivoglio (BO) ✉info@marposs.com

Finally, I would like to thank all the people who have supported me along this path.

Bologna, April 19, 2021 J. B.